BINDING SERVICES
Tel +44 (0)29 2087 4949
Fax.+44 (0)29 2037 1921
E-Mail Bindery@Cardiff.ac.uk

Determining the Role of Polyamine Metabolism in Two Human Pathogenic Protozoa: *Trichomonas vaginalis* and *Giardia intestinalis*

Submission for the degree of Ph.D.

by

KRISTINA MARIE HARRIS

Cardiff University School of Biosciences

ProQuest LLC
789 East Eisenhower Parkway
P.O. Box 1346
Ann Arbor, MI 48106-1346

ACKNOWLEDGMENTS

This work has been a journey – not only from New York to Cardiff, but everywhere I have gone in my quest to complete it. I wish to thank both of my wonderful supervisors, Professors David Lloyd and Burt Goldberg for seeing in me what I could not always see in myself, and for imparting their vast amounts of knowledge to me with patience and enthusiasm. Without their dedication, my experience would not have been nearly as broadening. Their exuberance and pure love for science emanates from them, and I could not help but take from this experience my own enthusiastic view of the work we have done, and an excitement for the work I will do in the future.

I would like to thank my mother, Carole Harris, for her consistent encouragement and support of my goals, and my father James Harris for encouraging me in secondary school math and sciences. I would also like to thank my Grandmother, Ruth Bateman, for her unconditional love and encouragement in my educational pursuits.

The people I have met in Cardiff and at NYU throughout this time have made my experience special. I would especially like to thank Dr. Victoria Hough for encouraging me to start a masters degree and her consistent support, Dr. Bethan Lewis and Majella O'Keeffe for their support of me during my time in Cardiff, Drs. Victoria Gray and Irina Guschina for their guidance in the lab and friendship, Dr. Katey Lemar for helping me learn new techniques and encouraging me to do the PhD, Rhian E. Lewis for working so hard, Coralie, Karla, Meryl, Joan, Anne and Sam for their encouragement, and Amanda Witt and Christopher P. Edelson for their friendship and support during difficult times.

Appreciation is expressed to the Boehringer Ingelheim Fond and Bateman Trust for funding this work, Professor Graham Coombs and Dr. Timothy Paget for providing cultures, and Dr. Richard Dickinson for graciously allowing us to use equipment. Collaboration and technical support was provided by: Dr. Anthony Hayes, Dr. Anthony Hann, Michael P. Turner, Michael O'Reilly, Dr. Giancarlo A. Biagini, Dr. Mark van der Giezen, and Leyda Evers.

ABSTRACT

This work relates the arginine dihydrolase and polyamine pathways to the synthesis of nitric oxide in *Trichomonas vaginalis,* a microaerophilic eukaryotic protozoan which is the causative agent of the sexually transmitted disease trichomoniasis. When organisms were grown overnight in the presence of 5mM difluoromethylornithine (DFMO), an inhibitor of polyamine synthesis: a combination of plasma and hydrogenosome membrane potential decreased, electron-dense inclusions appeared in greater numbers in hydrogenosomes, and the oxygen consumption rates of hydrogenosomes increased by approximately two-fold. Upon adding exogenous sources of spermine or spermidine, various effects inflicted by the presence of DFMO were virtually reversed. Based on enzyme assays conducted, polyamine depletion by DFMO also caused changes in activities of enzymes in the arginine dihydrolase pathway.

An important addition to the polyamine pathway was discovered in the body of this work: the production of nitric oxide by both *Giardia intestinalis,* an intestinal parasite that causes giardiasis, as well as *Trichomonas vaginalis*. Fluorimetric detection by confocal laser scanning microscopy and flow cytometry was performed after preincubation with the NO-specific fluorogen 4-amino-5methylamino-2'7'-difluorescein (DAF-FM). Microscopy indicated population heterogeneity with respect to NO production in freshly-harvested organisms and this was confirmed by the broad distribution of fluorescence intensities in the flow cytograms. Specific activities were determined for two nitric oxide synthases from *T. vaginalis*, one located in the cytosol and the other in the hydrogenosome, and one nitric oxide synthase from *G. intestinalis*, localized to the granular fraction. Bioinformatic searches confirmed the presence of two

NOS genes and contain protein motifs typically associated with NOS sequences. The N-terminal domains of both genes lack a NO synthase motif and instead contain motifs normally associated with various iron sulfur proteins (Fe-hydrogenase). Implications of NO production in the evolution, biology and pathogenicity of these important parasites are discussed.

Abbreviations:

Acyl-PG: O-acylphosphatidylglycerol

ADI: arginine deiminase

ADP: adenosine diphosphate

ATP: adenosine triphosphate

CDC: Center for Disease Control (USA)

CK: carbamate kinase

CL: cardiolipin (diphosphatidylglycerol)

CO_2: carbon dioxide

CSTE: Council of State and Territorial Epidemiologists (USA)

DAF-FM: 4-amino-5-methylamino-2'7'-difluorescein

DNA: deoxyribonucleic acid

DFMO: difluoromethylornithine

DioC6(3): 3,3-dihexyloxacarbocyanine iodide

EM: electron microscopy

ESI-MS: electrospray ionization mass spectrometry

$FADH_2$: 1,5-dihydro- flavin adenine dinucleotide

FAMEs: fatty acid methyl esters

Fd: ferredoxin

GDH: glutamate dehydrogenase

HIV: human immuno deficiency virus

iNOS: inducible nitric oxide synthase

LIT: linear ion trap

L-NAME: L-nitroarginine methyl ester

L-NNA: L-N^G-Nitroarginine

Metronidazole: Flagyl® (1-ethoxy 5-nitroimidazole)

NADPH:

NHS: National Health Service (UK)

NO: nitric oxide

NOS: nitric oxide synthase

NMR: nuclear magnetic resonance

ODC: ornithine decarboxylase

OCT: ornithine carbamyltransferase

PAO: polyamine oxidase

PC: phosphatidylcholine

PE: phosphatidylethanolamine

PFOR: pyruvate: ferredoxin oxidoreductase

PG: phosphatidylglycerol

PI: phosphatidylinositol

PS: phosphatidylserine

RNA: ribonucleic acid

SEM: scanning electron microscopy

SPD: spermidine

SSAT: spermidine:spermine N^1-acetyl transferase

SPM: spermine

STI: sexually transmitted infection

TEM: transmission electron microscopy

TLC: thin layer chromatography

TMRE: tetramethylrhodamine ethyl ester

TYM: tryptose/yeast/maltose medium

UK: United Kingdom

USA: United States of America

WHO: World Health Organization

FIGURES AND TABLES: **PAGE:**

DETERMINING THE ROLE OF POLYAMINE METABOLISM IN TWO HUMAN PATHOGENIC PROTOZOANS: *TRICHOMONAS VAGINALIS* AND *GIARDIA INTESTINALIS*

CHAPTER 1: INTRODUCTION

Determining the Role of Polyamine Metabolism in Two Human Pathogenic Protozoa: *Trichomonas vaginalis* and *Giardia intestinalis*

Protozoan parasites have some features in common with prokaryotic bacteria: they have short generation times, high rates of reproduction, and a tendency to induce immunity to reinfection on the part of the hosts that survive. However, they also have membrane-bounded organelles and several metabolic pathways similar to the eukaryotic cells of the host. Parasitic protozoa have evolved adaptations to allow them to better survive in the environments provided by their hosts. These characteristics include an ability to evade or counteract the immune response (Vickerman, 1978). Due to the parasite's ability to combat the immune system, infections of a host with parasitic protozoa are sometimes fatal to the host, and if not, often last longer than infections with bacteria. This study will focus on two parasitic protozoa: *Trichomonas vaginalis* and *Giardia intestinalis.*

1.1 Overview of two parasitic protozoa: *Trichomonas vaginalis* and *Giardia intestinalis.*

Trichomonas vaginalis will be the main organism studied in this work. This microaerophilic eukaryotic flagellate (Paget & Lloyd, 1990) of the human urogenital tract is the causative agent of the sexually transmitted disease trichomoniasis. The World Health Organization (WHO) estimates the worldwide prevalence of trichomoniasis is 170 million, which is greater than that of either gonorrhea or chlamydia. More than half of all females with gonorrhea also have trichomoniasis. As a rule, individuals with one

diagnosed STI frequently have one or more additional sexually-transmitted infections. It is estimated that approximately three million females are infected with trichomoniasis annually in the United States alone. The only drug approved by the United States Federal Drug Administration and the United Kingdom National Health Service to treat trichomoniasis is Flagyl® (1-ethoxy 5-nitroimidazole), commonly referred to as metronidazole, which was first introduced in the United States in 1963. In addition to the strong side effects caused by metronidazole, many negative characteristics of this drug have been discovered. Evidence of metronidazole's carcinogenic potential is mounting, the drug cannot be administered during the first trimester of human pregnancy, and it has been shown to cause abortions in cows (Rhyan *et al.*, 1988). All of these issues, in addition to the emergence of drug-resistant strains, necessitate finding a new drug treatment for patients with trichomoniasis.

Giardia intestinalis, a microaerophilic parasitic protozoan (Paget *et al.*, 1989), is the causative agent of one of the world's most common intestinal infections: giardiasis. Infection with this organism can be life-threatening to immunocompromised individuals, the very young, and the elderly. Currently the treatment of choice is also the administration of metronidazole or a different 5'-nitroimidazole drug, both of which present similar problems to those stated above for treatment regimes of *T. vaginalis*.

Both organisms contain, instead of the usual eukaryotic mitochondria, unique organelles which carry out essential redox reactions (Lindmark & Müller, 1973, 1975; Lloyd *et al.*, 2002; Tovar *et al.*, 2003). *T. vaginalis* contains hydrogenosomes, an organelle distinctly different from the mitochondrion in function, which carries out the same purposes (redox balancing and energy production) within the organism (Lindmark

& Müller, 1973), but using only substrate-level phosphorylation. Hydrogenosomes have been shown to be evolved forms of mitochondria (Biagini *et al.*,1997), although they do not carry out oxidative phosphorylation or the electron transport chain. *G. intestinalis* has only recently been found to have organelles with membrane potential (Lloyd *et al.*, 2002), and another "vestigial" organelle, the mitosome (Tovar *et al.*, 2003).

1.2 *Trichomonas vaginalis.*

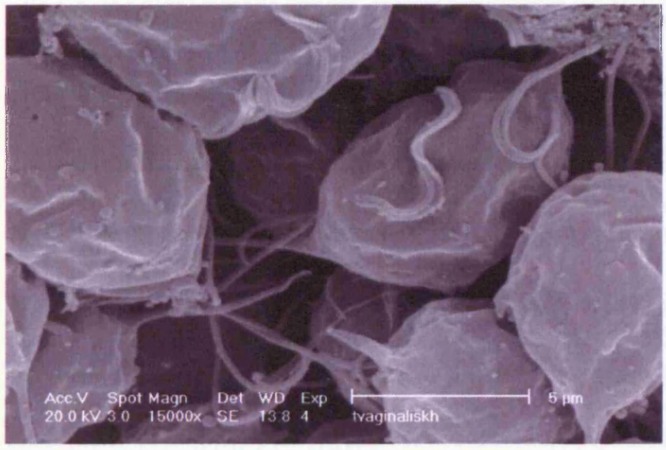

Figure 1.1: Scanning electron micrograph of fixed *Trichomonas vaginalis*. Scale bar = 5µm

1.2a. Structure of *Trichomonas vaginalis.*

Urogenital trichomonads vary in size and shape, and also vary depending on whether the sample is fresh or fixed (Fig 1.1, Appendix). Generally, however, in fixed and stained preparations they measure approximately 10µm x 7µm, while living organisms are about one third larger (Honigberg & Brugerolle, 1990). The shapes of organisms growing in TYM media tend to be more consistently ellipsoidal, ovoidal, or speroidal. The shape of the trichomonad also depends greatly on the strain; some are more circular in shape than others (Honigberg & Brugerolle, 1990). Among the most distinguishing structural characteristics are four anterior flagella, a nucleus, and an

axostylar trunk which is lined with hydrogenosomes generally positioned in three parallel rows (Fig. 1.2). The axostyle is thought to function as a supportive entity for the cell; it may also play a role in attachment to vaginal epithelial cells and therefore could be classed as a virulence factor (Petrin *et al.,* 1998, Benchimol, 2004). Apart from the lack of mitochondria and peroxisomes (Müller, 1973; Cavalier-Smith, 1987), *T. vaginalis* contains the usual intracellular organelles of eukaryotes such as a prominent nucleus, endoplasmic reticulum, Golgi complex and lysosomes; glycogen granules are also present (Benchimol, 2004). The organism has a recurrent flagellum that forms the undulating membrane (Fig 1.3a). This allows the cells to have a "quivering" motility. The undulating membrane and the costa originate in the kinetosomal complex at the anterior of the parasite. *Trichomonas vaginalis*, when interacting with epithelial cells, alters its cell morphology from a pear shape to an ameboid form which allows intimate contact between the parasite and the epithelial cell and may even result in plasma membrane continuity (Benchimol, 2004).

Figure 1.2: Cross-section of *T. foetus*. Hydrogenosomes can be viewed lined up along the axosytyle. A=axostyle, P=pelta, N=nucleus, H=hydrogenosome, V=vacuole. (Lopes *et al.*, 2001)

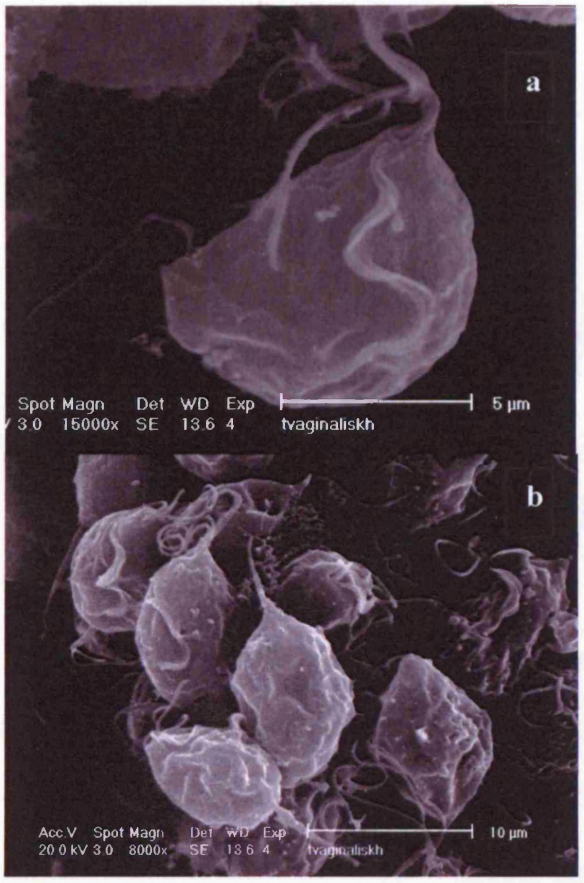

Figure 1.3: Scanning electron micrographs (SEM) of fixed *Trichomonas vaginalis*. a. One single organism. Notice the flagella and undulating membrane. b. A cluster of *T. vaginalis* organisms.

Trichomonads lack the ability to synthesize many macromolecules *de novo*. The parasite acquires these nutrients from vaginal secretions, lysis of bacterial cells (Petrin *et al.,* 1998) or aquires essential nutrients by the lysis of red blood cells and epithelial cells of the host. The lysis of the host cells occurs due to osmotic breakdown and cytoskeletal damage caused by the parasite's cytopathogenic mechanisms. The parasite then ingests the essential vitamins and minerals that were present within the lysed hosts cells, such as lipids and iron (Fiori *et al.,* 1999). Culture media for trichomonads must contain all the essential macromolecules, vitamins and minerals; serum is particularly essential for the growth of trichomonads as it provides lipids, amino acids, and trace metals. The most common medium used for culturing trichomonads is Diamond's Tryptone Yeast Maltose (TYM) medium (Diamond, 1957; Petrin *et al.,* 1998). Trichomonads only exist as

trophozoites and therefore lack a cyst stage of the life cycle, making them easy to maintain in culture. The trophozoite of *Trichomonas vaginalis* carries out cell division by binary fission (Petrin *et al.,* 1998).

1.2b. The hydrogenosome.

The hydrogenosome is a metabolic organelle which is unique to microaerophilic trichomonads, some fungi, and a few ciliates (Biagini *et al.*, 1997). Hydrogenosomes are electron-dense, microbody-like inclusions of about 0.5μm to 1.0μm in diameter (Figs 1.4 & 1.5; Appendix) (Benchimol *et al.*, 1996). These organelles have a unique ultrastructure. The matrix of these typically spherical bodies is finely granular and generally contains a dense, at times crystalline core, which is bound by two thin unit membranes. There is evidence that hydrogenosomes divide by binary fission and to date the structures of these organelles in all trichomonads have been identical (Benchimol *et al.*, 1996). This mitochondria-like redox balancing organelle is important when studying targets for development of anti–parasitic drugs for the treatment of trichomoniasis.

The hydrogenosome is a double membrane-bound organelle that carries out substrate-level phosphorylation to produce ATP using pyruvate or malate as the primary substrates (Bui *et al.,* 1996). The hydrogenosome, originally isolated from *Trichomonas vaginalis* in 1973 (Lindmark & Müller, 1973), derives its name from its ability to produce hydrogen gas from the oxidation of pyruvate or malate by using H^+ as its terminal electron acceptor (Biagini *et al.,* 1997). Pyruvate is decarboxylated by the hydrogenosomal enzyme pyruvate: ferredoxin oxidoreductase (PFOR) resulting in the formation of acetate and carbon dioxide. The electrons are donated via a redox carrier chain to hydrogenase to form molecular hydrogen. (Dyall *et al.,* 2004; Dunne *et al.,*

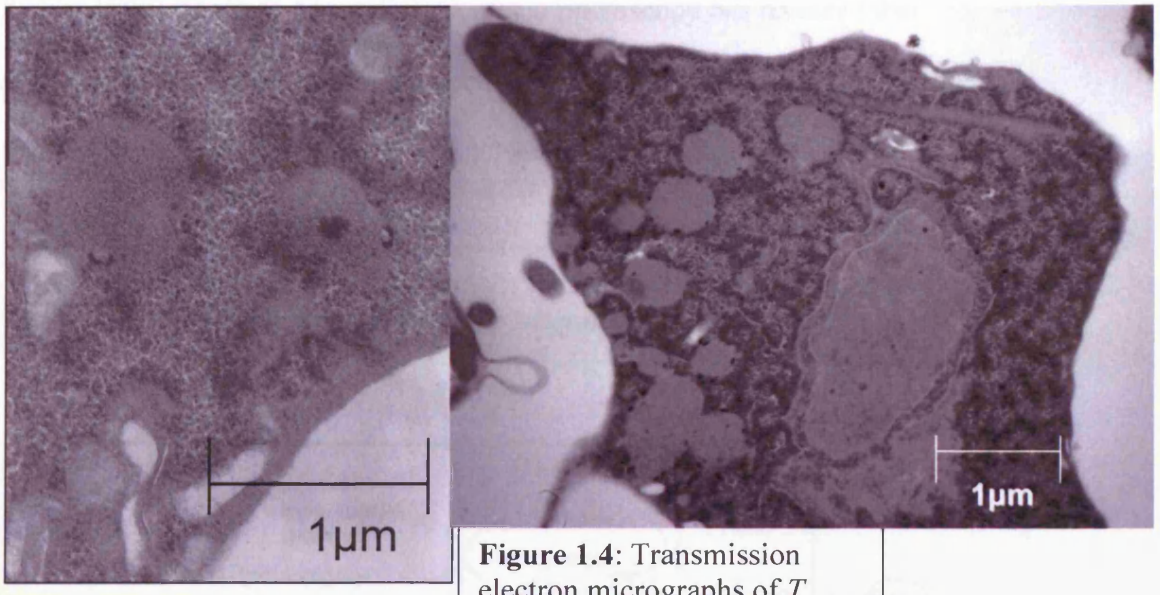

Figure 1.4: Transmission electron micrographs of *T. vaginalis* sections. Right: section representing a whole organism. Left: a higher magnification of two hydrogenosomes in a whole organism.

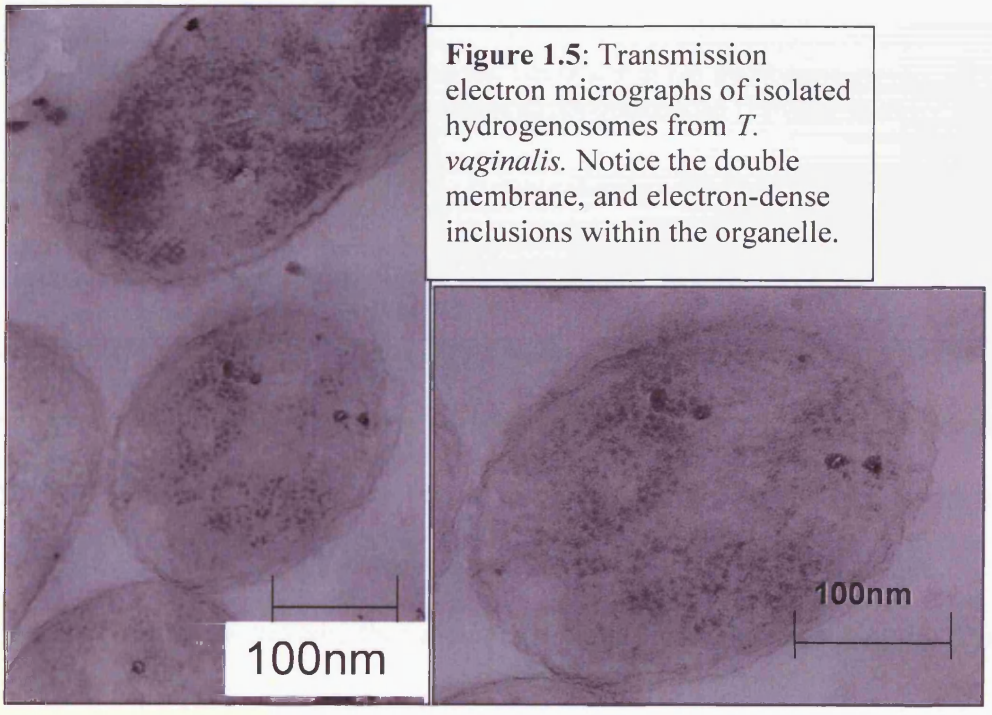

Figure 1.5: Transmission electron micrographs of isolated hydrogenosomes from *T. vaginalis*. Notice the double membrane, and electron-dense inclusions within the organelle.

2003; Kulda, 1999) (Fig 1.5; Appendix). Confocal microscopy has revealed that hydrogenosomes have a transmembrane electrochemical potential and also function as calcium stores for the cell (Humphreys *et al.,* 1998).

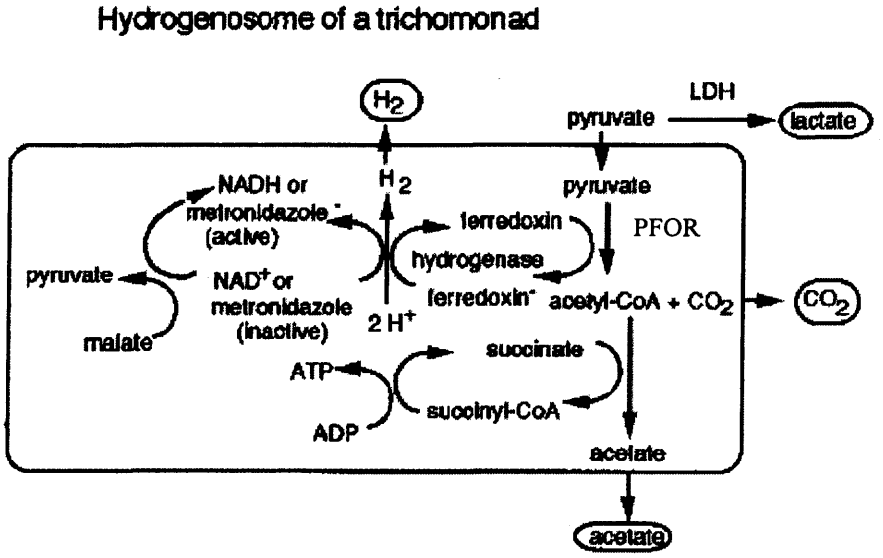

Figure 1.6: Metabolic pathway of *Trichomonas vaginalis* in the hydrogenosome. Metronidazole competes with pyruvate ferredoxin oxidoreductase (PFOR), thereby inhibiting the pathway. (Samuelson, 1999)

Hydrogenosomes and mitochondria are functionally analogous organelles sharing many common features. Mitochondria and hydrogenosomes both act as electron sinks for glycolysis–generated NADH; however mitochondria carry out oxidative phosphorylation while hydrogenosomes rely solely on substrate-level phosphorylation for the generation of ATP (Biagini *et al.,* 1997). In hydrogenosomes, electrons released by the PFOR reaction are accepted by ferredoxin, then reoxidized by the hydrogenase to form H_2 (Fig.

1.6). When metronidazole is introduced to these organisms, the drug competes preferentially with the hydrogenase for these electrons.

There has been much debate about the evolutionary ancestry of the hydrogenosome. Debates over whether hydrogenosomes are modified mitochondria (Biagini *et al.,* 1997; van der Giezen, 2005), or whether hydrogenosomes and mitochondria share a common endosymbiotic ancestor have dominated this controversy (Cavalier-Smith, 1987; Müller, 1992).

1.2c. Trichomoniasis.

Trichomoniasis is a sexually transmitted infection (STI) of worldwide importance; it is now thought to be the most common non-viral STI in the world (Petrin *et al.,* 1998; Soper, 2004). The World Health Organization (WHO) estimated that 170 million people (5 -74% in women and 5 -29% in men) will become infected worldwide annually, with the figure steadily rising (Swygard *et al.,* 2004; WHO, 2001). However this figure could be grossly underestimated due to the asymptomatic carrier state which has been observed in women and men (10 – 50% women and 15 – 50% men) and the fact that in many countries trichomoniasis is not a reportable disease (Petrin *et al.,* 1998; Soper, 2004; Lehker & Alderete, 2000). Trichomoniasis is mainly a disease of the reproductive years and clinical symptoms are rarely observed after menopause (Petrin *et al.,* 1998).

The most serious public health concern associated with trichomoniasis is its relationship to the transmission and acquisition of human immuno deficiency virus (HIV). It has been suggested that infection with *Trichomonas vaginalis* can increase the risk of acquiring HIV up to 5–fold (Lehker & Alderete, 2000). The incidence of

trichomoniasis was significantly associated with an increase of detectable specific antibodies to the HIV virus (seroconversion) and treatment of the trichomoniasis infection significantly reduced HIV RNA levels (Soper, 2004). It is thought that infection with *Trichomonas vaginalis* contributes to the spread and cause of the disease by increasing viral shedding of HIV as a result of the local inflammation produced by the trichomoniasis infection and increased susceptibility to HIV as a result of macro or microscopic breaks in mucosal barriers, thereby increasing the portal of entry (Sorvillo & Kerndt, 1998; Sorvillo *et al.*, 2001).

1.2d. Treatment of trichomoniasis.

Flagyl® (1-ethoxy 5-nitroimidazole), commonly referred to as metronidazole, is the only drug approved in the USA and the UK for treatment of trichomoniasis. The mutagenic potential of a drug that possesses a nitro group has raised questions about its carcinogenic potential, making it less than ideal (Bendesky *et al.*, 2002). In addition, pregnant women cannot take this medication as it is known to pass through the placental barrier (Visser *et al.*, 1984). Possibly the most convincing reason to look for another treatment arises from the emergence of drug-resistant strains (Forsgren & Forssman, 1979; Mammen-Tobin & Wilson, 2005), which makes the prescription of higher doses necessary. As doses increase, so do the adverse effects of the drugs on the patients ingesting them. Those taking high doses for more than three days are likely to experience vomiting and nausea, headache, dizziness, and darkening of the urine. Metronidazole refractory cases are abundant, currently estimated at about 10% of all trichomoniasis patients. Given the high rate of first treatment failure, the drug's carcinogenic potential,

and the ban on its use during pregnancy, there is an urgent need for the development of safe, effective alternatives (Rein, 1990).

The hydrogenosome plays a critical role in drug activation. Metronidazole enters the cell via passive diffusion and acts as a preferential electron acceptor and therefore competes for electrons with the hydrogenase (Fig 1.6). Hydrogen production is immediately inhibited; ferredoxin-mediated transport of electrons activates the drug. The reduction of the nitro group of metronidazole results in the production of toxic intermediates, which are thought to damage DNA, proteins, or interfere with protein trafficking. The mechanism is still not fully understood (Dunne *et al.*, 2003; Rasoloson *et al.*, 2002; Kulda, 1999). In addition to the toxic radicals, in the presence of metronidazole the production of molecular hydrogen is impaired resulting in an increase of intracellular hydrogen peroxide, which causes severe damage to the cell (Dunne *et al.*, 2003).

1.2e. Polyamine metabolism in *Trichomonas vaginalis*.

Polyamines are cationic molecules that are essential for cell proliferation and differentiation; overproduction has been linked to carcinogenesis (Marton & Pegg, 1995). Polyamines are abundant in rapidly proliferating cells and help to stabilize DNA by binding tightly to nucleic acids. Studying an organism's polyamine metabolism became more prevalent after it was shown that African trypanosomiasis, caused by infection with *Trypanosoma cruzi*, was cured in varying degrees by arresting polyamine metabolism using difluoromethylornithine (DFMO) (McCann *et al.*, 1981; Bitonti *et al.*, 1985; Bacchi & Yarlett, 1993). DFMO is known to deplete the supply of polyamines to the parasite by acting as a competitive inhibitor of ornithine decarboxylase (ODC), thereby arresting

polyamine synthesis (North *et al.*, 1986). The putrescine analog, 1,4-diamino-2-butanone (DAB) is also known to deplete the supply of polyamines by acting as a competitive inhibitor of ODC (Stevens *et al.*, 1977).

Several considerations set protozoan parasites, such as *T. cruzi* and *T. vaginalis,* apart from their mammalian hosts, and provide evidence that the parasite polyamine metabolism is selectively different from that of the host (McCann *et al.*, 1981; Yarlett *et al.*, 2000). Arresting polyamine metabolism was therefore seen as a prudent way of targeting the parasite's own survival needs, without adversely affecting the host's cells. In its mammalian host, *Trypanosoma brucei* is able to change the antigenic character of its surface coat, thereby evading the host's immune response (Vickerman, 1978). Therefore, regular treatments with drugs designed to target surface membranes of the organism would not work, so the idea of depleting the parasite's source of polyamines was an innovative one that proved successful (McCann *et al.*, 1981). As a result, several other groups began using the polyamine metabolic pathway as a target for drug therapy (Gillin *et al.*, 1984; Keithly, 1989; Keithly *et al.*, 1997; Yarlett *et al.*, 2000).

In vivo, *T. vaginalis* is exposed to polyamines, particularly spermine (White *et al.*, 1983). The parasite produces and excretes large amounts of putrescine via an energy-generating arginine dihydrolase pathway, but lacks the biosynthetic enzymes responsible for the synthesis of higher polyamines (Linstead & Cranshaw, 1983; Yarlett *et al.*, 1996). The limited nature of biosynthesis of polyamines in *T. vaginalis*, and therefore the reliance of the parasite on exogenous polyamines, makes this pathway a rational target for the development of new antimicrobial agents (Yarlett *et al.*, 2000).

Since *T. vaginalis* lacks *de novo* synthesis of spermine (Yarlett *et al.*, 1996; 2000), spermine is converted to spermidine via the combined actions of spermidine:spermine N^1-acetyl transferase (SSAT) and polyamine oxidase (PAO), while arginine is taken up and goes through a series of reactions to produce adenosine triphosphate (ATP) (Yarlett *et al.*, 2000). The polyamine metabolic pathway in *T. vaginalis* (Fig 1.6) contains both an energy-generating arginine dihydrolase pathway, and a unique backconversion pathway for spermine import. These pathways are connected by ornithine decarboxylase, the enzyme inhibited by difluoromethylornithine (DFMO), in that this reaction produces putrescine, which is exported from the organism via a spermine/putrescine antiport (Yarlett *et al.*, 2000). Therefore, the inhibition of ODC by DFMO would provide substantial depletion of polyamines to the parasite. It is not known whether the inhibition of polyamine production may affect the uptake of arginine, and thereby inhibit ATP generation.

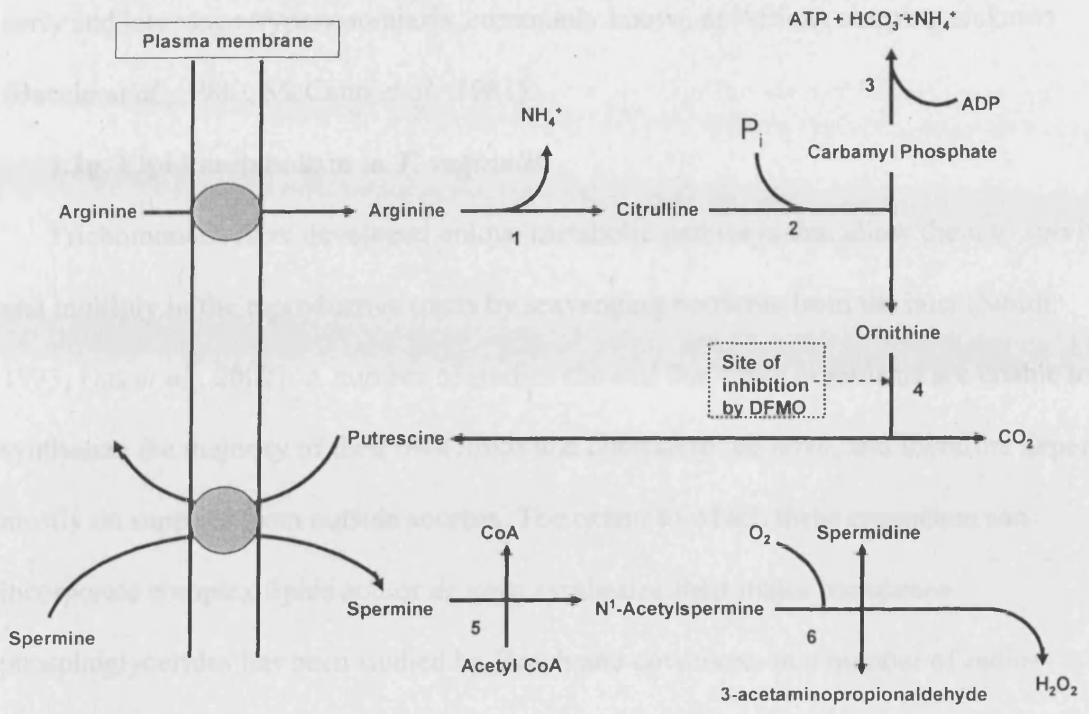

Figure 1.7: Polyamine metabolism in *T. vaginalis* (Yarlett *et al.*, 2000). 1. arginine deiminase 2. catabolic ornithine carbamyltransferase 3. carbamate kinase 4. ornithine decarboxylase 5. spermine:spermidine N^1-acetyltransferase 6. polyamine oxidase. Two putrescines are required to antiport with one spermine to balance the charge transfer.

1.2f. DL-α-difluoromethylornithine (DFMO)

DL-α-difluoromethylornithine (DFMO) is an analog of ornithine and an enzyme-activated irreversible inhibitor of ornithine decarboxylase (ODC), the enzyme responsible for the decarboxylation of ornithine to putrescine and CO_2 (Fig 1.7). The decarboxylation of ornithine is the starting point of polyamine synthesis in *Trichomonas vaginalis* and therefore treatment with DFMO depletes the supply of polyamines to the parasite (Yarlett *et al.*, 1993). Inhibition of the polyamine pathway at this point prevents the export of putrescine and therefore should prevent the uptake of spermine and the synthesis of spermidine. DFMO has been used with varying degrees of success as a treatment for

early and late stage trypanosomiasis, commonly known as African sleeping sickness (Bacchi *et al.*, 1980, McCann *et al.*, 1981).

1.2g. Lipid metabolism in *T. vaginalis*.

Trichomonads have developed unique metabolic pathways that allow them to survive and multiply in the reproductive tracts by scavenging nutrients from the host (Smith, 1993; Das *et al.*, 2002). A number of studies showed that these organisms are unable to synthesize the majority of their own lipids and cholesterol *de novo*, and therefore depend mostly on supplies from outside sources. The extent to which these organisms can incorporate complex lipids and/or *de novo* synthesize their major membrane phosphoglycerides has been studied by Beach and coworkers in a number of radio-labelled experiments (Beach *et al.*, 1991). They concluded that biosynthesis of phosphatidylethanolamine (PE) may proceed normally whereas that of phosphatidylcholine (PC) as well as phosphatidylinositol (PI), phosphatidylserine (PS), phosphatidylglycerol (PG) and O-acylphosphatidylglycerol (Acyl-PG) showed a major deficiency. Moreover, a limited potential for exchange reactions and turnover has also been shown for labeled phosphoglycerides incorporated directly from the environment. The trichomonads have been suggested to lack a variety of enzymatic activities involved in complex phosphoglyceride metabolism (Beach *et al.*, 1991).

However, trichomonads can synthesize glycolipids and glycophosphosphingolipids *de novo* (Singh *et al.*, 1991). Two major ethanolamine phosphate-substituted inositol phosphosphingolipids have been identified in the unsaponifiable acidic fractions of *T. foetus* and *T. vaginalis* by a combination of tandem mass spectrometry (MS-MS) and nuclear magnetic resonance (NMR) (Costello *et al.*, 1993). The authors suggested that

these glycosphingolipids may represent metabolic intermediates for new types of membrane anchors for surface glycopeptides or glycolipids that mediate the host-parasite relationship of these trichomonads (Costello *et al.*, 1993).

1.3 *Giardia intestinalis.*

Giardia intestinalis, a eukaryotic, microaerophilic protozoan (Paget & Lloyd, 1989), is the causative agent of one of the world's most common intestinal infections: giardiasis (Adam, 2001). Infection with this organism can be life-threatening to immunocompromised individuals, the very young, and the elderly. This parasite exists in two stages: the dormant cyst, and the flagellate trophozoite. The focus of our studies will be on the trophozoite, as it is the causative agent of giardiasis.

1.3a. Structure of *G. intestinalis*

Each trophozoite has eight flagella and a striated disk, which plays a role in the parasite's adhesion to the intestinal wall (Holberton, 1974; Inge *et al.*, 1988) (Fig 1.8). *Giardia* contains lysosome-like organelles (Bockman *et al.*, 1968; Thirion *et al.*, 2003), two identical nuclei (Bernander *et al.*, 2001; Kabnick *et al.*, 1990; Wiesehahn *et al.*, 1984), Golgi apparatus (most prominently during encystation) (Lujan *et al.*, 1995), mitosomes (Tovar *et al.*, 2003), but are devoid of mitochondria (Cavalier-Smith, 1987) and peroxisomes.

The duodenum and jejunum are regions of the small intestine hostile for microbes, which explains why very few microbes make up the normal flora in this portion of the digestive system (McFarland, 2000). Due to peristaltic movement, mucus and epithelial shedding, and high flow of liquids, in addition to its relatively short generation time, *G. intestinalis* must attach to the small intestine strongly. The cytoskeleton of *Giardia*, consisting of eight flagella (four pairs), the median body, the funis and the adhesive disk, is essential to adhesion of the parasite to the intestinal wall (Elmendorf *et al.*, 2003). The adhesive disk plays a pivotal role in adhesion to

of the host, and is unique to *Giardia intestinalis* (Inge *et al.*, 1988; Magne *et al.*, 1991; McCabe *et al.*, 1991) (Fig 1.8). It was recently shown that disk proteins are stored within the cyst, ready to be used after excystation (Palm *et al.*, 2005).

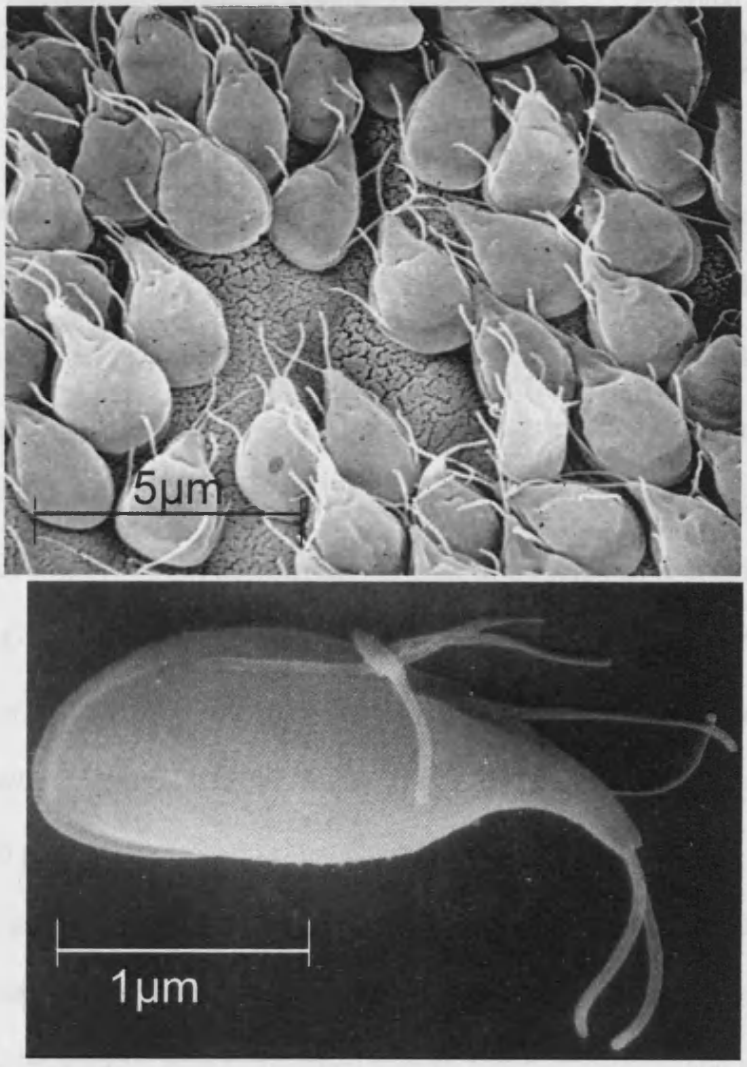

Figure 1.8: Scanning electron micrographs of *G. intestinalis*. Top: Organisms infecting the epithelial tissue of the small intestine *(Stan Erlandsen)*. Bottom: one single organism. Note the undulating membrane and flagella *(Stan Erlandsen)*.

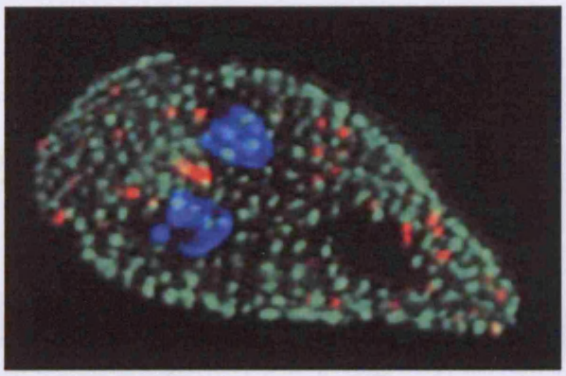

Figure 1.9: Fluorescence microscopy of *G. intestinalis*. Note the presence of 2 nuclei (blue). (Courtesy of Dr. Adrian Hehl, Univeristy of Zurich, Switzerland. Personal communication to D. Lloyd)

Although hypotheses have been presented, no studies have determined why *G. intestinalis* contains two nuclei (Fig 1.9). The nuclei replicate at exactly the same time (Wiesehahn *et al.*, 1984), are both transcriptionally active (Kabnick *et al.*, 1990), and contain similar quantities of DNA (Bernander *et al.*, 2001; Kabnick *et al.*, 1990). Each nucleus contains at least one copy of the complete genome (Yu *et al.*, 2002). Although some *G. intestinalis* organisms have been found that only contain one nucleus, they are rare, and it has not been determined whether these organisms are viable.

G. intestinalis has been termed 'amitochondrial' (Cavalier-Smith, 1987). However, redox-active organelles and mitosomes have recently been found in *G. intestinalis* (Lloyd *et al.*, 2002; Tovar *et al.*, 2003). Recently, *Giardia intestinalis* was found to produce hydrogen, a characteristic formerly thought to be unique to hydrogenosome-containing organisms (Lloyd *et al.*, 2002). These discoveries have promoted discussions about the possible presence of redox-generating organelles in *Giardia intestinalis* with similarities to both hydrogenosomes and mitochondria.

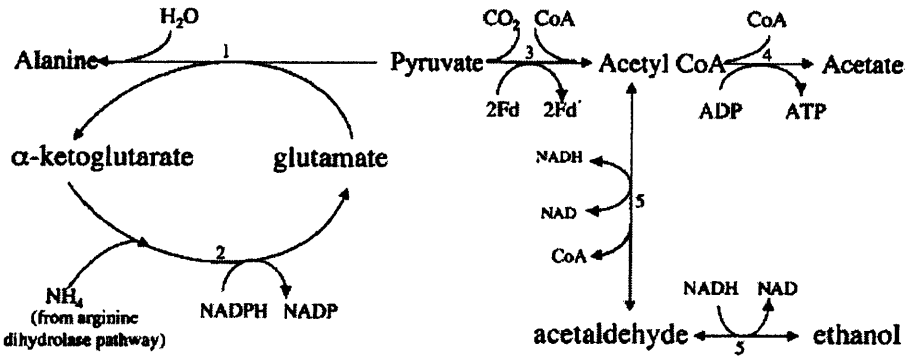

Figure 1.10 (Adam, 2001): End product synthesis from pyruvate. The enzymes involved are: 1. alanine aminotransferase; 2. glutamate dehydrogenase (GDH); 3. pyruvate ferredoxin oxidoreducatse (PFOR); 4. acetyl-CoA synthetase; 5. alcohol dehydrogenase. Acetate is the major product under aerobic conditions, while ethanol and alanine are preferentially produced under anaerobic conditions (Paget *et al.*, 1990; 1993).

G. intestinalis oxidizes exogenous and endogenous carbohydrates to ethanol, acetate, and CO_2; energy production is carried out only by substrate-level phosphorylation (Lindmark, 1980) (Fig 1.10). The balance of endproduct formation is sensitive to the amount of O_2 present, as well as the amount of glucose present in the medium (Adam, 2001). Acetate is the major product under aerobic conditions, while ethanol and alanine are preferentially produced under anaerobic conditions (Paget & Lloyd, 1990; Paget *et al.*, 1993). It is believed, since a mitochondria-like organelle has not been found in *Giardia*, that the glycolytic pathway occurs in the cytosol (Lindmark, 1980). The enzyme catalyzing the conversion of pyruvate to coenzyme A is pyruvate:ferredoxin oxidoreductase (PFOR), which in many protists was a marker protein specific for hydrogenosomes. Its existence in *Giardia intestinalis*, which is thought not to have hydrogenosomes, has raised many

questions. Why does this protist contain an enzyme so specific to hydrogenosomes if it does not contain hydrogenosomes? Did *Giardia* used to contain hydrogenosomes? Why is energy production in *Giardia* via the actions of PFOR occurring outside a membrane-bound organelle such as a hydrogenosome or mitochondria?

The location of both *Giardia* and *Trichomonas* in evolutionary taxonomy has been debated mostly due to their lack of classic mitochondria. *Giardia* were considered to be among the most 'primitive' organisms on the eukaryotic evolutionary tree due to their lack of traditional mitochondria, peroxisomes, and nucleoli, as well as their possession of only rudimentary Golgi stacks and their limitation to substrate-level phosphorylation for producing energy (Cavalier-Smith, 1987; Adam, 2001; Sogin & Silberman, 1998).

The discovery of nuclear genes with putative mitochondrial ancestry in *Giardia* led to more studies of these organisms (Hashimoto *et al.*, 1998; Roger *et al.*, 1998; Tachezy, 2001; Morrison, 2001; Arisue *et al.*, 2002). The culmination of these studies was the discovery of membrane-bound organelles (Lloyd *et al.*, 2002), followed by the discovery of mitosomes in *Giardia* (Tovar *et al.*, 2003). Several groups have confirmed the theory that *Giardia* evolved from organisms containing mitochondria (Lloyd, Ralphs & Harris, 2002; van der Giezen *et al.*, 2005).

1.3b. The mitosome.

The organelle recently discovered in *Giardia intestinalis*, named the mitosome, has been labeled as a mitochondrial relic. The mitosome is double membrane-bound, and only approximately 100nm in diameter (Fig. 1.11). These very small organelles are distributed throughout the cytosol, where they contribute

to Fe-S protein maturation, but lack other functions (Tovar *et al.*, 2003). Their role in Fe-S maturation is believed to have stemmed from that of the same protein in mitochondria, which is necessary for regeneration of Fe-S proteins as part of an electron transport chain. It remains unknown why these organisms would no longer need the other constituents of mitochondria, and why so much was lost. Most recently, mitosomes were shown to contain the following key mitochondria marker proteins: Cpn60, mtHsp70, ferredoxin (Fd), IscS, and IscU. The mitosome has also been found to divide and segregate during mitosis (Regoes *et al.*, 2005).

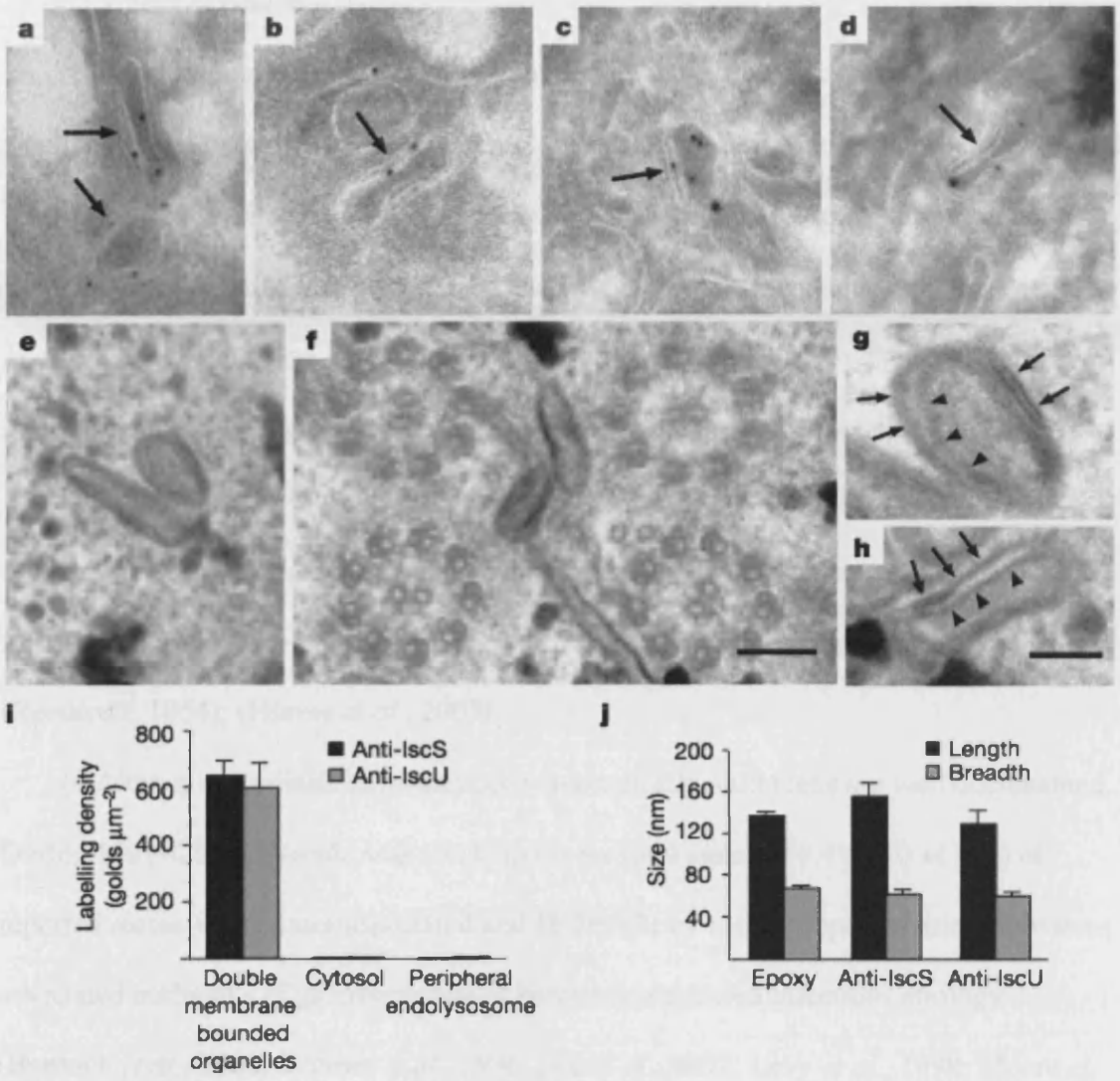

Figure 1.11: From Tovar *et al.*, 2003.

| Localization of IscS and IscU in *Giardia* trophozoites by transmission electron immunomicroscopy. **a–d**, Thawed frozen cryosections of glutaraldehyde-fixed *Giardia* were labelled with anti-IscS (**a**) and anti-IscU antibodies (**b**) or double-labelled (**c** and **d**) for anti-IscU (8 nm gold particles) followed by anti-IscS antibodies (12 nm gold particles). Arrows indicate double-membrane-bounded structures. Membranes appear as white profiles with this methodology. **e–h**, Epoxy resin sections of glutaraldehyde-fixed trophozoites. **f**, Double-membrane-bounded structures are shown in close proximity to flagellar axonemes. **g**, **h**, High-magnification images showing organelle double membranes. Arrows point towards outer membranes while arrowheads identify inner membranes. **i**, Densities of labelling from typical labelling experiments were obtained as explained in Methods ($n = 8$ for IscS and $n = 7$ for IscU; n = number of scanned micrographs). **j**, Sizes of double membrane bounded organelles in epoxy resin and cryosections labelled with antibodies to either IscS or IscU ($n = 43$ for epoxy resin, $n = 13$ for IscS and $n = 11$ for IscU; n = number of organelles). Intermembrane spacing in epoxy resin was 9.36 ± 0.49 nm ($n = 29$). Scale bars, 100 nm (**a–f**) and 50 nm (**g**, **h**).

1.3c. Giardiasis.

Giardia intestinalis is the most common intestinal parasite in the United States (Kappus *et al.*, 1994). This flagellated protozoan causes giardiasis, which is characterized by diarrhea, abdominal cramps, bloating, weight loss, and malabsorption. A zoonotic disease, giardiasis also affects domestic and wild mammals (e.g., cats, dogs, cattle, deer, and beavers) (Thompson, 2000). *Giardia* infection is transmitted by the fecal-oral route and results from the ingestion of *Giardia* cysts through the consumption of fecally contaminated food or water, or through person-to-person or animal-to-person transmission. The cysts are infectious immediately upon being excreted in feces. The infectious dose is low; ingestion of 10 cysts has been reported to cause infection (Rendtorff, 1954); (Hlavsa *et al.*, 2005).

Although giardiasis cases can occur sporadically, outbreaks are well documented. During 1991--2000, *Giardia* was identified as a causal agent of 9.4% (10 of 106) of reported recreational water-associated and 16.2% (21 of 130) of reported drinking water-associated outbreaks of gastroenteritis of known or suspected infectious etiology (Barwick *et al.*, 2000; Kramer *et al.*, 1996; Lee *et al.*, 2002; Levy *et al.*, 1998; Moore *et al.*, 1993). Additionally, foodborne outbreaks of giardiasis linked to infected foodhandlers and uninfected foodhandlers who cared for infected children have been reported (Quick *et al.*, 1992). Outbreaks resulting from person-to-person transmission in child care centers also have been reported (Ang, 2003).

In 1992, the Council of State and Territorial Epidemiologists (CSTE), an organization that works with the Center for Disease Control in the USA to improve the American public's health by supporting the efforts of epidemiologists, assigned giardiasis

an event code to facilitate transmission of reported giardiasis data to Center for Disease Control in the USA. Reporting of giardiasis as a nationally notifiable disease in the USA began in 2002.

1.3d. Treatment of giardiasis.

The choice of a therapeutic agent for treatment of the infection is difficult; of the three drugs commonly used, metronidazole and furazolidone have been shown at high doses to be carcinogenic in animal studies, while quinacrine causes frequent side effects. In previous studies, both metronidazole and quinacrine were more effective than furazolidone, but quinacrine caused side effects which may have been responsible for poor compliance. With regard to the carcinogenicity of these compounds, it appears likely that there is no large short-term risk from the use of metronidazole, but long-term follow-up studies have not been done and no clinical studies have been done regarding the risk of furazolidone or quinacrine. The lack of clear confidence in animal studies is evident in the fact that the Food and Drug Administration has approved ongoing studies with drugs related to metronidazole (Davidson, 1984; Harris *et al.*, 2001; Wright *et al.*, 2003).

1.3e. Applications of polyamine metabolism research in *G. intestinalis*.

Very little is known about the polyamine pathway in *G. intestinalis*, but it was made clear that the parasite contains ornithine decarboxylase, when DFMO inhibited the growth of the parasite (Gillin, Reiner & McCann, 1984). This enzyme is a part of the arginine dihydrolase pathway, which is probably very similar to that of *T. vaginalis* (Minotto *et al.*, 1999). Although a precise mechanism has not been proposed for the polyamine pathway in *G. intestinalis*, the existence of an ODC in the organism, coupled

with the close evolutionary relationship between *T. vaginalis* and *G. intestinalis*, supports using the mechanism of *T. vaginalis* as a model for that in *G. intestinalis*. Whilst this area of work may eventually provide a target for chemotherapy for *Trichomonas vaginalis* and *Giardia intestinalis,* the main focus of this study involves further characterizing the pathway and defining the role of the unique redox balancing organelles found in these organisms.

1.4 Nitric oxide production.

Nitric oxide is an important signaling molecule, a component of the host immune response in combating pathogens and parasites as well as a molecule responsible for a wide diversity of physiological control functions (Broillet, 1999; Albina *et al.*, 1998; Hess *et al.*, 2005; Nisoli & Caruba, 2006; Kato & Giulivi, 2006). NO synthases are traditionally associated with a guanylyl cyclase which is tightly associated with a heme group, and depend on the presence of Ca^{2+}. This guanylyl cyclase is induced when NO binds to the heme group and thereby activates cGMP production.

Nitric oxide plays an important role in the mammalian immune system, where it is primarily produced by macrophages in response to cytokines or microbial invaders. It acts as a tumoricidal and antimicrobial molecule *in vitro* and *in vivo* (Nathan, 1992; Bogdan, 2001a). Its structure is unstable and its action brief; within seconds it will undergo oxidation to nitrite or nitrate. Due to its structure, it is also easily diffused through membranes, thereby allowing it to take part in intercellular as well as intracellular control mechanisms (Gaston & Stamler, 1999). All isoforms of NOS [nNOS (neuronal), iNOS (inducible), and eNOS (endothelial)] except mtNOS (mitochondrial NOS) function in the human immune system (MacMicking et al., 1997; Stuehr, 1999).

The interaction of NO is not restricted to a single defined receptor; it can react with inorganic molecules (i.e. oxygen, superoxide or transition metals), structures in DNA, prosthetic groups (i.e. heme) or proteins (causing the S-nitrosylation of thiol groups) (Broillet, 1999; Bogdan, 2001b). Many of these targets are responsible for regulatory processes, thus making nitric oxide capable of inducing other processes including various signaling cascades (Bogdan, 2001b).

NOS catalyzes the net reaction:

L-Arginine + NADPH + O_2 = Citrulline + Nitric oxide + $NADP^+$

The metabolic conversion of arginine to citrulline via the actions of nitric oxide synthase (NOS), with nitric oxide (NO) as the main product, has been studied in numerous mammalian cell-types, tissues and organs. With respect to parasitic protozoa, however, NO production has been dominated by a one-sided exploration: effects of the release of NO from the host's immune system and its cytotoxic manifestations in the parasites. However, only a few studies have explored the production of NO by the parasites themselves.

NOS activity has been shown in *Trypanosoma cruzi* and was found to be sensitive to typical NOS inhibitors, such as N^W-methyl-L-arginine (Paveto *et al.*, 1995). It was also found that *Leishmania donovani* produces NO and contains a NOS similar to that of the mammalian enzyme (Basu *et al.*, 1996). *Entamoeba histolytica* was shown to have NOS activity and responded to typical NOS inhibitors (Hernandez-Campos *et al.*, 2003). It is possible that nitric oxide production is a mechanism utilized by many protozoan parasites. NOS or NOS-like enzymes are present in several non-protozoan parasites,

including *Hymenolepis diminuta* (Gustafsson *et al.*, 1996), *Brugia malayi* (Pfarr and Fuhrman, 2000), *Ascaris suum* (Bascal *et al.*, 2001), *Diphyllobothrium dendriticum* (Lindholm *et al.*, 1998), *Schistosoma mansoni* (Kohn *et al.*, 2001), and *Trichinella britovi* (Masetti *et al.*, 2004). *Trichomonas vaginalis* has recently been found to contain an enzyme that degrades nitric oxide (Sarti *et al.*, 2004); this is presumed to function as defense mechanisms against the host's immune response.

CHAPTER 2

GENERAL MATERIALS AND METHODS

2.1 Maintenance, growth, and harvesting of *Trichomonas vaginalis*. C1 (ATCC 30001) cultures and G3 cultures were grown in Diamond's Tryptone/Yeast Extract/Maltose (TYM) medium, pH 6.2, without agar and with (v/v) 10% horse serum, at 37 °C for 24 h (Diamond, 1957). Cell cultures were centrifuged at 1,000 x g for 15 min at 20 °C, then washed in a Doran's Buffer: 30mM Na_3PO_4, 74mM NaCl, 0.6mM $CaCl_2$, and 1.6mM KCl, pH 6.2.

2.2 Maintenance and growth of *Giardia intestinalis*. JKH strain was a gift of Timothy Paget, University of Hull, UK, and was isolated by Victoria Hough. Trophozoites were cultured axenically at 37 °C, in Diamonds modified medium containing (w/v): 2% tryptone, 1% yeast extract, 0.5% glucose, 0.106% arginine, 0.2% sodium chloride, 0.1% dipotassium hydrogen phosphate, 0.1% potassium dihydrogen phosphate, 0.1% cysteine, 0.02% ascorbic acid, 0.0023% ammonium ferric citrate, 0.1% bovine bile (Keister, 1983; Edwards *et al.*, 1989). Log phase cultures were harvested at 500 x g for 10 min at 4 °C in a Beckman Coulter Avanti J-E centrifuge (Fullerton, California, USA).

2.3 Confocal microscopy. Living *T. vaginalis,* stained with varying concentrations of fluorophores (to be stipulated in individual chapters) and immobilized with 2% (w/v) methyl cellulose, were observed using a Leica Microsystems DM6000B (Milton Keynes, UK) laser scanning confocal microscope using a X63 oil immersion objective. Images were subsequently stacked into three dimensional representations using the proprietary software.

2.4 Flow cytometry. Samples of whole organisms or hydrogenosome-enriched fractions were analyzed using a Becton Dickinson FACSCalibur Flow Cytometer (Franklin Lakes, New Jersey, USA). The photomultiplier voltage was set to 550V. The argon ion laser was programmed for excitation and emission signals were acquired for wavelengths specific to the individual fluorophores for 100,000 cells in each sample at a flow rate of 60µl/min. Organisms grown overnight in TYM in the presence or absence of 5mM DFMO were harvested and washed. Finally, samples were loaded with fluorescent dye for 20 min and washed again in Doran's Buffer before being analyzed by the flow cytometer. A similar dye-loading procedure was carried out on isolated hydrogenosomes. In this case, the photomultiplier voltage was increased to 950V so as to detect the fluorescence of smaller particles.

Table 2.1: Flow Cytometry Fluorophores & Incubation Times

Fluorophore used	**Concentration**	**Incubation Time**	**Excitation**	**Emission**
TMRE*	0.5 nM	20 min	488 nm	550—700 nm
$DioC_6(3)$	0.5 nM	20 min	488 nm	550—700 nm
DAF-FM**	200 nM	20 min	488 nm	550—700 nm

*TMRE: tetramethylrhodamine ethyl ester
**DAF-FM: 4-amino-5-methylamino-2'7'-difluorescein

2.5 Transmission electron microscopy. All procedures were carried out at 4 °C, unless otherwise specified. Sedimented organisms or subcellular fractions were fixed in a solution containing 2.5% (v/v) glutaraldehyde, 0.05M sodium cacodylate (pH 6.8), 2mM $CaCl_2$, and 0.2M sucrose, and incubated for 1 h. The pellet was then washed in a buffer containing 0.1M calcium cacodylate, 2mM $CaCl_2$, and 0.2M sucrose, and incubated overnight. The samples were then incubated in 1.0% osmium tetroxide in 0.1M cacodylate buffer for 1 h. The samples were dehydrated at 20 °C by exposure to successive ethanol washes, each lasting 5 min: 30%, 50%, 70%, 90%, and finally three successive washes in 100% ethanol (v/v). The samples were then incubated for 10 min in pure propylene oxide at 20 °C. Samples were subsequently incubated overnight in a 1:1 mixture of propylene dioxide and araldite CY212 at 20 °C. The following day, samples were embedded into new resin and allowed to incubate at 60 °C for 48 h. Thin sections were then cut, stained for 10 min with 2% uranyl acetate (w/v) and subsequently with lead citrate for 5 min (Reynolds, 1963), washed briefly and finally examined using a Philips Electron Microscope 208, operated at 80kV.

2.6 Determining cell counts. Cultures were diluted 100-fold prior to preparing a haemocytometer slide. The slide was observed on a M16 Student and laboratory phase-contrast microscope (Vickers Instruments, Sheffield, UK), counted, and multiplied by 100 for the dilution factor, and then 1000 as stipulated by the manufacturers of the haemocytometer slide for final calculation of number of cells per ml.

2.7 Hydrogenosome isolation from *T. vaginalis*. All procedures were carried out at 4 °C. The organisms were washed and resuspended in a buffer containing 250mM sucrose, 50mM Tris-HCl, 10mM β–mercaptoethanol, pH 7.0. Disruption was carried out by shaking in a Braun MSK cell disintegrator with acid-washed glass beads (400μm diameter) twice, for 30 s each time, at 2,000 Hz. The homogenate was centrifuged at 500 x g for 5 min to remove unbroken cells, nuclei, and membrane fragments. The supernatant was then centrifuged at 4,000 x g for 10 min to sediment the hydrogenosome-enriched large granular fraction. This pellet was resuspended in approximately 100μl of 250mM sucrose, 50mM Tris-HCl, pH 7.0. (de Duve & Berthet, 1953; de Duve *et al.*, 1955; de Duve, 1964; Lindmark & Müller, 1973; Cerkasóv *et al.* 1978).

2.8 Subcellular fractionation of *T. vaginalis*. Two log phase cultures of *T. vaginalis,* one having been grown overnight in 5mM DFMO and the other in the absence of DFMO, were harvested at 500 x g for 10 min in a Beckman Coulter Avanti J-E centrifuge (Fullerton, California, USA). All procedures were carried out at 4 °C. The organisms were washed and resuspended in a buffer containing 250mM sucrose, 50mM Tris-HCl, 10mM β–mercaptoethanol, pH 7.0. Disruption was carried out twice using a Braun MSK cell disintegrator with acid-washed glass beads (400μm diameter), for 20 s each, at 2,000 Hz. The homogenate was centrifuged at 400 x g for 10 min to remove unbroken cells, nuclei, and membrane fragments. The supernatant was then centrifuged at 2,200 x g for 10 min to separate the hydrogenosome-rich large granular fraction. The remaining supernatant was centrifuged at 7,840 x g for 15 min to separate the small granular from the cytosolic

fraction (de Duve & Berthet, 1953; de Duve *et al.*, 1955; de Duve, 1964; Lindmark & Müller, 1973; Cerkasóv *et al.* 1978).

2.9 Subcellular fractionation of *Giardia intestinalis*. All procedures were carried out at 4 °C. Log phase cultures of *G. intestinalis* were harvested at 500 x g for 10 min in a Beckman Coulter Avanti J-E centrifuge (Fullerton, California, USA). The organisms were washed and resuspended in a buffer containing 250mM sucrose, 50mM Tris-HCl pH 7.0, 10mM β–mercaptoethanol. Disruption was carried out using a Braun MSK cell disintegrator with acid-washed glass beads (400μm diameter) for 20 s at 2,000 Hz. The homogenate was centrifuged at 400 x g for 10 min to remove unbroken cells, nuclei, and membrane fragments (referred to as the primary sedimenting fraction). The supernatant was then centrifuged at 2,200 x g for 10 min to separate the hydrogenosome-rich large granular fraction. The remaining supernatant was centrifuged at 10,000 x g for 15 min at 4 °C to separate the small granular from the cytosolic fraction. Marker enzyme assays were conducted on all fractions, according to the protocols previously stated (de Duve & Berthet, 1953; de Duve *et al.*, 1955; de Duve, 1964; Ellis *et al.*, 1993a).

2.10 Marker enzyme assays to determine purity of fractions.

2.10a. NAD^+ -dependent malic enzyme assay. The assay mixture contained 50 mM KCl, 5 mM $MgCl_2$, 20 mM Tris HCl (pH 7.6), 20 mM L- malate, 0.05 mg of protein and 0.3 mM of NAD^+ in a total volume of 1 ml. The absorbance was monitored at 340nm over a 15 min period at room temperature using a Unicam SPI8000 Ultraviolet Spectrophotometer (Cerkasóv *et al.*, 1978; Lindmark & Müller, 1978; Hrdý & Müller, 1995; Drmota *et al.*, 1996).

2.10b. $NADP^+$ -dependent malic enzyme assay. The assay mixture contained 50 mM KCl, 5 mM $MgCl_2$, 20 mM Tris HCl (pH 7.6), 20 mM L- malate 0.025 mg of protein and 0.3 mM of $NADP^+$ in a total volume of 1 ml. The absorbance at 340nm was monitored over a 15 min period at room temperature using a Unicam SPI8000 Ultraviolet Spectrophotometer. (Hrdý & Mertens, 1993)

2.10c. Acid phosphatase enzyme assay. The assay mixture contained 0.25M glycine-HCl, pH 3 containing 0.5% Triton X 100, 0.3 mg protein and 50mM para-nitrophenol phosphate (substrate) in a final volume of 250 µl (Padh, 1989). The reaction was incubated at 37 °C for 10, 15, 20 and 30 min respectively. The assay was stopped by addition of 2.75ml of ice cold Na_3PO_4, pH 12. The increase in absorbance was read at 410 nm using a Unicam SPI8000 Ultraviolet Spectrophotometer (Nielsen *et al.*, 1974).

2.10d. Lactate dehydrogenase assay. The 1 ml assay mixture contained: 0.1M Tris-HCl, pH 7.1; 0.01M pyruvate, and 0.3mM NADH, and 0.2 mg protein. Linear reduction in absorbance was measured at 340nm using a Unicam SPI8000 Ultraviolet Spectrophotometer at room temperature (Bergmeier, 1970).

2.11 Protein determination. Ten µl, 20 µl and 40 µl volumes of each 1:5 diluted protein sample were added to 990, 980 and 960 µl of distilled H_2O, respectively, in acetone cleaned test tubes. Five ml of a solution containing: 0.19M Na_2CO_3, 0.1M NaOH, 0.01M NaKTartrate, and 0.02M $CuSO_4$ was added to the samples and then incubated for 10 min at room temperature with continuous shaking. After 10 min, 0.5 ml of Folin's solution (1:1 Folin's: distilled water) was added to each tube. This was then incubated for a further 30 min with continuous shaking. The absorbance of the samples was measured at 650nm using a Unicam

SPI8000 Ultraviolet Spectrophotometer; protein concentration was calculated using a standard curve (Lowry *et al.*, 1951).

2.12 Carbamate kinase assay. A 1ml assay contained the following: 1mM ADP, 20mM glucose, 1mM NADP, 30mM $MgCl_2$, 2u glucose-6-phosphate dehydrogenase, 14u hexokinase, 1mM carbamyl phosphate, 0.1 mg protein, and 10mM Hepes, pH 6. Absorbance was measured at 340nm by a Unicam SP1800 Ultraviolet Spectrophotometer (PYE Unicam). Assays were carried out on fractions from control cultures as well as those grown overnight in 5mM DFMO. Substrate concentrations were varied and the assays conducted in order to produce a Michaelis-Menten plot. K_M and V_{max} values were then determined from a Lineweaver-Burk plot (Yarlett *et al.*, 1994). The activity of the carbamate kinase enzyme was measured indirectly using an enzyme linked assay. This assay utilizes the enzymatic activity of glucose-6-phosphate dehydrogenase and hexokinase (Fig 2.1); this results in the increasing formation of NADPH which could then be measured over time at 340nm using a spectrophotometer.

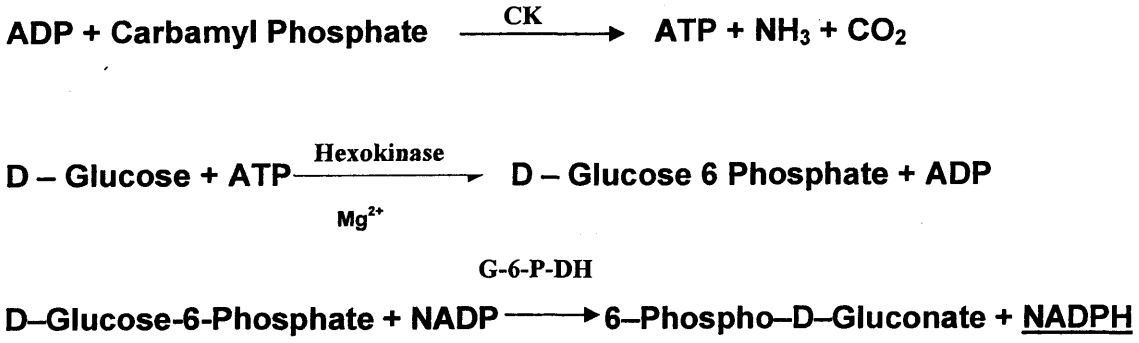

Figure 2.1. Mechanism of the enzyme-linked carbamate kinase enzyme assay. The linked enzymes assay produces NADPH which is measured at 340nm using a spectrophotometer. CK = Carbamate Kinase, G-6-PHD = Glucose-6-phosphate dehydrogenase.

2.13 Arginine deiminase assay. A 1ml assay (Fig 2.2) was carried out containing the following: 1mM L-arginine, 0.1 mg protein, and 40mM MES, pH 6. This reaction was incubated at RT for 15, 30, 60, and 120 min, after which each sample was stopped with 100 µl trichloroacetic acid solution (TCA), and the formation of citrulline was measured (Rahmatulah & Boyd, 1980). Five mg of thiosemicarbazide was added to 100 ml of: 25% concentrated sulfuric acid, 20% concentrated phosphoric acid, 0.25% iron chloride. Fifty ml of 5mM 2,3-butanedione monoxime was added subsequently. The resulting solution is referred to as the chromogenic solution. Three ml of chromogenic solution was added to 0.1 ml of supernatant from the assays and mixed with a spin mix vortex (Gallenkamp & Co. Ltd., UK) for 20 s. Samples were then boiled at 100 °C for 5 min, and cooled to RT on the bench before measuring the absorbance at 530 nm by a Unicam SP1800 Ultraviolet Spectrophotometer (PYE Unicam). Assays were carried out on fractions from control cultures as well as those grown overnight in 5mM DFMO. Substrate concentrations were varied and the assays conducted in order to produce a Michaelis-Menten plot. K_M and V_{max} values were then determined from a Lineweaver-Burk plot. (Yarlett *et al.*, 1994).

Arginine Deiminase Reaction in *T. vaginalis*

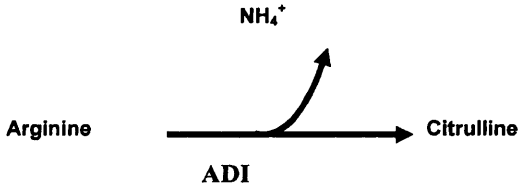

Figure 2.2: Arginine catabolism to citrulline via the actions of arginine deiminase.

2.14 Ornithine carbamyltransferase (OCT) assay. A 1ml assay (Fig 2.3) was carried out containing the following: 10mM ornithine, 10mM carbamyl phosphate, 0.1mg protein, 0.1M Tris, pH 8. Reactions were incubated at 25 °C for 5, 10, and 15 min, after which they were stopped with 100 µl of 7.5% TCA. Samples were developed using the method described by Boyd & Rahmatulah (1980), as described above. Absorbance was measured at 530nm, using 1ml cuvettes with a 1 cm path length, by a Unicam SP1800 Ultraviolet Spectrophotometer (PYE Unicam). Assays were carried out on fractions from control cultures as well as those grown overnight in 5mM DFMO. Substrate concentrations were varied and the assays conducted in order to produce a Michaelis-Menten plot. K_M and V_{max} values were then determined from a Lineweaver-Burk plot.

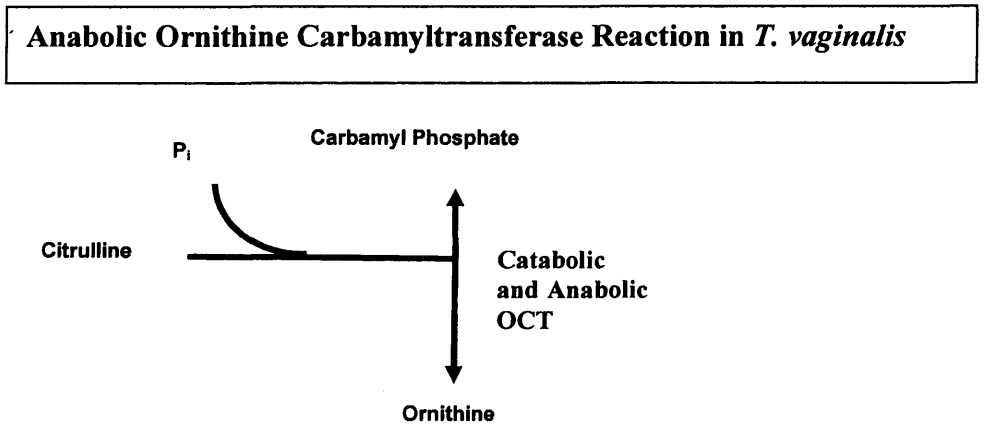

Figure 2.3: Conversion of citrulline to carbamyl phosphate and ornithine via the actions of ornithine carbamyl transferase. The assay used in this study, however,

measured the activity of anabolic OCT, and therefore measured the amount of citrulline produced.

2.15 Oxygen consumption measurements. Harvested organisms, after growth in the presence or absence of DFMO, were injected into a 2ml Clark oxygen electrode closed reaction vessel at 37 °C, containing 1.9ml of Doran's Buffer. Endogenous rates of oxygen consumption were measured, followed by those supported by 5mM malate. Organisms were counted using a haemocytometer for calculations of specific oxygen consumption rates.

2.16 NO-synthase assay. Harvested organisms were broken open by freezing and thawing the organisms three times to yield a homogenate. Assays were conducted on the homogenates to optimize the procedure. Once the procedure had been optimized, new cultures were harvested and a subcellular fractionation was conducted on both *G. intestinalis* and *T. vaginalis*, according to the protocols above, to determine the location of the NOS. The assay was done according to the protocol already published (Fernandez-Cancio *et al.*, 2001). The 1 ml assay contained the following: 0.1mM L-arginine, 1μM NADPH, 0.5mM $FADH_2$, 0.5mM $FMNH_2$, 0.5mM BH4, 0.5mM EDTA, 1.2mM $CaCl_2$, 0.5mM $MgCl_2$, 0.2 units nitrate reductase, 0.5mM glucose-6-phosphate, 0.4 units G-6-phosphate dehydrogenase, and the cell extract which contained 0.5 mg protein. The mixture was incubated at 37 °C for 1 h. The reaction was then stopped by adding 100μl of 0.5M HCl.

$$NO_3^- + NADPH + H^+ \longrightarrow NO_2^- + NADP^+ + H_2O$$

Figure 2.4: NOS activity was determined by measuring the amount of NO_2^- formed.

Since NADPH and $NAPD^+$ have been shown to interfere with the Griess reaction, the use of a small amount of NADPH was necessary, in addition to glucose-6-phosphate dehydrogenase to recycle the NADPH, thereby making the Griess reaction more effective.

The amount of nitrite formed (Fig 2.4) was then detected by the Griess method (Green *et al.*, 1982). The Griess Reagent consists of 1 part 0.1% napthylethylenediamine dihydrochloride in distilled water, and 1 part 1% sulfanilamide, in 5% concentrated phosphoric acid; the two parts must be mixed together within 12 h and kept at 4 °C. Enzyme assay samples were incubated 1:1 with Griess reagent for 15 min before the absorbance at 540 nm was measured using a Unicam SP1800 Ultraviolet Spectrophotometer (PYE Unicam).

2.17 Preparation of *G. intestinalis* for detection by NO electrode.

2.17a. Harvesting whole organism *G. intestinalis*. Tubes were incubated on ice for 20 min, after which they were gently shaken to resuspend adherent organisms in media. A culture of intact *G. intestinalis*, was harvested at 1000 x g for 10 min in a Beckman Coulter Avanti J-E centrifuge (Fullerton, California, USA) at 4 °C. Cells were washed with Doran's Buffer: 30mM Na_3PO_4, 74mM NaCl, 0.6mM $CaCl_2$, and 1.6mM KCl, pH 6.2.

2.17b. Mitochondria-like organelle isolation from *G. intestinalis*. All procedures were carried out at 4 °C. Cultures of *G. intestinalis* were harvested at 1,000 x g for 10 min in a Beckman Coulter Avanti J-E centrifuge (Fullerton, California, USA). The organisms were washed and resuspended in a buffer

containing 250mM sucrose, 50mM Tris-HCl pH 7, 10mM β–mercaptoethanol. Disruption was carried out using a Braun MSK cell disintegrator with acid-washed glass beads (400μm diameter) for 20 s at 2,000Hz. The homogenate was centrifuged at 1,000 x g for 10 min to remove unbroken cells, nuclei, and membrane fragments. The supernatant was then centrifuged at 10,000 x g for 10 min to give the mitochodria-like organelle-enriched large granular fraction. The pellet was resuspended in approximately 200μl of 250mM Sucrose, 50mM Tris-HCl, pH 7 (de Duve & Berthet, 1953; de Duve, 1964; Ellis *et al.*, 1993).

2.18 Monitoring NO production. An Iso-NO Isolated Nitric Oxide Meter connected to an NO electrode (World Precision Instruments, Florida, USA) was used to detect the production of NO. A Clark Oxygen Electrode was used to monitor oxygen consumption simultaneously. The temperature was held at 37 °C by thermostatically maintained water which was circulated around the reaction vessel. Stirring was at a constant rate of 150 rev min^{-1}. In the case of hydrogenosomes, 2ml of buffer containing 250mM sucrose, 50mM Tris-HCl, pH 7, was added to the reaction vessel. In the case of whole organisms, 2ml of Doran's Buffer was added to the reaction vessel: 30mM Na_3PO_4, 74mM NaCl, 0.6mM $CaCl_2$, and 1.6mM KCl, pH 6.2. In both cases, the sample was then injected into the reaction vessel and the gas output monitored on a chart recorder. Subsequently, in both cases, varying concentrations of arginine, L-NAME, and L-NNA were injected into the reaction vessel. Calibration was carried out by adding known amounts of NO-saturated buffer to 2mL of buffer.

2.19 Production of NO-saturated buffer. A closed reaction train set up for the production of nitric oxide (NO) was purged with nitrogen for 30 min. A saturated sodium nitrite solution was added dropwise from a funnel into concentrated sulfuric acid, which was constantly stirring. The NO generated was passed through a series of four Drechsel bottles with sintered glass bubblers: the first two contained 10M NaOH to absorb any acid, while the second two contained distilled water to wash the NO. The NO was bubbled through a syringe into a container containing buffer, sealed with a Suba-Seal closure with a turnover rubber flange (Merck Ltd., Poole). The NO was bubbled into the solution until it was saturated which, from calibration experiments, was known to be complete in 30 min for 10 ml of buffer. Once the solution was saturated, samples of the NO-saturated solution were removed by a Hamilton syringe within one day of the solution's production. The solution was stored at 4 °C. Saturated NO solution concentrations for various temperatures were noted from published tables, and NO concentration at RT was found to be 1.85mM.

2.20 Lipid analysis. Lipids were extracted by a modified Folch method as described by Garbus *et al.* (1963). Polar lipids were separated by two-dimensional TLC on 10 x 10 cm silica gel G plates using chloroform/methanol/water (65:25:4,by vol.) in the first dimension and then chloroform/acetone/methanol/acetic acid/water (50:20:10:10:5, by vol.) in the second direction. Plates were sprayed with 0.05% (wt/vol) 8-anilino-4-naphthosulphonic acid in methanol and viewed under U.V. light to reveal lipids or visualized under iodine vapor. Identification was made by reference to authentic standards and confirmed using specific color reagents (Kates, 1986). Lipids containing phosphorus were identified by using Zinzade's reagent,

which contains phospholipase DM. This reacted with phospholipids (i.e. those lipids containing phosphorus) to produce a primary or secondary alcohol derivative. Dragendorff reagent was used to detect alkaloids and other nitrogen compounds. The presence of amino groups was detected with the aid of a ninhydrin spray.

2.21 Fatty acid analysis. Fatty acid methyl esters (FAMEs) were prepared by transmethylation with 2.5% H_2SO_4 in dry methanol/toluene (2:1, by vol). Profiles of the fatty acid of individual lipids were determined using a Clarus 500 gas chromatograph with a flame ionising detector (FID) (Perkin-Elmer 8500, Norwalk, Connecticut). It was fitted with a 30m x 0.25mm i.d. capillary column (Elite 225, Perkin Elmer). The oven temperature was programmed as follows: 170°C for 3 min, then heated to 220°C at 4°C/min, and heated at 220°C for 15 min. The carrier was nitrogen at a flow rate of 20 ml/min. Sample (3µl) was injected, and a split ratio of 20:1 was employed. FAMEs were identified by comparing retention times with those of FA standards (Nu-Chek Prep. Inc., Elysian, USA). Quantification was made by reference to an internal standard of pentadecanoate (All GC work was performed by Irina Guschina in the laboratory of John Harwood).

2.22 Electrospray ionization mass spectrometry (ESI-MS). For the structural identification, individual lipid classes separated by TLC were eluted from silica gel and analyzed by using both the single stage MS mode and the tandem MS mode. ESI-MS was performed with a quadrupole instrument (Finnigan –Navigator. Model ISO 9001). All samples were appropriately diluted in 1:1 chloroform/methanol prior to direct infusion into the ESI chamber using a syringe pump at a flow rate of 100 µL/min. Lipids were directly ionized in negative or positive mode by ESI source.

The nebulizing gas (N_2) pressure was 100 psi, and the drying gas (N_2) flow and temperature were 300 L/h and 120 °C, respectively. A mass/charge (*m/z*) range from *m/z* 100-1600 was acquired. The data were processed into chromatograms using Xcalibur software (ThermoFinnigan).

2.23 Tandem mass spectrometry (ESI-MS/MS). Electrospray MS/MS data were obtained on a Q-Trap instrument (Applied Biosystems 4000 Q-Trap) operating in the negative mode. Lipid extracts were diluted in 1:1 chloroform/methanol and introduced at 10 µl/min in methanol using a Hamilton syringe. All scans were executed using an ionspray voltage of –4500 V and a declustering potential of –140 V. Q1 scans were performed scanning a mass range of 600-1000 amu over 4 sec, with 20 scans acquired and averaged. MS/MS scans using the ion trap mode of the Q-Trap were run at a scan rate of 1000 amu/sec with collision energies of –50 and –60V, and a linear ion trap (LIT) fill time of 150 msec with Q0 trapping enabled. Again 20 scans were acquired and averaged. The spectrograms were analyzed using the software Analyst 1.4.1. (Work done in collaboration with Irina Guschina and Michael O'Reilly).

CHAPTER 3

Effects of Polyamine Depletion by Difluoromethylornithine on Hydrogenosomes in *Trichomonas vaginalis*

3.1 Summary.

The correlation between polyamine metabolism and the hydrogenosomes in *Trichomonas vaginalis* was examined using four methods. When examined by confocal microscopy, in organisms stained with 5 μM Rhodamine123, morphological clarity of the hydrogenosomes was lost due to a decrease in membrane potential after *T. vaginalis* was exposed overnight to 5mM difluoromethylornithine (DFMO); this compound arrests polyamine synthesis. When examining hydrogenosome samples prepared for transmission electron microscopy, those from organisms grown overnight in 5 mM DFMO contained more electron-dense inclusions inside the hydrogenosomes than controls. Using flow cytometry, a decrease in fluorescence of polyamine-depleted cultures stained with 0.5 nM tetramethylrhodamine ethyl ester (TMRE) was observed in whole organisms as well as less $DioC_6(3)$ uptake in isolated hydrogenosomes from polyamine-depleted cultures when compared with controls. Thus, since fluorophore uptake correlates with trans-membrane electrochemical potentials, the hydrogenosomal and plasma membrane potentials decreased after arresting polyamine synthesis. Upon exposing these polyamine-depleted cells to 5 mM spermine or 5 mM spermidine for 7h in starvation buffer the fluorescence, as measured by flow cytometry, recovered. Further, the rate of oxygen consumption by polyamine-depleted hydrogenosomes was approximately two times greater than the rate of consumption by those from controls. From this it may be concluded that the depletion of polyamines using DFMO disturbs hydrogenosomal structure and function.

3.2. Introduction.

The arginine dihydrolase pathway in *T. vaginalis* provides these amitochondrial parasites with a second important source of energy (Fig 1.7). Difluoromethylornithine (DFMO), an analog of ornithine and an irreversible competitive inhibitor of ODC (Bitonti *et al.*, 1985), is known to deplete the supply of polyamines to the parasite (North *et al.*, 1986). According to published work, inhibition of the polyamine pathway prevents the export of putrescine and therefore also the uptake of spermine. Thus, spermidine synthesis is also arrested. This energy-generation associated with the arginine dihydrolase pathway and the closely coupled polyamine metabolic pathway is of great importance in an organism where substrate-level phosphorylation is its only means of producing ATP. Evidence for the degenerative effects of polyamine depletion by DFMO was obtained from a study in which mitochondrial structure was adversely affected in rat brain tumor cells *in vitro* (Oreddson *et al.*, 1983). Similar structurally degenerative effects on hydrogenosomes have been obtained after exposing *Tritrichomonas foetus* to the putrescine analog 1,4-diamino-2-butanone (DAB), another inhibitor of polyamine synthesis (Reis *et al.*, 1999).

Polyamines play a role in maintaining transmembrane electrochemical potentials, which stems from the electrogenic consequences of their transport across membranes. When the pathway is fully functional, these charged molecules are constantly transported through both the plasma membrane and the hydrogenosomal membrane (Yarlett *et al.*, 1996, 2000). If transport of these charged molecules is diminished, as is the case with DFMO-grown cells where ornithine decarboxylase has been inhibited, the pathway flux is decreased. In the absence of this charge balancing, the charge difference affects the organism's membrane potential.

In this study, the aim was to determine how the depletion of polyamines in *T. vaginalis* by

DFMO affected: the ultrastructure as revealed by electron microscopy, bioenergetic function of the hydrogenosome as observed by confocal microscopy, and changes in transelectrochemical potential as observed by flow cytometry (Mason *et al.*, 1995) using the membrane potential-sensitive fluorescent dyes tetramethylrhodamine ethyl ester (TMRE) and $Dio(C_6)_3$.

3.3. Results.

3.3a. Transmission electron microscopy.

Ultrastructural differences between *T. vaginalis* grown in the presence and absence of DFMO were observed in electron micrographs of thin sections (Fig. 3.1). Numerous electron-dense granules were observed surrounding and within the hydrogenosomes, with some appearing between the inner and outer membranes, in organisms grown overnight with 5mM DFMO (Fig 3.1a,c,e,g). These electron-dense granules were not observed in the same frequency in samples from cultures that had been grown without DFMO (Fig 3.1b,d,f,i). These structural differences were even more evident after isolation of hydrogenosome-enriched fractions from organisms. The peripheral location of the electron-dense inclusions between the two membranes is clearly evident in the hydrogenosomes isolated from the DFMO-grown sample (Fig 3.1e,i). In the hydrogenosomes isolated from control cultures, these electron-dense granules are much less frequent (Fig 3.1d,h).

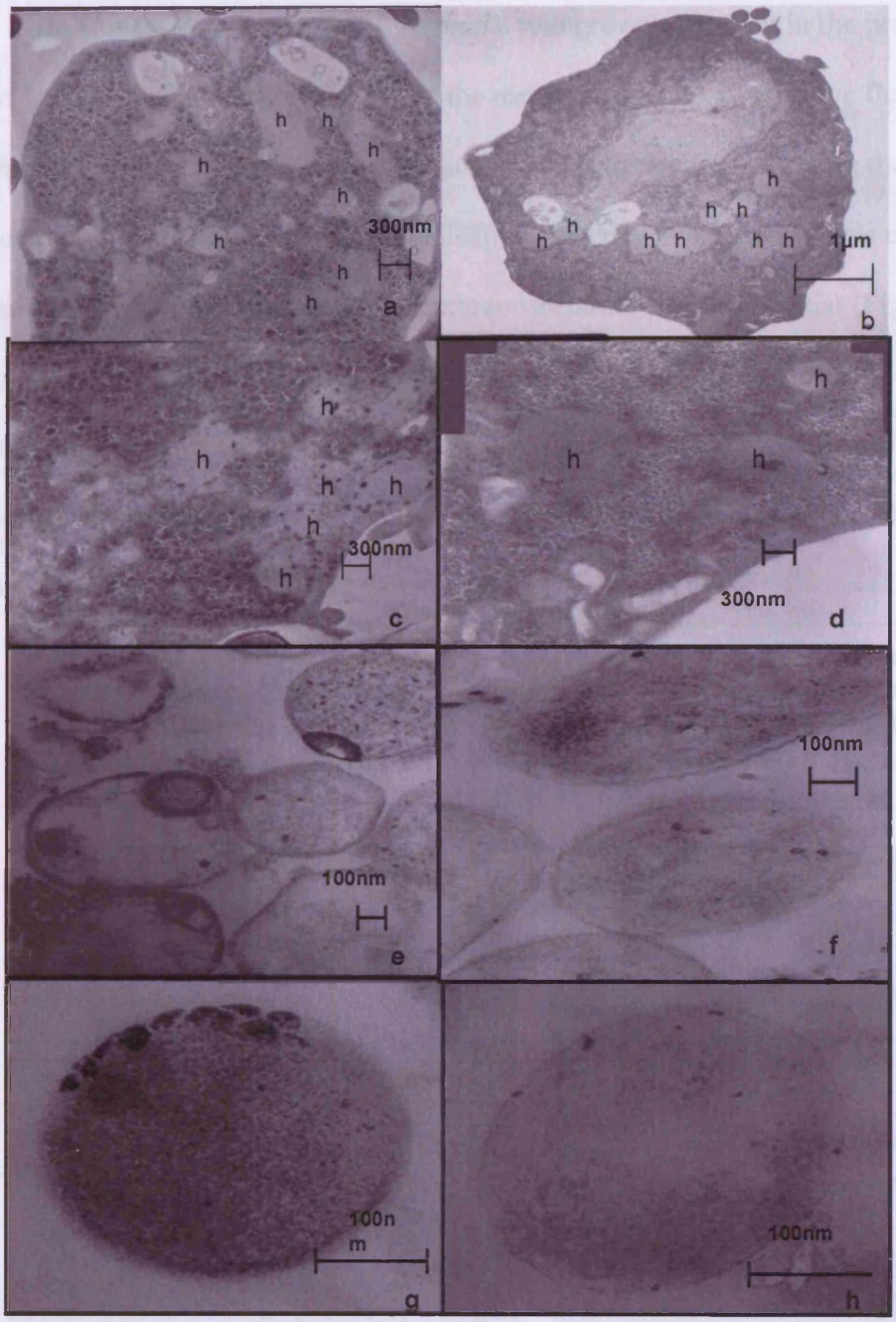

Figure 3.1: Transmission electron microscopy sections of *T. vaginalis*. Organisms grown overnight with 5mM DFMO: a, c, e & g (left column). Cultures grown without DFMO: b, d, f & i (right column). Top two rows (a, b, c & d) are sections from whole organisms. Hydrogenosomes are denoted with ah 'h'. Bottom two rows are isolated hydrogenosomes (e, f, g, & h). Note the different scales in each picture.

3.3b. Confocal microscopy. *T. vaginalis* was grown overnight in the presence or absence of 5mM DFMO, then stained with 5μM of the membrane potential-sensitive fluorophore Rhodamine123 (Fig 3.2). In the control organism, the hydrogenosomes were the most intensely fluorescent of the intracellular features, indicating the extensive uptake of this cationic lipophilic dye into organelles with a normal transmembrane electrochemical potential (Fig 3.2a). However, hydrogenosomes within the organisms grown overnight in DFMO were hardly visible, as Rhodamine123 was not accumulated within these organelles (Fig. 3.2b). In both cases, fluorescence was also observed within the nucleus. Within the DFMO-grown trichomonads, this intensity was greater.

Figure 3.2: *T. vaginalis*, stained with 5μM Rhodamine 123, viewed under the confocal microscope. a. one *T. vaginalis* organism grown overnight in tryptose/yeast/maltose medium (TYM). Note the intense areas of fluorescence, which are hydrogenosomes. b. one *T. vaginalis* organism grown overnight in TYM with 5mM difluoromethylornithine (DFMO).

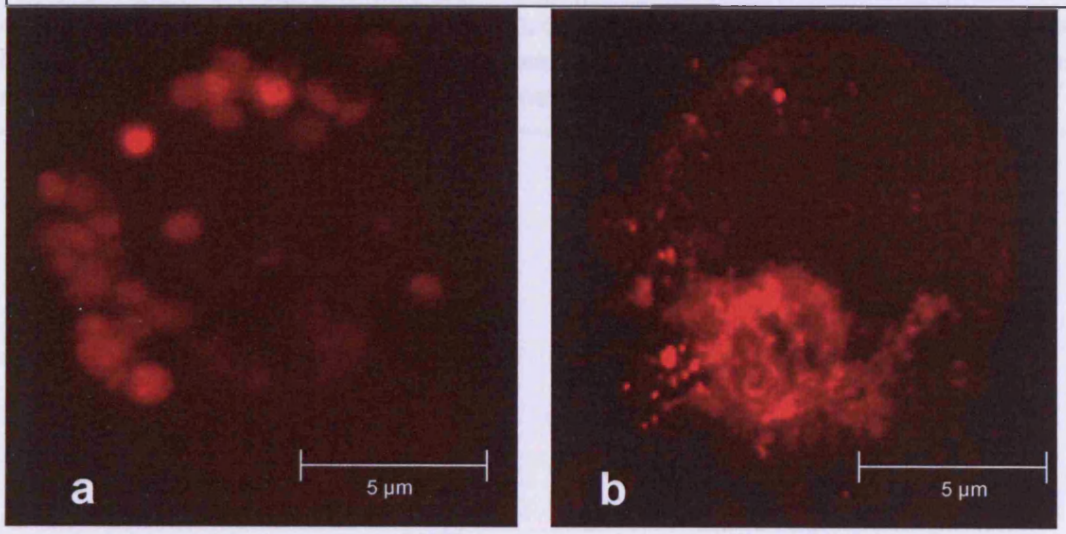

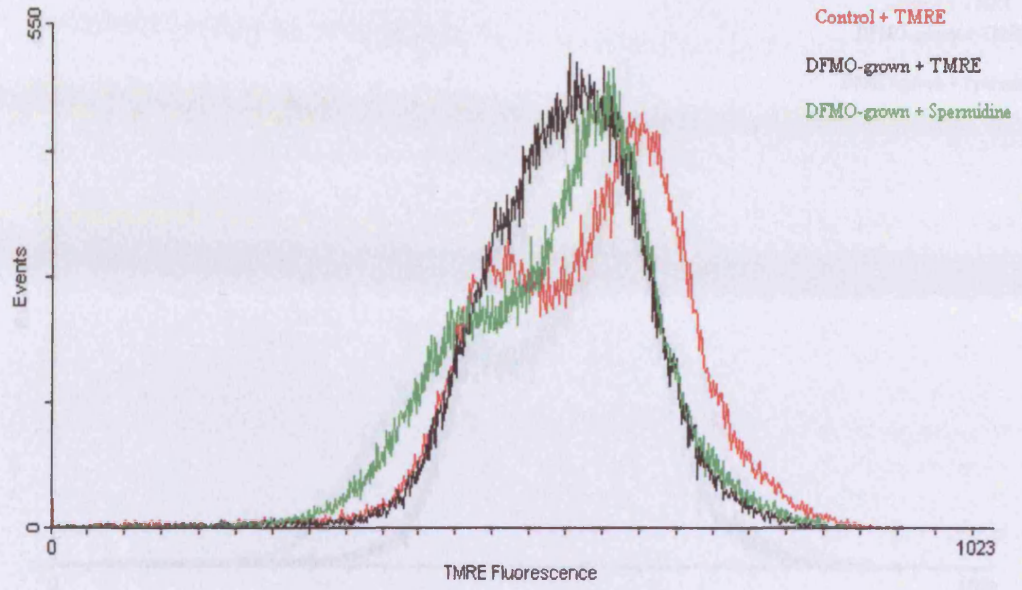

Figure 3.3: Flow cytometry histogram from cultures of *T. vaginalis*: control and difluoromethylornithing (DFMO)-grown cultures with 0.5nM tetramethylrhodamine ethyl ester (TMRE), DFMO-grown cultures incubated with 5mM spermidine, then loaded with TMRE. The y axis represents the number of individual organisms analyzed. The x axis is the fluorescence emission in from 500-700nm.

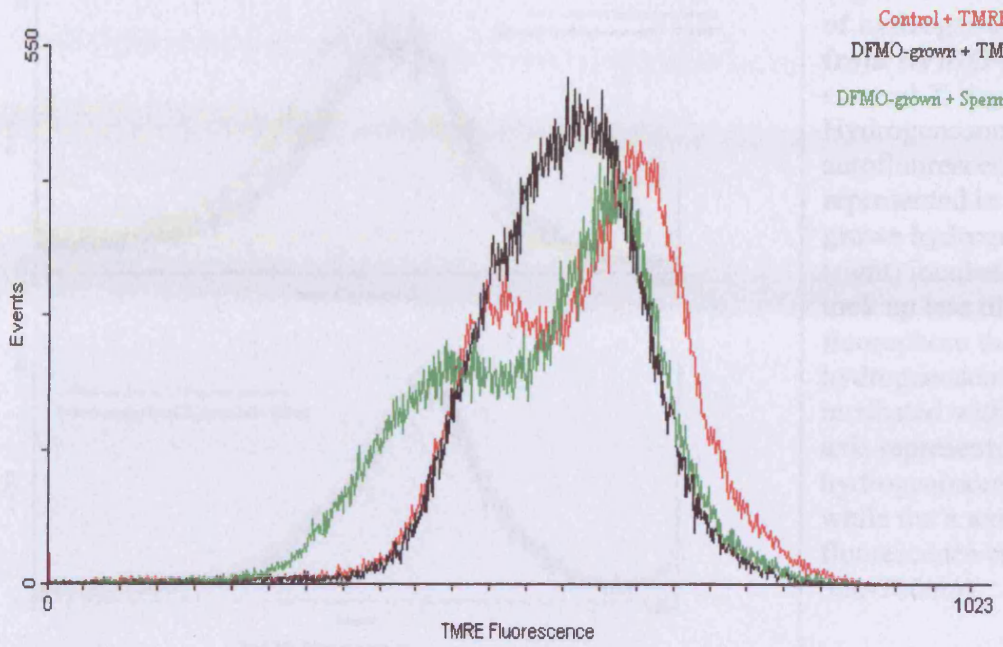

Figure 3.4: Flow cytometry histogram of cultures of *T. vaginalis*: control and difluoromethylornithing (DFMO)-grown cultures with 0.5nM tetramethylrhodamine ethyl ester (TMRE), DFMO-grown cultures incubated with 5mM arginine, then loaded with TMRE. The y axis represents the number of individual organisms analyzed. The x axis is the fluorescence emission in from 500-700nm.

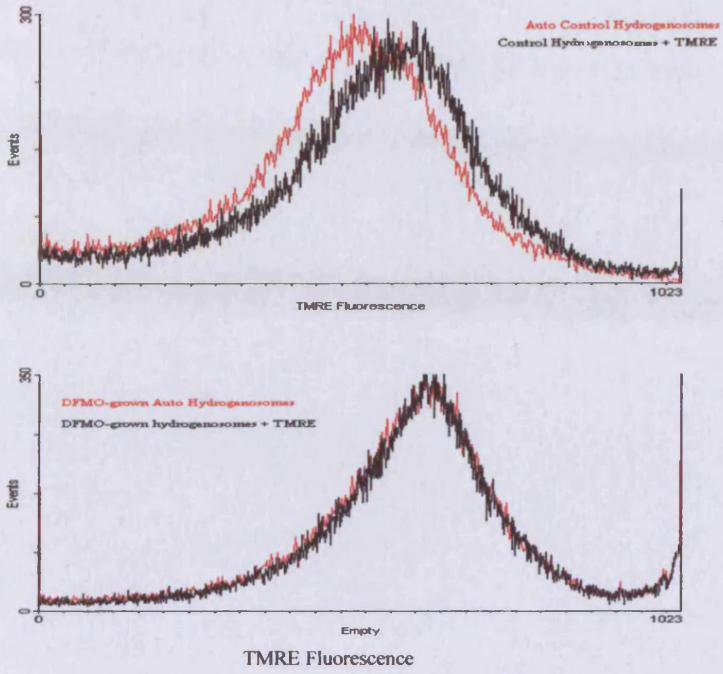

Figure 3.5: Flow cytometry of hydrogenosomes isolated from DFMO-grown vs. control *T. vaginalis*. Hydrogenosome autofluorescence is represented in red. DFMO-grown hydrogenosomes (right) incubated with TMRE took up less of the fluorophore than control hydrogenosomes (left) also incubated with TMRE. The y axis represents the number of hydrogenosomes analyzed, while the x axis represents the fluorescence emitted (between 500-700nm).

3.3c. Flow cytometry. The uptake of both voltage-sensitive dyes, and therefore the intensity of fluorescence of organisms from DFMO-grown cultures, was less than that of control cultures (Figs 3.4 & 3.4) (Lloyd & Hayes, 1995; Humphreys et al., 1994a). Organisms grown overnight in the presence or absence of 5 mM DFMO were incubated for 7 h at room temperature in Doran's buffer without the inhibitor, then loaded with TMRE. When loaded with TMRE, cultures grown overnight in DFMO exhibited a lower distribution of fluorescence than was the case in control organisms (compare Fig 3.3a & 3.3c). After DFMO-grown cultures were incubated in Doran's buffer containing 5 mM spermine for 7 h, increased accumulation of the membrane potential-sensitive dyes occurred (Fig 3.3b), indicating that the transmembrane electrochemical potentials had recovered inhibitor-treated organisms. The DFMO-grown cells, after exposure to 5 mM spermine in Doran's during the 7 h incubation, showed recovery of

fluorescence intensity distributions and therefore membrane potential-mediated fluorophore accumulation. When DFMO-grown cells were incubated with 5 mM spermidine (Fig 3.3d; Fig 3.4), the recovery of membrane potential was slightly less than the cultures incubated with spermine. On the other hand, samples grown in the presence of DFMO which were incubated with 5 mM arginine or 5 mM putrescine for 7 h prior to being assessed by flow cytometry (data not shown), did not show any membrane potential recovery.

When loaded with Dio(C_6)$_3$ (Fig 3.5), hydrogenosomes isolated from organisms grown in the presence of DFMO take up less of the fluorophore than control hydrogenosomes also incubated with Dio(C_6)$_3$. Since membrane potential correlates with fluorophore uptake, the membrane potential of hydrogenosomes isolated from DFMO-grown organisms was less than that of control hydrogenosomes.

Table 3.1: Mean of Oxygen Consumption of Isolated Hydrogenosomes from *T. vaginalis*

	Endogenous	**Malate-supported**	**Malate-supported minus endogenous**
DFMO-grown * (n=15)	**93.4 (± 17.9)**	**740 ± (127)**	**647 ± (123)**
CONTROL * (n=11)	**64 ± (7.42)**	**304 ± (47.5)**	**240 ± (48.0)**

*** nmoles/min/mg protein ± (Standard Deviation)**

3.3d. Oxygen consumption measurements. The rates of oxygen consumption by hydrogenosomes isolated from cultures grown overnight in 5 mM DFMO had significantly higher rates of oxygen consumption than hydrogenosomes isolated from control cultures (Table 3.1).

3.4. Discussion.

Polyamine depletion of *T. foetus* by the putrescine analog 1,4-diamino-2-butanone (DAB)

was previously observed to adversely affect hydrogenosomal structure (Reis *et al.*, 1999). The changes in ultrastructure of the hydrogenosomes in *T. vaginalis* by DFMO shown in Figs 3.2 and 3.3 provide further evidence of the importance of the polyamine metabolic pathway to maintaining the healthy hydrogenosome. The decrease in the intensity of fluorescence of Rhodamine123 accumulated within hydrogenosomes, viewed by confocal microscopy after growth overnight in 5 mM DFMO, indicates a decrease in the hydrogenosomal membrane potential upon exposure to the drug. This phenomenon is easily explained; arresting a pathway responsible for transporting cationic molecules across both the plasma membrane and the hydrogenosomal membranes was likely to affect these organelles' membrane potentials (Yarlett *et al.*, 2000).

Based on the TEM images in Fig 3.2, hydrogenosomal structure was altered after growth in the presence of DFMO. The results are similar to those found in *T. foetus* upon depleting cellular contents of polyamines using the inhibitor DAB (Reis *et al.*, 1999). In the current study, electron-dense granules were observed inside and surrounding the hydrogenosomes in greater frequency in polyamine-depleted cultures than in cultures grown without DFMO. Membrane-associated inclusions of hydrogenosomes in *T. vaginalis* have previously been found to have high levels of Mg^{2+} and Ca^{2+} (Humphreys *et al.*, 1994b). This suggested that divalent cation accumulation by hydrogenosomes is important in the regulation of cytosolic ion concentrations (Chapman *et al.*, 1985). The electron-dense granules observed in the present work may be precipitates formed in part by Ca^{2+}, since calcium uptake may have been affected by polyamine depletion as a result of the blocking of ODC. Attempts made to determine the components of these inclusions using transmission electron microscopy were unsuccessful thus far.

The accumulation of the lipophilic cationic voltage-sensitive dye TMRE within

mitochondria increases as inner mitochondrial membrane potentials are increased (Scaduto & Grotyohann, 1999); since hydrogenosomes are evolved forms of mitochondria, their membrane should act similarly (Biagini *et al.*, 1997). The flow cytometry data (Figs 3.4-3.6) confirms the decrease of hydrogenosomal membrane potential of *T. vaginalis* organisms after growth in the presence of DFMO. Organisms from cultures incubated overnight in 5 mM DFMO, and subsequently loaded with TMRE in starvation buffer, had a decreased fluorescence compared with trophozoites grown in the absence of DFMO. This was true for both whole cell cultures (Figs 3.4 & 3.5) and isolated hydrogenosomes (Fig 3.6). I concluded that, as a result of the depletion of polyamines in *T. vaginalis*, hydrogenosomal membrane potentials decrease. The amount of fluorescence in whole cells that can be attributed to the plasma membrane potential is yet to be determined.

In *T. vaginalis* from DFMO-grown cultures, the reintroduction of spermine or spermidine gave an increased intensity of fluorescence when examined by flow cytometry, indicating some functional recovery of the membrane potential in whole cells (Figs 3.4 & 3.5). Recovery was slightly more pronounced after the introduction of spermine into the environment of the organism than was the case for spermidine. The spermine-spermidine interconversion is reversible, although the forward direction is kinetically favorable (Yarlett *et al.*, 2000). Thus, the introduction of spermidine would be expected to cause less recovery than the introduction of spermine. We conclude that polyamine synthesis is a process essential for the maintenance of physiologically active membrane potentials of the hydrogenosomal membranes in *T. vaginalis*.

Interestingly, the presence of an antiport has been postulated (Yarlett *et al.*, 2000), but evidence presented in this report suggests that such an antiport does not exist. If there had been an antiport, the spermine and spermidine should not have been able to travel into the organism

without the export of putrescine; due to the organism's treatment with DFMO, the putrescine production would have been significantly lower than under normal conditions and therefore would not have been present in the quantity needed to export via an antiport. Preliminary work suggests there is a cation-polyamine antiport which exports ammonium rather than putrescine.

In the case of the DFMO-grown cells that were exposed to arginine in starvation buffer, no recovery of membrane potential was observed. As previously stated, DFMO inhibits ODC; based on enzyme assays done (see Chapter 4; Section 4.3.d), the energy-producing arginine dihydrolase pathway was also affected. The enzyme activities of both arginine deiminase and carbamate kinase decreased significantly when organisms were grown overnight in the presence of 5 mM DFMO. Putrescine production and excretion would therefore proceed more slowly, and the charge difference between the inside and outside of the plasma membrane would be different from those under normal conditions. In the case of the cells that were exposed to putrescine, no recovery in fluorescence was seen after its introduction into the organism in starvation buffer. The role of putrescine in polyamine metabolism is minor when ODC has been inhibited, so it is not surprising that the addition of putrescine to the environment of the organism does not affect the membrane potential.

Hydrogenosomes isolated from cells grown in the presence of DFMO increased their endogenous rate of oxygen consumption by 50% (Table 3.1). The endogenous carbon source is from glycogen metabolism catalyzed by glycogen phosphorylase, to produce glucose-6-PO_4. This oxidation is dependent on NADH and NADPH oxidases (Tanabe, 1979). The addition of malate to hydrogenosomes causes a 2.7-fold increase of O_2 consumption in hydrogenosomes isolated from DFMO-treated cells. When malate is present the increased rates of oxygen consumption by hydrogenosomes confirm the need of the parasite to compensate for the loss of

ATP production by the polyamine pathway by increasing the rate of its energy-producing malate metabolism, a pathway which consumes oxygen. When ODC was inhibited, the polyamine pathway no longer consumed oxygen (a component of the spermine-spermidine conversion). Therefore, all of the oxygen consumption can be attributed to other pathways. DFMO-grown hydrogenosomes have an endogenous rate of oxygen consumption of approximately 1.5 times that of control hydrogenosomes. The significant increase in oxygen consumption by DFMO-grown hydrogenosomes is most likely a result of increased oxidation of NAD-NADH oxidase in the hydrogenosome. Within the DFMO-grown cells, the reliance on this pathway for ATP is greater than that of the control cells which are also capable of producing ATP through an intact polyamine metabolism. This data confirms the importance of the energy produced by the polyamine pathway to the parasite and therefore affirms the possibility of this pathway being used as a target for therapy.

When studying polyamine metabolism in *T. vaginalis* and its effects on the hydrogenosome, it is important to consider the energetic role of this pathway. When DFMO inhibited ODC, the energy-generating portion of the arginine dihydrolase pathway was adversely affected. The effects of inhibiting ODC with DFMO may extend even further and impact the pyruvate:ferredoxin oxidoreductase pathway, which also relies upon the hydrogenosome being fully-functional. Although these possibilities must be explored further to determine how far-reaching the effects of ODC inhibition proves to be within the organism, it is clear that utilizing DFMO as an inhibitor of polyamine synthesis prevents the hydrogenosome from being fully-functional.

CHAPTER 4: Effects of Difluoromethylornithine on the Arginine Dihydrolase Pathway in *Trichomonas vaginalis*

4.1 Summary.

Trichomonas vaginalis, the eukaryotic microaerophilic parasite of the human urogenital tract, has a unique bioenergetic metabolism. This organism is auxotrophic for spermine as it lacks the enzymes for the synthesis of higher polyamines; the organism therefore obtains spermine from the host. This process is driven, and putrescine biosynthesis carried out, by the energy-generating arginine dihydrolase pathway linked to the spermine:spermidine acetyl transferase:polyamine oxidase (SSAT-PAO) pathway. By using subcellular fractionation techniques, 70% of carbamate kinase activity was localized to the hydrogenosome-rich large granular fraction, while 83% of the arginine deiminase activity was found in the small granular fraction. Further evidence from this study suggests carbamate kinase is associated with the hydrogenosomal membrane. For arginine deiminase: the apparent V_{max} was 1.45 x 10^{-5} moles/L/min, apparent K_M was 1.86 x 10^{-6} moles/L and the specific activity was 7.5μmol/mg protein/min. For carbamate kinase: the apparent V_{max} was 1.13 x 10^{-6} moles/L/min, the apparent K_M 7.04 x 10^{-6} moles/L, and the specific activity 145 nmoles/mg protein/min. Ornithine carbamyl transferase (OCT) was cytosolic (49%); the apparent K_M was 1.23 x 10^{-6} moles/L , the apparent V_{max} was 8.17 x 10^{-6} moles/L/min, and the specific activity was 12μmoles/mg protein/min. Cultures of *Trichomonas vaginalis* grown in the presence of 5mM DFMO, an irreversible inhibitor of ornithine decarboxylase (ODC), displayed more than 50% decreased carbamate kinase and arginine deiminase enzyme activities, while the activity of anabolic ornithine carbamyl transferase increased by 42%. Polyamine depletion by DFMO disrupted the arginine dihydrolase pathway by affecting the activity of the enzymes involved.

4.2 Introduction.

The arginine dihydrolase pathway is one of the critical substrate-level ATP generating pathways used as an alternative to glucose metabolism in *Trichomonas vaginalis*. The putrescine formed by the arginine dihydrolase pathway is excreted from the cell as a byproduct of the pathway (Fig. 1.7) (Yarlett *et al.*, 1996). The polyamine pathway is estimated to contribute 10% of the parasite's energy requirements (Yarlett & Bacchi, 1994; Linstead & Cranshaw, 1983). Recent evidence has indicated that the pathway contributes a larger percentage of energy to the parasite's metabolism (Harris *et al.*, unpublished). The importance of this pathway *in situ* can also be inferred from the disappearance of arginine from the vaginal fluid of infected patients and the significant amount of putrescine produced (Yarlett, 1988). It has been discovered recently that the polyamine metabolism of *Trichomonas vaginalis* is linked to the ability of the organism to adhere to the host cell and stimulate cytotoxic effects (Garcia *et al.*, 2005).

Arginine is brought into the organism by a dedicated transporter where it is presumably transported across the hydrogenosomal membrane where is is deaminated to citrulline (Yarlett et al., 1994; 1996), and then phosphoryltically cleaved to ornithine and carbamyl phosphate (Fig 1.7). It is at this point the pathway splits, ornithine then being decarboxylated to form putrescine. This reaction links the arginine dihydrolase pathway to the spermidine:spermine acetyl transferase:polyamine pathway (Yarlett *et al.*, 2000). It has been stated that the putrescine: spermine antiport pumps out 2 molecules of putrescine for every one molecule of spermine that is selectively transported into the cell to balance the charge across the membrane (Yarlett *et al.*, 2000). The carbamyl phosphate generates ATP, NH_3^+ and bicarbonate by carbamate kinase (Lindstead & Cranshaw, 1983).

Previous studies of using subcellular fractionation techniques on *T. vaginalis* have localized carbamate kinase, ornithine carbamyl transferase and ornithine decarboxylase to the

cytosolic fraction, while the arginine deiminase was localized to the hydrogenosomal fraction (Yarlett *et al.*, 1994). In these previous studies the cells where disrupted by homogenization, which could have led to intracellular membrane damage. In the current study, the arginine deiminase and carbamate kinase were found to be hydrogenosomal while the ornithine carbamyltransferase was located in the cytosol.

4.3 Results.

4.3a. Marker enzyme assays to determine purity of fractions.

$NADP^+$-dependent malic enzyme activity was found in all the fractions; this was likely due to cytosolic contamination. The primary sediment, large granular and small granular fractions contained 26%, 13% and 20% of recovered activity, respectively (Fig 4.1), while the cytosolic fraction displayed 41% of the total activity.

To further check the validity of the cytosolic fraction lactate dehydrogenase (Ldh) asssays were conducted; more than 90% of Ldh activity was localized to the cytosolic fraction (Fig 4.1).

NAD^+-dependent malic enzyme activity was present within the large granular fraction (38%); however there was a large percentage of recovered activity in the small granular fraction, containing 35% recovered enzyme activity. The presence of this enzyme activity indicated that hydrogenosomes were also present within the small granular fraction.

Acid phosphatase activity, a marker for lysosomes, was found in the small granular fraction (68%) as expected (Fig 4.1). Small amounts of acid phosphatase activity were detected within the primary sediment and large granular fraction having 10% and 22% recovered enzymatic activity of acid phosphatase, respectively. No lysosomal enzymatic activity was found in the cytosolic fraction.

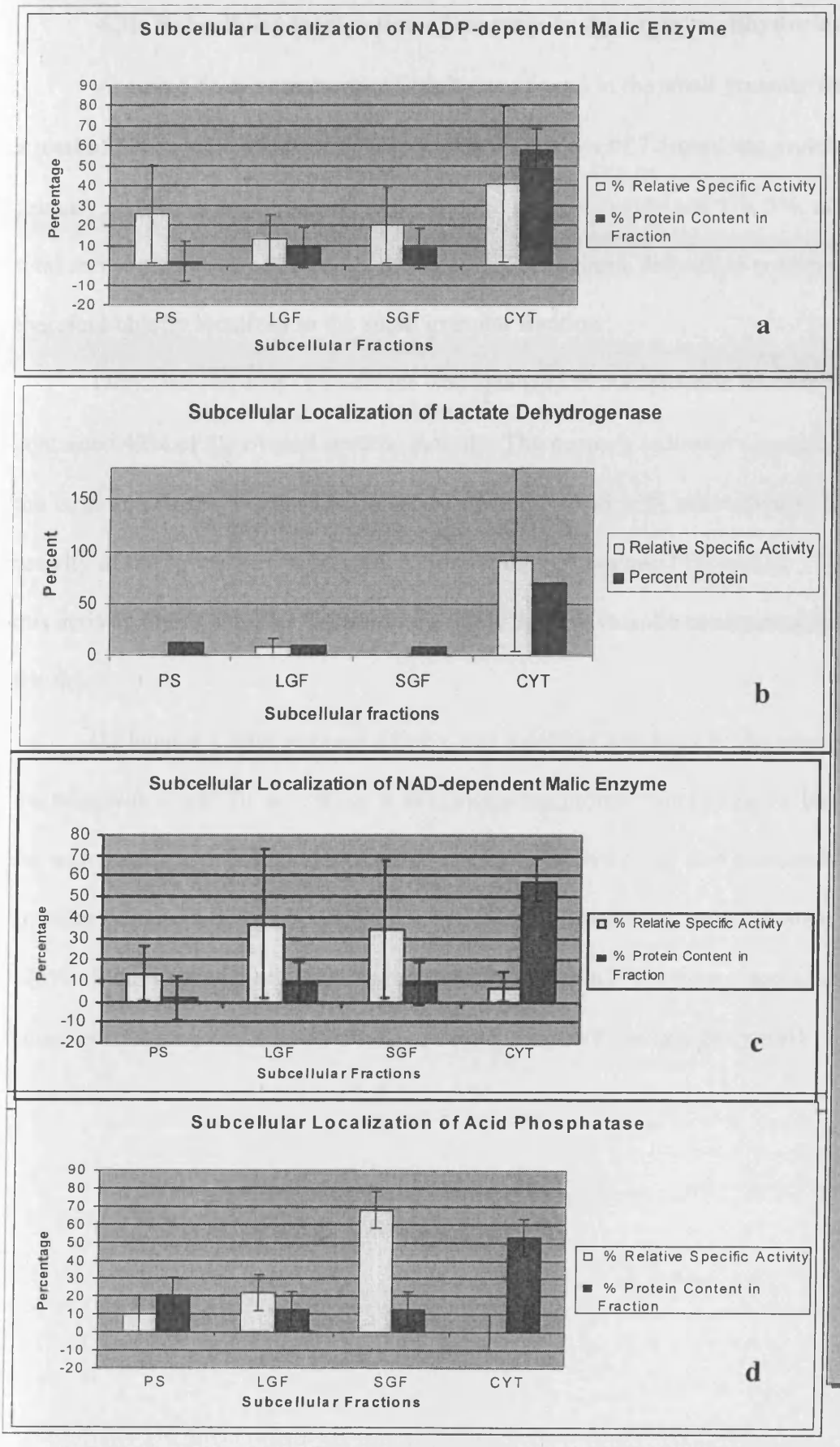

Figure 4.1. Subcellular localization of marker enzymes from *Trichomonas vaginalis* expressed as percentage of relative specific activity of each fraction. a. $NADP^+$-dependent malic enzyme (cytosolic marker). b. NAD^+-dependent malic enzyme (hydrogenosome marker). c. acid phosphatase (lysosomal marker) & d. lactate dehydrogenase (cytosolic marker), The results represent a typical experiment of triplicate repeats. The error bars display 95% confidence intervals. PS = primary sediment (contains whole cells, plasma and nuclear membranes), LGF = large granular fraction, SGF = small granular fraction, & CYT = non-sedimentable fraction.

4.3b. Subcellular localization of enzymes in the arginine dihydrolase pathway.

Arginine deiminase enzyme activity was found in the small granular fraction and had a total of 83% recovered activity with a specific activity of 7.5μmol/mg protein/min. The primary sediment, large granular and cytosolic fractions contained 5%, 5%, and 6% of the total recovered activity (Table 4.1 & Fig 4.2). The arginine deiminase enzyme activity was therefore chiefly localized to the small granular fraction.

Ornithine carbamyl transferase was localized to the cytosolic fraction (Fig 4.2), which contained 49% of the overall specific activity. The primary sediment contained 24%, while the large and small granular fractions contained 14% and 13%, respectively. The specific activity of the cytosolic fraction was 12μmole/mg protein/min (Table 4.2). The presence of this activity in the granular fractions was likely due to cytosolic contamination of these fractions.

Carbamate kinase enzyme activity was localized primarily to the large granular fraction, with a specific activity of 0.145μmoles/mg protein/min (Table 3), containing 70% of the recovered activity (Fig 4.2). A small amount of activity was also localized in the small granular fraction having a specific activity of 0.0533μmoles/mg protein/min and containing ~26% of the recovered activity. No significant (less than 5%) enzyme-specific carbamate kinase activity was recovered from the primary sediment fraction or cytosol.

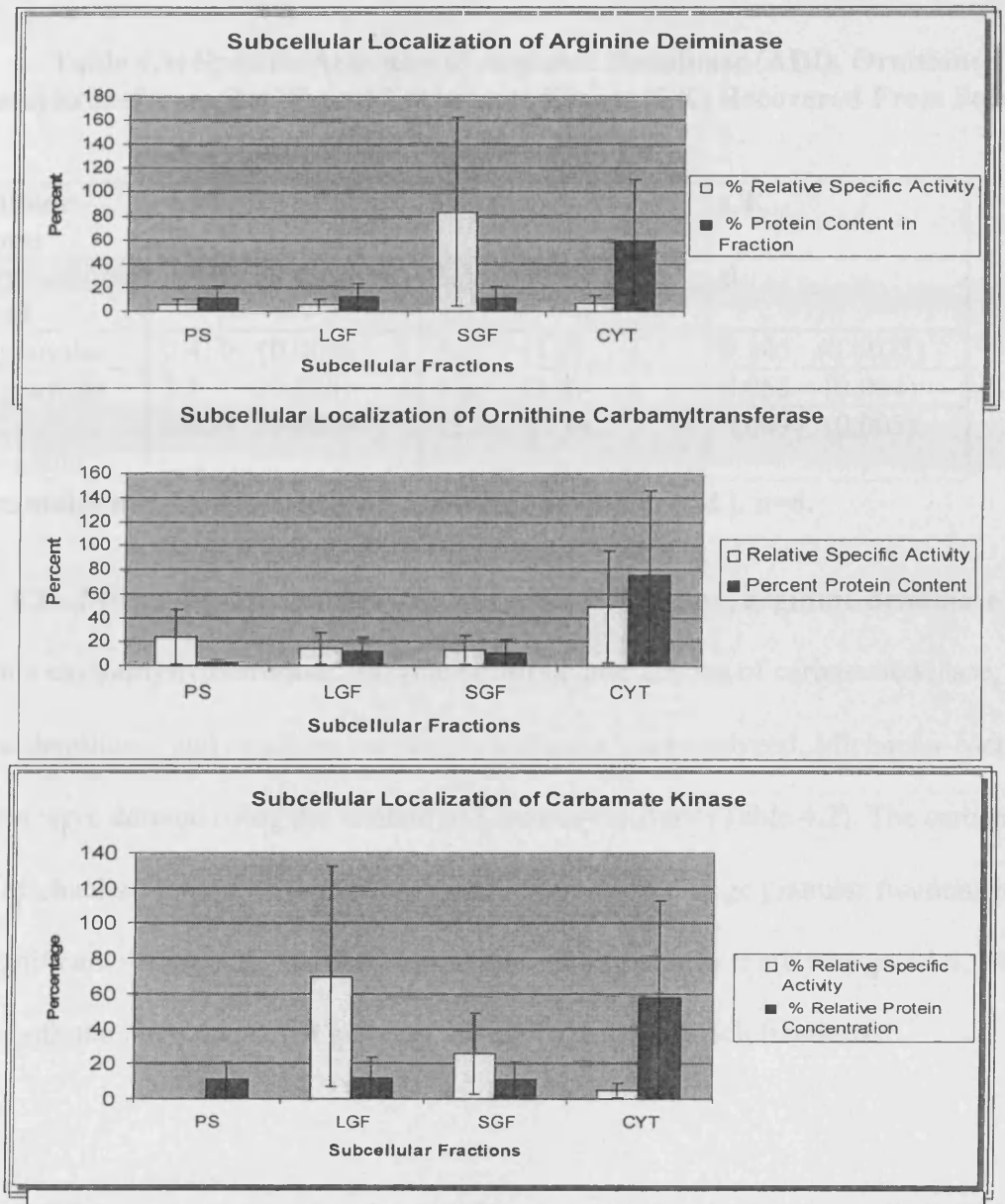

Figure 4.2. Subcellular localization of arginine deiminase, ornithine carbamyltransferase & carbamate kinase from *Trichomonas vaginalis*, expressed as a percentage of specific activity of each fraction. Experiments were repeated six times for each fraction. The error bars represent 95% confidence intervals. PS = primary sediment (contains whole cells, plasma and nuclear membranes), LGF = large granular fraction, SGF = small granular fraction, and CYT = non-sedimentable fraction.

Table 4.1: Specific Activities of Arginine Deiminase (ADI), Ornithine Carbamyltransferase (OCT) and Carbamate Kinase (CK) Recovered From Subcellular Fractions of *T. vaginalis* *

Subcellular Fractions	ADI	OCT	CK
Primary sediment	0.450 (0.003)	5.8 (0.34)	0
Large granular	0.450 (0.004)	3.5 (1.0)	0.145 (0.0025)
Small granular	7.5 (0.004)	3.2 (1.5)	0.053 (0.004)
Non-sedimentable	0.600 (0.003)	12.0 (1.9)	0.0097 (0.005)

***S.A.=μmoles/mg protein/min (+/-) standard deviation (s.d.). n=6.**

4.3c. Michaelis–Menten kinetics of carbamate kinase, arginine deiminase and ornithine carbamyltransferase. Enzyme-substrate interactions of carbamate kinase, arginine deiminase, and ornithine carbamyltransferase were analyzed. Michaelis–Menten constants were derived using the method of Lineweaver-Burk (Table 4.2). The carbamate kinase Michaelis-Menten values for both small granular and large granular fractions have little significant difference. For that reason, as well as the marker enzyme profiles, we believe both the large and small granular are hydrogenosome-rich fractions.

Table 4.2. Kinetics analysis of carbamate kinase, arginine deiminase, and ornithine carbamyltransferase apparent V_{max} and K_M were derived from Lineweaver–Burk Plots.

Enzyme	Apparent V_{max} (moles/L/min) x 10^{-6}	Apparent K_M (moles/L) x 10^{-6}
Arginine deiminase	0.145	1.86
Carbamate kinase : Large granular fraction	1.13	7.04
Carbamate kinase : Small granular fraction	1.46	16.0
Ornithine carbamyltransferase Cytosolic	8.17	1.23

4.3d. Analysis of the arginine dihydrolase pathway of DFMO treated

Trichomonas vaginalis. DFMO-treated *Trichomonas vaginalis* displayed the same pattern of subcellular enzyme distribution as observed in the untreated fractions for all three enzymes. However, the activity of carbamate kinase substantially decreased in all fractions, especially the large granular fraction where the enzyme was predominantly localized (Fig. 4.3). The specific activity of carbamate kinase recorded for the DMFO-treated large granular fraction (0.076 μmol/mg protein/min) reduced by half of that found for the control large granular fraction (0.16μmol/mg protein/min). A Student's T Test was carried out to compare the control carbamate kinase enzyme activity and the DFMO treated enzyme activity of carbamate kinase. The test confirmed that the difference between the specific activity of carbamate kinase in the DFMO-treated and the control fractions of *Trichomonas vaginalis* was significant (Table 4.3).

Trichomonas vaginalis grown in the presence of 5mM DFMO also displayed a significant decrease in arginine deiminase activity (Fig 4.3) within the small granular fraction; specific activity was reduced by 2 and a half-fold (3μmol/mg protein/min) compared to the specific activity within the small granular fraction of the untreated control (7.5μmol/mg protein/min). A Students T Test confirmed that the decrease in activity of the treated small granular fraction and cytosol compared to the untreated fractions was significant (Table 4.4).

The effect of DFMO on the activity of the ornithine carbamyl transferase enzyme was quite different from the other two enzymes of the arginine dihydrolase pathway. In subcellular fractions obtained from *T. vaginalis* grown overnight in 5mM DFMO, the activity of OCT increased (Fig. 4.3).

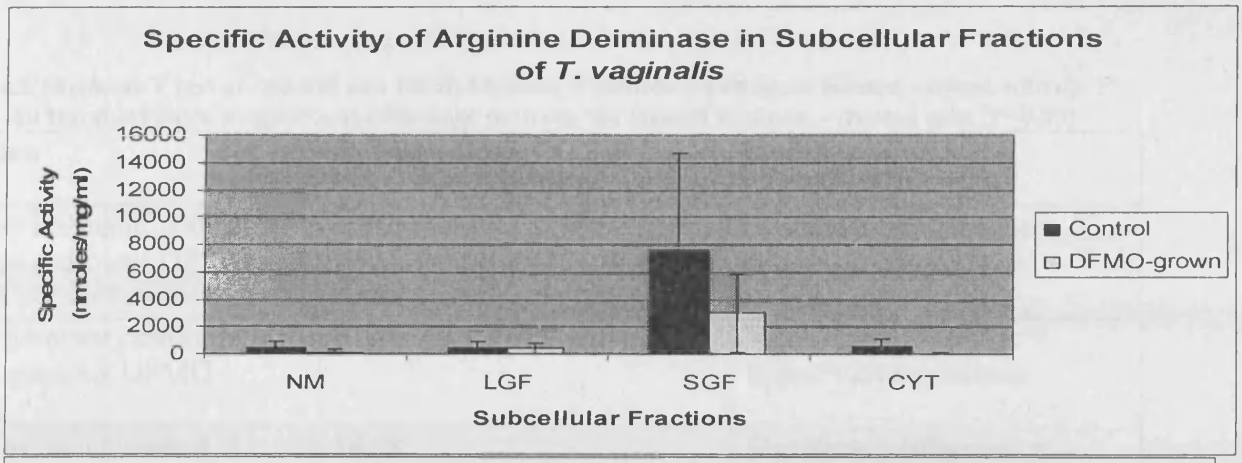

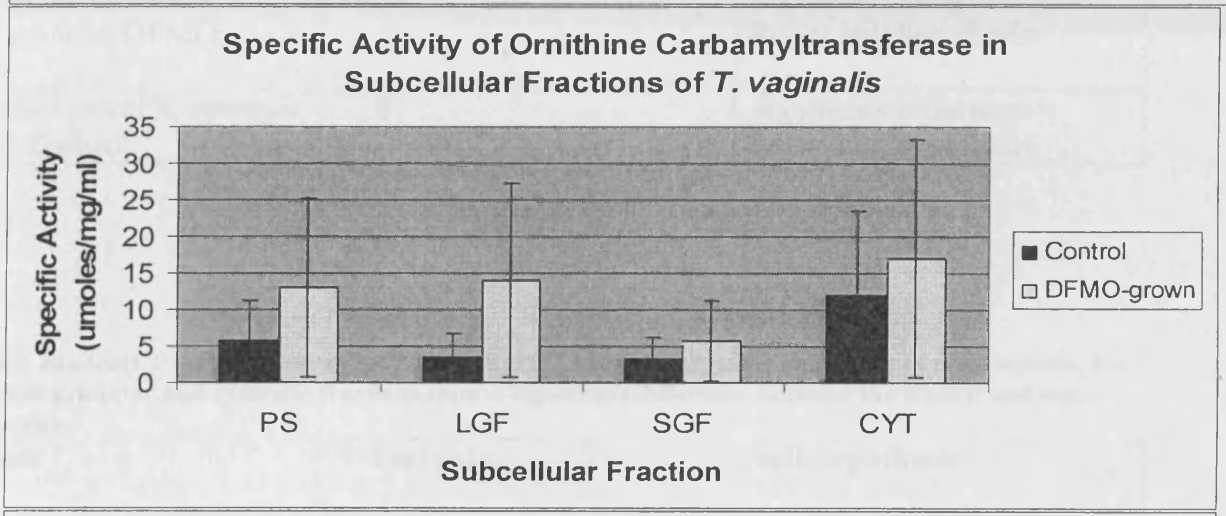

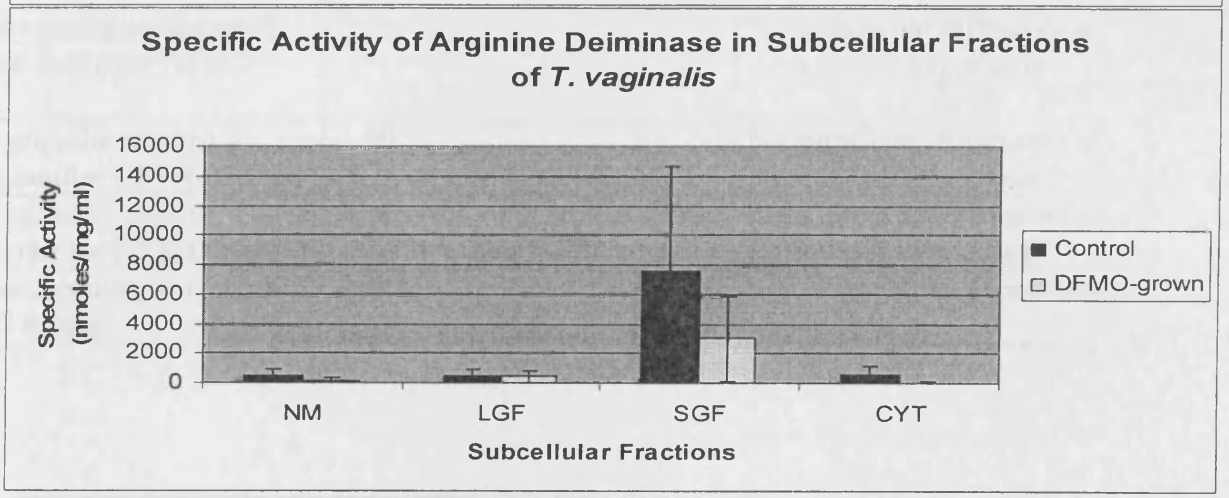

Figure 4.3. Specific activities of arginine deiminase, ornithine carbamyltransferase & carbamate kinase enzymes from subcellular fractions of *Trichomonas vaginalis* cultures grown in the presence of difluoromethylornithine (DFMO) compared to those grown in the absence of this inhibitor or polyamine synthesis. Results are expressed as a percentage of specific activity of each fraction. PS = primary sediment (contains whole cells, plasma and nuclear membranes), LGF = large granular fraction, SGF = small granular fraction, and CYT = cytosolic fraction (non-sedimentable). Experiments were repeated six times for each fraction. Error bars represent 95% confidence intervals.

Table 4.3. Students T test on control and DFMO treated Fractions Carbamate Kinase enzyme activity. P = 0.05. All fractions show a significant difference between the treated and non – treated cells (P<0.05)

Fraction	T-Test value	Null-hypothesis
Primary sediment control V Primary sediment DFMO treated	1.95	Significant Difference = Reject null hypothesis
Large granular control V Large granular DFMO treated	210.0 (Wilcoxon Statistic)	Significant difference = Reject null hypothesis
Small granular control V Small granular DFMO treated	14.98	Significant difference = Reject null hypothesis
Cytosolic control V cytosolic DFMO Treated	12.87	Significant difference = Reject null hypothesis

Table 4.4. Students T test on control and DFMO treated fractions arginine deiminase enzyme activity. P= 0.05. Small granular and cytosolic fractions show a significant difference between the treated and non – treated cells.

Fraction	T-Test value	Null-hypothesis
Primary sediment control V primary sediment DFMO treated	0.51	No significant difference = Accept null hypothesis
Large granular control V large granular DFMO treated	1.30	No significant difference = Accept null hypothesis
Small granular control V small granular DFMO treated	1041.54	Significant difference = Reject null hypothesis
Cytosolic control V cytosolic DFMO treated	268.41	Significant difference = reject null hypothesis

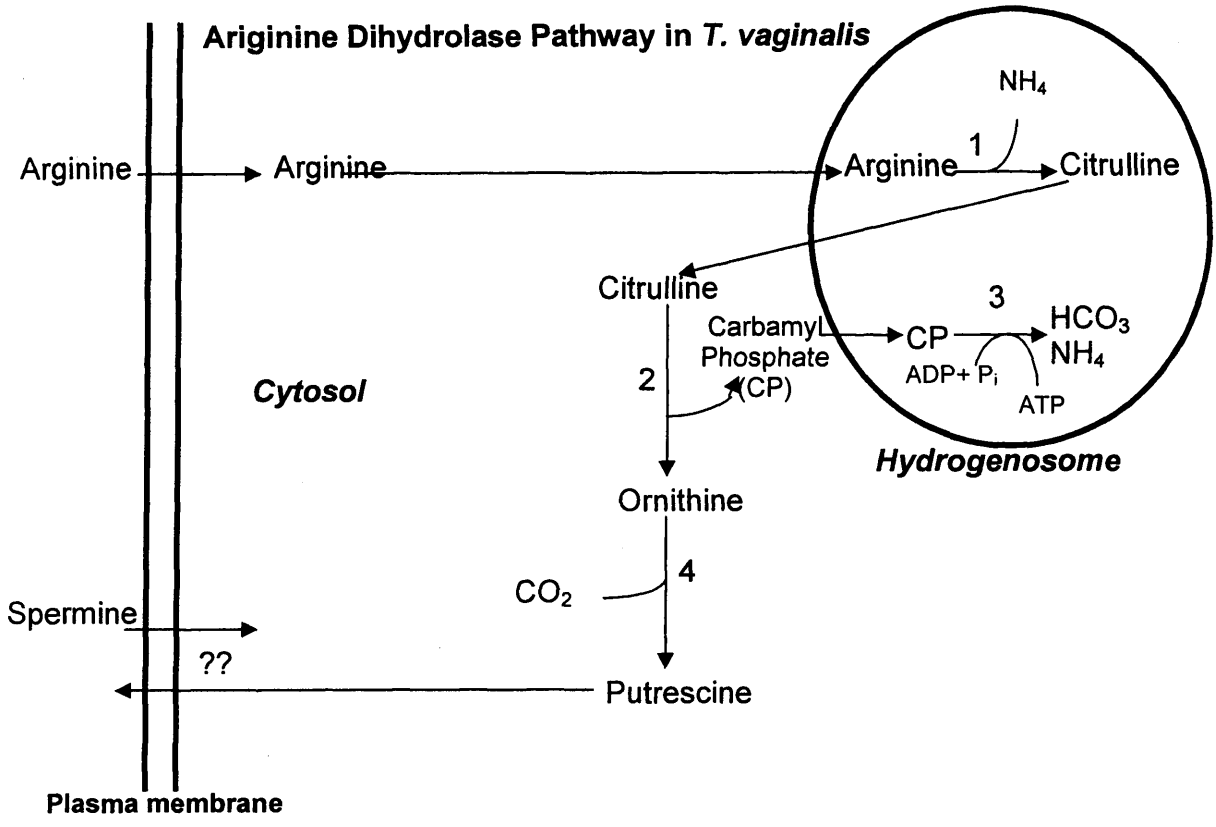

Figure 4.4: Proposed revision of arginine dihydrolase pathway in *T. vaginalis*. Enzymes numbered: 1. arginine deiminase. 2. catabolic ornithine carbamyltransferase. 3. carbamate kinase. 4. ornithine decarboxylase. Evidence from this study supports the absence of a spermine/putrescine antiport, but no transport system has yet been proposed in its place.

4.3.e. Proposed revision of arginine dihydrolase pathway in *T. vaginalis*.

Based on the localization assays done in this work, a proposed revision of the arginine dihydrolase pathway was created (Fig. 4.4). The main difference between this pathway and that of Yarlett *et al.* (2000) is the localiztion of the carbamate kinase enzyme to the hydrogenosome. There is also evidence to suggest that a nitric oxide synthase may be functioning in conjunction with or in competition with the arginine deiminase. Further work conducted in subsequent chapters will examine this question.

DISCUSSION

The distribution of NAD^+- dependent malic enzyme activity confirmed that hydrogenosomes were located in both the small and large granular fractions (Fig 4.2). The presence of hydrogenosomes within the small granular fraction was probably due to the difference in size of these organelles, the smaller hydrogenosomes having been removed at a later stage during the fractionation. This is important when considering the localization of carbamate kinase to both the large granular fraction and the small granular fraction (Fig 4.3). Clearly both of the granular fractions contained hydrogenosomes, which supports our evidence that carbamate kinase in *T. vaginalis* is hydrogenosomal.

Hydrogenosomes carry out substrate-level phosphorylation to produce ATP using pyruvate or malate as the primary substrate (Bui *et al.*, 1996a, b). It is therefore not surprising that this important energy-generating reaction would be located in these metabolically important redox organelles. Carbamate kinase enzyme had high substrate affinity (apparent K_M) and a high initial velocity (apparent V_{max}) (7.04×10^{-6} moles/L and 1.13×10^{-6} moles/L/min, respectively) indicating the high affinity of this enzyme to carbamyl phosphate in the production of ATP.

It has been previously reported (Yarlett *et al.*, 1994, Yarlett *et al.*, 1996) that the carbamate kinase enzyme, and hence the energy-generating portion of the arginine dihydrolase pathway, was present within the cytosol of *Trichomonas vaginalis* containing 70% of recovered activity with only a minor portion of activity being present within the large granular fraction. The current study differs from the previously reported results. Little activity was found within the cytosolic fraction (4.7% recovered activity) compared to the 69.7 % recovered activity reported from the hydrogenosomal rich large granular fraction. The kinetic values of this study are significantly different from those found in the previous

study, but since they used u/mg protein for velocity we cannot compare our Michalis-Menten constants with those specific activities (Table 4.2).

Previous work carried out to elucidate the location of arginine deiminase within *Trichomonas vaginalis* stated that the enzyme was located in the large granular fraction, where the fraction was reported to contain 40–46% of the recovered activity, and when density gradient centrifugation was carried out, a single peak of activity was recovered which was neither associated with the hydrogenosomes or the contaminating lysosomes (Yarlett *et al.*, 1994). That study concluded that arginine deiminase was a membrane associated protein and was probably associated with the plasma membrane (Yarlett *et al.*, 1994). In the current study, however, very little arginine deiminase activity was recovered from the large granular fraction, which contained only 5% of the total recovered activity. Instead, the small granular fraction contained the greatest amount of arginine deiminase activity having a total of 83.3% of the total recovered activity. Since both of these granular fractions contain hydrogenosomes, it is likely that the arginine deiminase may be associated with the hydrogenosomal membrane, since so much of the activity was prevalent in the small granular fraction, where membrane debris would have likely been collected.

The deamination of L-arginine to citrulline by arginine deiminase is the first step in the arginine dihydrolase pathway. The importance of L-arginine, and hence the arginine dihydrolase pathway to the organism, is illustrated during *Trichomonas vaginalis* infection, when arginine, which is normally present in high concentrations within vaginal exudates and seminal fluid, is practically absent from the fluid (Chen *et al.*, 1982). Given the parasite's need for arginine, the elucidation of the location of this enzyme could act as an attractive chemotherapeutic drug target.

The results obtained in this study are reliable as the enzyme assay experiments were repeated six times. All control arginine deiminase assay experiments and also the DFMO

drug treated experiments demonstrated that the largest percentage of recovered arginine deiminase activity was present within the small granular fraction. The difference in results obtained by the Yarlett group (Yarlett *et al.,* 1994) and the results obtained by this study are not due to experimental differences as the assays carried out were identical to the assays used in the Yarlett study.

Cultures of *Trichomonas vaginalis* grown in the presence of 5mM DFMO, an irreversible inhibitor of ornithine decarboxylase, displayed significantly reduced enzyme activities of both carbamate kinase and arginine deiminase. The drug reduced the specific activity of carbamate kinase by half compared to the control. The effect of the drug on the specific enzyme activity of arginine deiminase was even greater, with the enzymatic activity of the treated organisms having reduced by approximately two and a half fold. Therefore polyamine depletion by DFMO, through the inhibition of ODC, also causes inhibition of the arginine dihydrolase pathway. This reduction in enzymatic activity could have serious implications for the organism, not only with respect to polyamine synthesis, but more importantly would likely result in reduced ATP formation. The reduction in the specific activities of both enzymes could have been a result of the build up of citrulline and carbamyl phosphate due to blockage of the pathway by the ODC inhibitor, which may be causing feedback inhibition in arginine deiminase and carbamate kinase. The decreased specific activity of the enzymes of the arginine dihydrolase pathway could result in the prevention of arginine – uptake.

Anabolic ornithine carbamyltransferase activity, on the other hand, increased, indicating the importance of citrulline production under these conditions. It is possible that citrulline formed by anabolic OCT could then condense with aspartate to form arginosuccuinate mediated by arginosuccunate synthase, and the arginosuccinate could then be cleaved to fumarate and arginine by arginosuccinate lyase. The arginine could then also be

converted to citrulline by arginine deiminase. This would utilize the aspartate pool in a cycle to form fumarate. Fumarate can be metabolized to succinate by fumarate reductase and malate by fumarase. Although a fumarase gene has been found in *T. vaginalis*, the expression of fumarase has not been shown (Gerbod *et al.*, 2001). It is possible that the expression of fumarase is inducible by the inhibition of ODC and the anabolic OCT production of citrulline.

Recent work carried out (Reis *et al.,* 1999, Chapter 3) has revealed that polyamine depletion as a result of inhibition of ODC by DFMO disturbs the structure and function of the hydrogenosomes and has adverse effects on the plasma membrane and hydrogenosomal membrane potentials. This data supports the subcellular locations of carbamate kinase and arginine deiminase (if associated with the hydrogenosomal membrane) elucidated in this study. If the hydrogenosomal structure was disturbed or damaged and the membrane potential decreased, it would almost certainly have an adverse affect on the specific activity of the enzymes of the pathway. The reverse could also be true: the reduced specific activity of the enzymes, and therefore the decrease in arginine uptake, could be a factor in causing hydrogenosomal disturbance and result in a decrease in hydrogenosomal membrane potential.

This work provides further understanding of how *Trichomonas vaginalis* responds to polyamine depletion and the importance of the arginine dihydrolase pathway to the function and energy production of the organism. Given the significant role this pathway plays in the organism, further work on this pathway is needed to explore possible targets for drug therapy.

CHAPTER 5

Redox organellese from *Trichomonas vaginalis* and *Giardia intestinalis* produce nitric oxide and display NO-synthase activity

5.1 Summary.

The arginine-dependent production of nitric oxide (NO) in the microaerophilic parasitic protists *Trichomonas vaginalis* and *Giardia intestinalis* were studied. Potentiometric measurement of washed, non-proliferating suspensions of *T. vaginalis* with a NO electrode indicated that the basal production rate (15.3 nmoles NO/min/10^6 organisms) was increased eight-fold on starvation for 4 h and sixteen-fold after 4 days. Fluorimetric detection by confocal laser scanning microscopy and flow cytometry was performed after preincubation with the NO-specific fluorogen 4-amino-5methylamino-2'7'-difluorescein (DAF-FM). Microscopy indicated population heterogeneity with respect to NO production in freshly-harvested organisms in both organisms, and this was confirmed by the broad distribution of fluorescence intensities in the flow cytograms. The weakly fluorescent organisms in images of *T. vaginalis* showed fluorescent reaction product spread uniformly throughout the area of the cytosol, whereas more intensely fluorescent organisms showed organellar localization. These organelles in *T. vaginalis* were distributed along the axostyle and around the costa in the configuration characteristic of hydrogenosomes. Confocal microscopy of *G. intestinalis* stained with 5μM of the voltage-sensitive fluorophore tetramethylrhodamine ethyl ester (TMRE) showed localization of membrane potential-containing organelles inside the plasma membrane around the cytosolic periphery of the organism. *G. intestinalis* stained with DAF-FM, a NO-specific fluorogen, also showed a localization of NO production in the periphery of the cytosol. Nitric oxide synthase activity measured in cell-free extracts

using the NO electrode and by NO_3^- formation from arginine in a coupled assay system indicated the presence of both particulate and non-sedimentable activities in *T. vaginalis*, but only particulate activity in *G. intestinalis*. Specific activity of the NO synthase in the granular fraction of *G. intestinalis* was 2.1 μmoles/mg protein/min. The apparent K_M and V_{max} values of the NOS from the granular fraction were 8.28 x 10^{-3} moles/L and 6.0 x 10^{-9} moles/L/h, respectively. A NO electrode indicated production of NO by whole organisms of *G. intestinalis*, and was stimulated by the addition of as little as 0.238 mM arginine. Subcellular fractionation of *G. intestinalis* yielded a fraction containing particles sedimented at 10,000 x g for 15 min; this fraction produced NO with a specific activity of 0.624 μmoles/mg protein/min in the presence of 2.38 mM arginine. Analysis of the *G. intestinalis* genome confirmed the presence of an iNOS (GenBank accession number AACB01000174). Bioinformatic searches of the *T. vaginalis* genome confirmed the presence of two NOS genes that contain C-terminal protein motifs typically associated with NOS sequences. The N-terminal domains of both genes lack a NO synthase motif and instead contain motifs normally associated with various iron sulfur proteins (Fe-hydrogenase). The presence of nitrosylation motifs in the glycogen phosphorylase gene of *T. vaginalis* provides a possible explanation as to the role of nitric oxide within the parasite. This study suggests that *T. vaginalis* contains two nitric oxide synthases, and redox-active organelles capable of generating a membrane potential in *G. intestinalis* may contain nitric oxide synthase. The production of NO by mitochondria-like organelles in this microaerophile provides further evidence for the hypothesis that *G. intestinalis* may have been a recent derivative of an aerobic lineage. Implications are discussed of NO production in the evolution, biology and pathogenicity of these unique parasites.

5.2 Introduction.

Nitric oxide is an important signaling molecule, a component of the host immune response in combating pathogens and parasites as well as a molecule responsible for a wide diversity of physiological control functions (Broillet, 1999; Albina *et al.*, 1998; Hess *et al.*, 2005; Nisoli & Carruba, 2006; Kato *et al.*, 2006). The metabolic conversion of arginine to citrulline via the actions of nitric oxide synthase (NOS), with nitric oxide (NO) as the main product, has been studied in numerous mammalian cell-types, tissues and organs. With respect to parasitic protozoa, however, NO production has been dominated by a one-sided exploration: effects of the release of NO from the host's immune system and its cytotoxic manifestations in the parasites. Only a few studies have explored the production of NO by the parasites themselves.

Nitric oxide synthase (NOS) activity has been shown in *Trypanosoma cruzi* and was found to be sensitive to typical NOS inhibitors (e.g. N^{W}-methyl-L-arginine, Paveto *et al.*, 1995). *Leishmania donovani* and *Entamoeba histolytica* also produce NO and responded to typical NOS inhibitors (Basu *et al.*, 1997; Hernandez-Campos *et al.*, 2003). NOS or NOS-like enzymes are also present in several non-protozoan parasites, including *Hymenolepis diminuta* (Gustafsson *et al.*, 1996), *Brugia malayi* (Pfarr & Fuhrman, 2000), *Ascaris suum* (Bascal *et al.*, 2001), *Diphyllobothrium dendriticum* (Lindholm *et al.*, 1998), *Schistosoma mansoni* (Kohn *et al.*, 2001), and *Trichinella britovi* (Masetti *et al.*, 2004).

G. intestinalis has been termed 'amitochondrial' (Cavalier-Smith, 1987). However, redox-active organelles and mitosomes have recently been found in *G. intestinalis* (Lloyd *et al.*, 2002; Tovar *et al.*, 2003). The location of both *Giardia* and

Trichomonas in evolutionary taxonomy has been debated mostly due to the organisms' reported lack of mitochondria (Cavalier-Smith, 1987). Both organisms are considered to be among the most 'primitive' organisms on the eukaryotic evolutionary tree due to their lack of mitochondria, peroxisomes, and nucleoli (Cavalier-Smith, 1987; Keeling, 1998), as well as their possession of only rudimentary Golgi stacks and the limitations that stem from their sole use of substrate-level phosphorylation reactions for energy production. I have found that NO is produced by redox potential-generating organelles from *G. intestinalis*. Previous studies have shown that mitochondria produce NO (Bates *et al.*, 1996; Ghafourifar & Richter, 1997; Biagini *et al.*, 1997; van der Giezen *et al.*, 2005). These results therefore add to the evidence that *G. intestinalis* has evolved from organisms containing fully-functional mitochondria and retained the ability to produce NO. Recently, *Giardia intestinalis* was found to produce H_2, a characteristic formerly thought to be unique to hydrogenosome-containing organisms (Lloyd *et al.*, 2002). In this study, I show that redox generating organelles in *G. intestinalis* possess another similarity to mitochondria (Bates *et al.*, 1996; Giulivi *et al.*, 1998) and hydrogenosomes in *Trichomonas vaginalis* (Harris *et al.*, 2006): they produce NO.

Trichomonas vaginalis has the ability to degrade nitric oxide (Sarti *et al.*, 2004); this was presumed to function as a defense mechanism against the host's immune response. However, based on the results of the present study, it is possible that this mechanism may also play a role in degrading nitric oxide produced by the parasite itself, providing a mechanism of regulation for the production and use of this volatile gas.
In this study, using four different methods, *T. vaginalis* has been shown to produce NO and contain two novel NOS enzymes. NOS activity was found in both the cytosol and

hydrogenosomal fractions, leading us to conclude this organism has at least two distinct nitric oxide synthases. Further, more organisms exposed to starvation conditions (no exogenous glucose in Doran's Buffer) displayed increased rates of nitric oxide production. Under the same conditions there was a dramatic increase of CO_2 production (approximately 2.5 fold) (Harris *et al.*, in preparation). In support of initial observations, a bioinformatic analysis of the nearly completed *T. vaginalis* genome revealed the presence of two potential NOS encoding genes. The relevance of this data on parasite physiology and pathology are discussed.

5.3 Materials and Methods.

5.3a. Confocal microscopy of *T. vaginalis*. Harvested *T. vaginalis* cultures were incubated with 10 μM 4-amino-5-methylamino-2'7'-difluorescein (DAF-FM) at 37 °C for 45 min, then centrifuged at 500 x g for 5 min and washed in Doran's buffer. Subsequently, the pellet was resuspended in fresh Doran's buffer. These organisms were immobilized with 2 % (w/v) methyl cellulose and mounted on polylysine-coated slides. Fluorescence signals from DAF-FM were collected on a Zeiss Pascal confocal microscope through a Plan-Apochromat 63x 1.4 N.A. water immersion objective. Excitation of DAF-FM was performed using an argon ion laser at 488 nm. Emitted light was reflected through a 505–550 nm band pass filter from a 540 nm dichroic mirror (Done in collaboration with Dr. Giancarlo Biagini, Liverpool School of Tropical Medicine, UK).

5.3b. Confocal microscopy of *G. intestinalis*. Harvested organisms were incubated with 10μM 4-amino-5-methylamino-2'7'-difluorescein (DAF-FM) and 5μM tetramethylrhodamine ethyl ester (TMRE) at 37 °C for 45 min. Cultures were then

incubated at 4 °C for 20 min, and once again centrifuged at 500 x g for 5 min. Organisms were washed in Doran's buffer. The pellet was resuspended in Doran's buffer and mounted on poly-L-lysine-coated slides. Fluorescence signals from DAF-FM were collected on a Zeiss Pascal confocal microscope through a Plan-Apochromat 63x 1.4 N.A. water immersion objective. Excitation of DAF-FM was performed using an argon ion laser at 488 nm. Emitted light was reflected through a 505–550-nm band pass filter from a 540-nm dichroic mirror. Excitation of TMRE was performed using an argon laser at 530 nm. Emitted light was was reflected through a 580—630-nm band pass filter from a 540-nm dichroic mirror (Done in collaboration with Dr. Giancarlo Biagini, Liverpool School of Tropical Medicine, UK).

5.3c. Flow cytometry. Samples of whole organisms were analyzed using a Becton Dickinson FACSCalibur Flow Cytometer (Franklin Lakes, New Jersey, USA). The argon ion laser provided excitation at 488 nm, and fluorescence emission signals were acquired between 550-700 nm for 100,000 cells in each sample at a flow rate of 60 µl/min. Harvested and washed organisms were preincubated with 200 nM DAF-FM for 20 min before analysis by the flow cytometer.

5.3d. Bioinformatic searches in *T. vaginalis* genome. The inducible nitric oxide synthase from *Homo sapiens* (accession no. AAC83553) was used as a seed for tBLASTn searches of the *T. vaginalis* genome at http://www.tigr.org/tdb/e2k1/tvg/. The obtained potential NOS sequences were subsequently used as query sequences for reciprocal tBLASTn and BLASTp searches using the nr GenBank database. Sequences returning NOS sequences as search results were subsequently analyzed for primary and secondary sequence features using SMART (Letunic *et al.*, 2004). Similar searches using the human

endothelial or neuronal nitric oxide synthases (accession no. NP_000594.2 and NP_000611, respectively) as seeds, returned the same sequences as when the inducible form was used (Done in collaboration with Dr. Mark van der Giezen, Queen Mary College, University of London, UK).

5.3e. Bioinformatic searches in *G. intestinalis* genome. The gene annotated in the *G. intestinalis* genome as iNOS (accession # AACB01000174) was tested for homology with NOS genes in other organisms, using a protein-protein BLAST and online genome databases (NCBI).

5.4 Results.

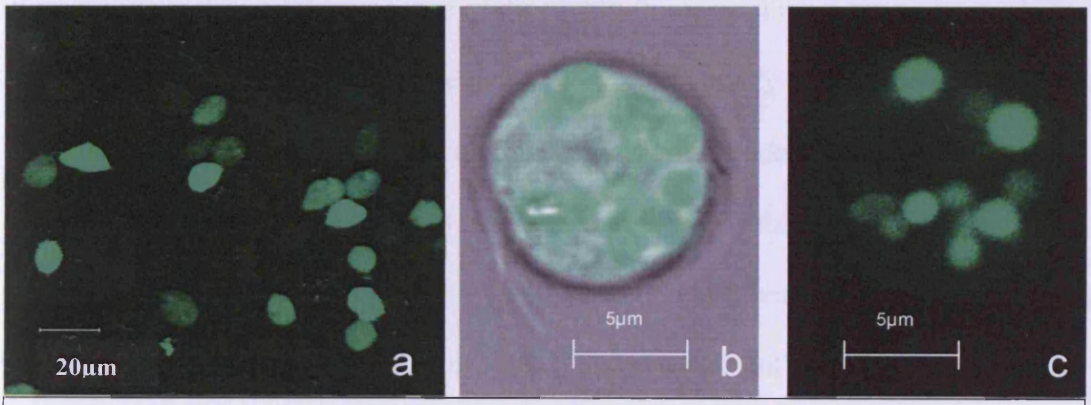

Figure 5.1: *Trichomonas vaginalis* stained with 10 µm DAF-FM, a fluorogen specific for nitric oxide. **a.** a single section of a monolayer of *T. vaginalis* **b.** transmission overlayed with fluorescence of the same organism as depicted in 1c. **c.** 2-D representation of a 3-D reconstruction from 20 sections of one *T. vaginalis* stained with DAF-FM. 1b and 1c are images of the same organism.

5.4a. Confocal microscopy of *T. vaginalis*. *T. vaginalis* preincubated with 10 µM DAF-FM, a fluorogen specific for nitric oxide, revealed large differences in the fluorescence intensities of individual organisms (Fig 5.1a). The heterogeneity of the stained population suggested a cell cycle dependence of NO production. Furthermore, differences in the intracellular locations of the fluorescent reaction product were also

evident between individual organisms. In some individuals, reaction product was also evident throughout the cytosol as well as in the hydrogenosome. Fig 5.1b shows an organism with both the fluorescence and transmission channels overlayed; Fig 5.1c, a two dimensional representation of a three-dimensional reconstruction of the same *T. vaginalis* organism (Fig 5.1b, c) reveals that, at some point in its cell cycle, nitric oxide is present in the hydrogenosomes, and some hydrogenosomes are more active NO producers than others.

5.4c. Confocal microscopy of *G. intestinalis*. Images of *Giardia intestinalis*, after incubation with the fluorogen DAF-FM (Figs 5.2, 5.3 & 5.4), indicated that many of the organisms showed the presence of the highly fluorescent reaction product, which correlates with NO production. The population heterogeneity of the product formation led me to believe that NO production could be cell cycle-dependent. The fluorescent organisms showed a localization of NO in the periphery of the cytosol just inside the plasma membrane, which correlated with the location of membrane potential-generating organelles accumulating TMRE (Fig 5.2a). This suggests that these peripheral organelles produce NO (Fig 5.2b). Some organisms showed a more diffuse concentration of fluorescent reaction product, again supporting the hypothesis that intracellular NO production varies in location at different times in the cell-cycle (Fig 5.2a). Still others (approximately 20%) did not show any fluorescent reaction product within the organism (Figs 5.3 & 5.4).

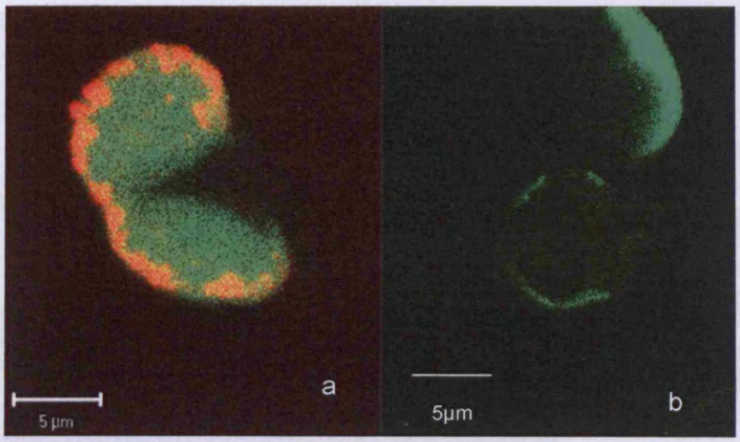

Figure 5.2. a. A dividing *G. intestinalis* organism stained with both TMRE (red) and DAF-FM (green). The vesicles exhibiting membrane potential on the periphery are mitochondria-like redox balancing organelles. b. A single *G. intestinalis* organism stained with DAF-FM, showing a localization of the fluorescence in the periphery of the cell. Both scale bars represent 5µm.

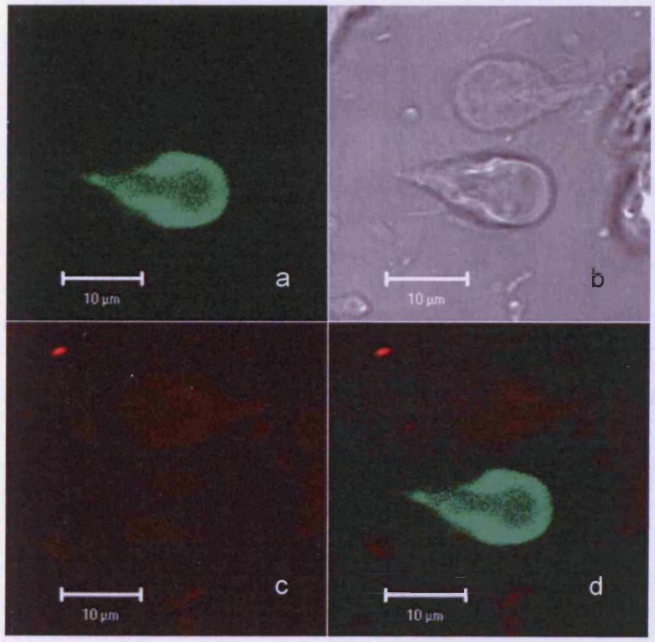

Figure 5.3. Images of *G. intestinalis* after incubation with TMRE and DAF-FM, viewed under different wavelengths of light. All four panels are identical fields of view. All scalebars represent 10µm a. DAF-FM is localized on the periphery of the organism in one, but not the other. b. Through transmitted light two distinct organisms can be seen. c. TMRE localization to the periphery is present in the organism toward the top of the field of view, but not the organism producing nitric oxide. d. When both channels were viewed simultaneously, there was little, if any, overlap.

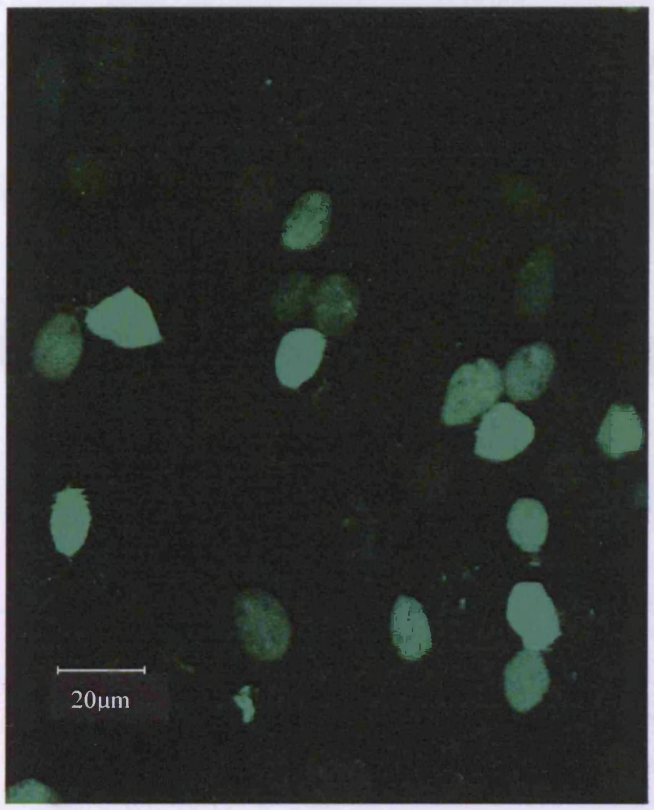

Figure 5.4: Images of *G. intestinalis* after incubation with DAF-FM. Note the heterogeneity of the fluorescent product. The scale bar represents 20μm.

5.4c. Flow cytometry of *T. vaginalis*. When *T. vaginalis* organisms were stained with DAF-FM, a slight increase in fluorescence was observed (Fig 5.5). This increase in fluorescence caused by the addition of DAF-FM correlated with nitric oxide production. In addition, the range of side scatter represented by the organisms became more uniform. The addition of DAF-FM seemed to have changed the organism's shape, perhaps causing it to be more round and therefore to produce less of a range of side scatter.

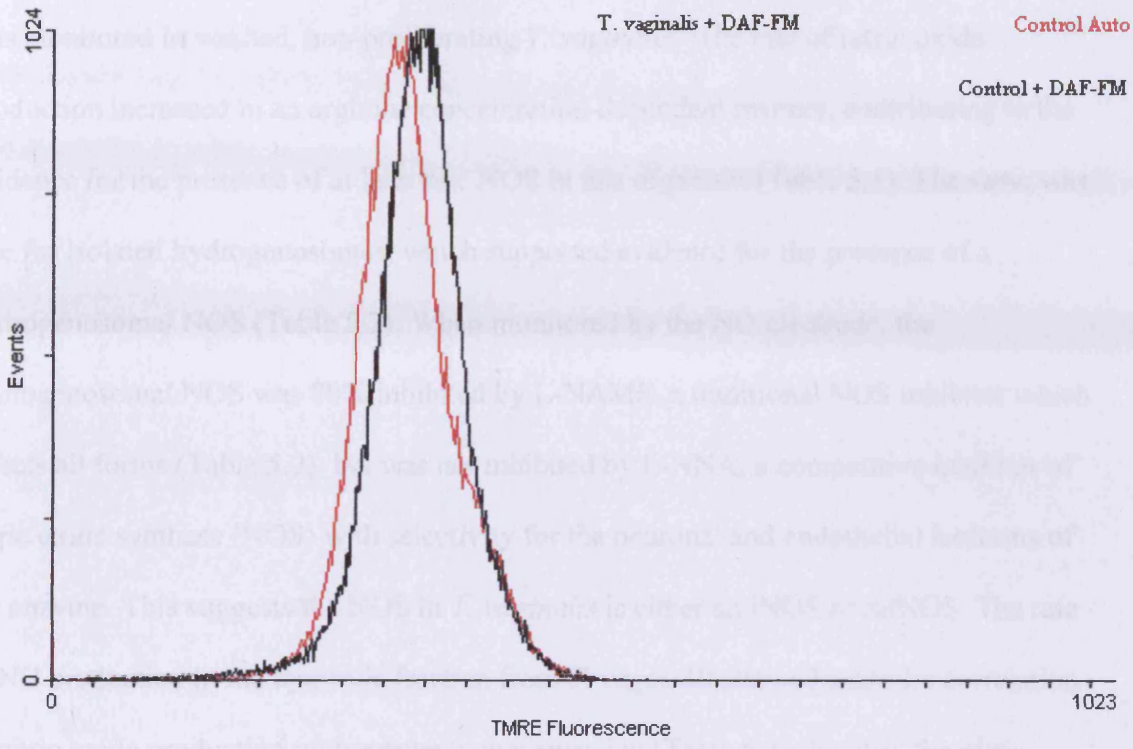

Figure 5.5: Flow cytometry histogram of *T. vaginalis* autofluorescence and *T. vaginalis* cultures incubated with the NO-specific fluorogen, DAF-FM. Note the increase of fluorescence upon adding DAF-FM to cultures of *T. vaginalis*, indicating the presence of NO. The y axis represents the number of individual organisms analyzed. The x axis is the fluorescence emission in from 500-700nm.

5.4d. Potentiometric monitoring of NO production. Nitric oxide production was monitored in washed, non-proliferating *T. vaginalis*. The rate of nitric oxide production increased in an arginine concentration-dependent manner, contributing to the evidence for the presence of at least one NOS in this organism (Table 5.1). The same was true for isolated hydrogenosomes, which supported evidence for the presence of a hydrogenosomal NOS (Table 5.2). When monitored by the NO electrode, the hydrogenosomal NOS was 80% inhibited by L-NAME, a traditional NOS inhibitor which affects all forms (Table 5.2), but was not inhibited by L-NNA, a competitive inhibitor of nitric oxide synthase (NOS) with selectivity for the neuronal and endothelial isoforms of the enzyme. This suggests the NOS in *T. vaginalis* is either an iNOS or mtNOS. The rate of NO production in the cytosolic fraction from *T. vaginalis* showed a similar correlation of nitric oxide production with substrate concentration (Table 5.3). Finally, the nitric oxide produced by starved *T. vaginalis* (incubated at 25 °C in Doran's Buffer) was found to be much greater than the nitric oxide produced by freshly harvested *T. vaginalis* (Table 5.4).

TABLE 5.1: Rate of NO production by Different *T. vaginalis* Cultures As Measured by the Nitric Oxide Electrode (n=3)

Concentration of Arginine Additions mmoles/L	Rate of NO production (standard deviation) nmoles NO/min/10^6 cells
0.024	3.37 (1.6)
0.238	7.71 (1.8)
0.476	7.66 (1.7)
4.76	22.4 (5.8)
24.4	26.9 (4.8)

TABLE 5.2: Rate of NO production by Hydrogenosomes Isolated from *T. vaginalis* As Measured by the Nitric Oxide Electrode (n=3)

Concentration of Arginine Additions mmoles/L	Rate of NO production Control (standard deviation) nmoles NO/mg protein min	Rate of NO production In presence of L-NAME (percent inhibition) nmoles NO/mg protein min
0.238	129 (3.9)	0 (100%)
0.476	168 (10)	Not done
4.76	425.6 (43.2)	65.8 (85%)
24	Not done	219
49	2411 (310)	1447 (40%)

TABLE 5.3: Rate of NO production by Cytosol Isolated from *T. vaginalis* As Measured by the Nitric Oxide Electrode (n=3)

Concentration of Arginine Additions mmoles/L	Rate of NO production (standard deviation) nmoles NO/mg protein min
Increase of NO concentration upon adding cytosol to reaction vessel	282 (53.4)
0.0119	86.4 (20)
4.76	294 (70)

Table 5.4: Increase in Nitric Oxide Concentration Upon Adding Various Types of *T. vaginalis* to Reaction Vessel, as Measured by the Nitric Oxide Electrode (n=3)

	***T. vaginalis* freshly harvested (standard deviation)**	***T. vaginalis* starved in Doran's Buffer for 4 hours (standard deviation)**	***T. vaginalis* starved in Doran's Buffer for 4 days (standard deviation)**
Concentration of NO increased in µmoles/min/10^6 cells	15.3 (5)	121.6 (16.5)	225 (14.9)

5.4e. NO electrode. Live *Giardia intestinalis* organisms, as well as the large granular fraction isolated from a large culture of organisms, were monitored for NO production by a nitric oxide electrode. The rate of nitric oxide production by whole cell *G. intestinalis* was 27.7 nmoles/min/10^6 cells. The rates of NO production increased as the substrate concentration increased (Table 5.5). Kinetics analysis was done (Fig 5.6) on the NO electrode data obtained from the large granular fraction of *G. intestinalis*. Apparent K_M and V_{max} values were found to be 10×10^{-3} moles/L and 3.33×10^{-6} moles/L/min, respectively.

TABLE 5.5: Rate of NO production by Granular Fraction from *G. intestinalis*, As Measured by the Nitric Oxide Electrode

Concentration of Arginine Additions mmoles/L	Rate of NO production (standard deviation) µmoles NO/mg protein/min
0.238	**0.416** (0.39)
2.38	**0.624** (0.15)
4.76	**1.09** (0.14)
24.4	**2.11** (0.87)

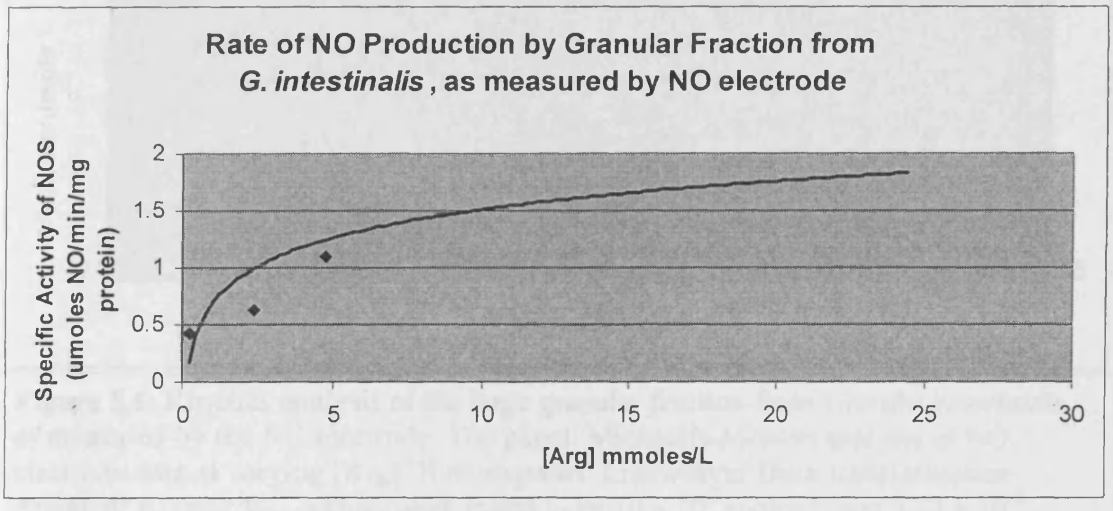

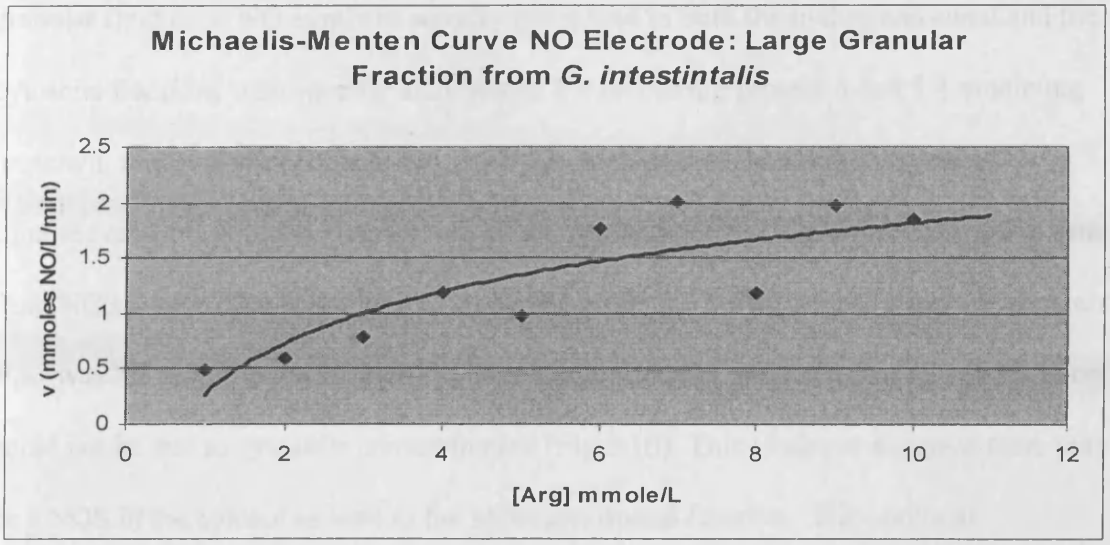

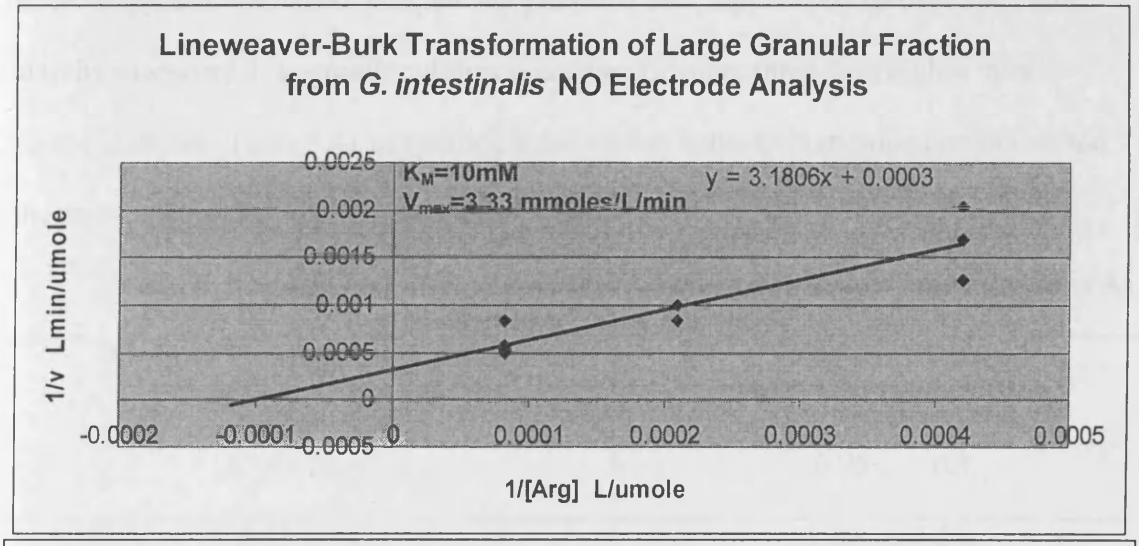

Figure 5.6: Kinetics analysis of the large granular fraction from *Giardia intestinalis*, as measured by the NO electrode. Top panel: Michaelis-Menten analysis of NO electrode data at varying [Arg]. Bottom panel: Lineweaver-Burk transformation. Apparent K_M and V_{max} values were found to be 10×10^{-3} moles/L and 3.33×10^{-6} moles/L/min, respectively. Note the rate is per min, whereas the assay rates are noted per h in conjunction with the incubation time.

5.4f. NOS activity assays in *T. vaginalis*. NOS assay activities increased with increasing substrate concentrations (Table 5.6). Based on marker enzyme assays (Fig. 5.10), the similiarity of activities in the small and large granular fractions for hydrogenosomal markers indicated the presence of hydrogenosomes in both of these

granular fractions. NO-synthase activity was found in both the hydrogenosomal and the cytosolic fractions with specific activities of 2.4 nmole/mg protein/h and 5.4 nmole/mg protein/h, respectively (Table 5.7 & Fig. 5.7). Michaelis-Menten kinetics and a Lineweaver-Burk plot were performed on the cytosolic NOS (Fig. 5.8 & 5.9), using data from NOS assays. The apparent K_M for arginine was 2.5 x 10^{-4} moles/L, and the apparent V_{max} was 7.3 x 10^{-6} moles/L/hour. Marker enzyme assays indicated that this distribution could not be due to cytosolic contamination (Fig 5.10). This evidence suggests there may be a NOS in the cytosol as well as the hydrogenosomal fraction. The confocal microscopy data combined with the NO electrode data support this theory. The NOS activity in starved *T. vaginalis* cultures was approximately three-fold higher than in control cultures (Table 5.4), suggesting a correlation between starvation conditions and the parasite's production of nitric oxide.

TABLE 5.6: Kinetics of *T. vaginalis* at Varying Substrate Concentrations As Measured by NOS Assays

Arginine Concentration (mM)	Apparent Vmax µmol/L/h (Standard Dev.)
0.001 (n=4)	0.05 (0)
0.01 (n=4)	1.72 (0.25)
0.5 (n=4)	2.45 (0.21)
1 (n=4)	2.5 (0.5)
10 (n=10)	2.8 (0.65)
50 (n=5)	3.7 (0.75)

TABLE 5.7: Specific Activity of Subcellular Fractions of *T. vaginalis* As Measured by NOS Assays (n=6)

	Primary Sediment	Large Granular Fraction	Small Granular Fraction	Cytosol
Specific Activity nmoleNO/mg protein/h	0	2.4	1.8	5.4
(Standard Deviation)	(0)	(0.99)	(0.023)	(0.049)

TABLE 5.8: Specific Activity of Starved vs. Freshly Harvested *T. vaginalis* (n=6)

***T. vaginalis* Starved vs. Freshly Harvested**	**NOS Specific Activity** nmoleNO/mg protein/h (Standard Dev.)
Freshly harvested *T. vaginalis*	2.6 (0.33)
Starved *T. vaginalis*	6.1 (1.67)

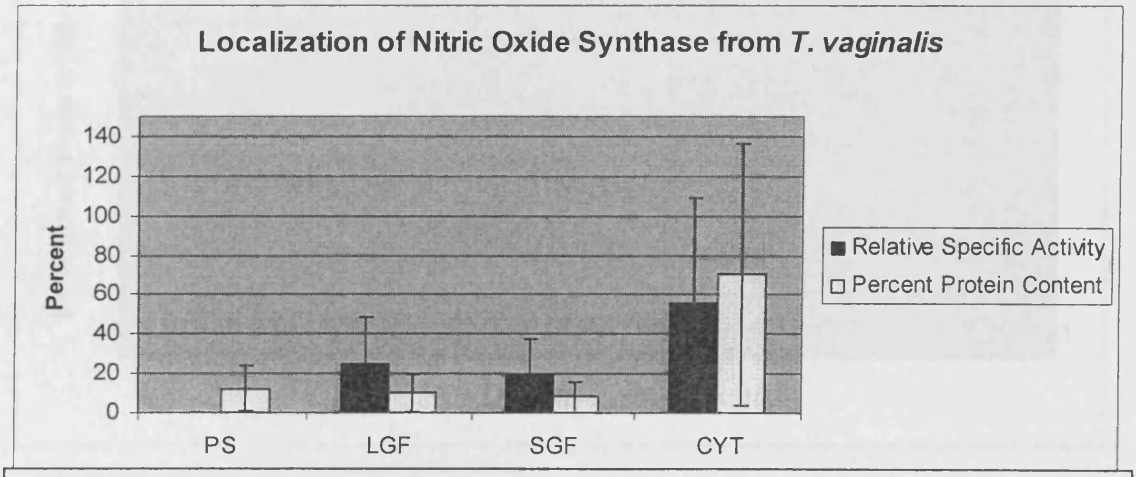

Figure 5.7: Relative specific activity of NOS in subcellular fractions from *T. vaginalis*. Error bars represent 95% confidence intervals. Note the high NOS activity in the cytosolic fraction, as well as activity in the large and small granular fraction. Marker enzyme assays showed this distribution could not be due to cytosolic contamination (Fig 5.6). This led us to believe there may be a NOS in the cytosol as well as the hydrogenosomal fraction. n=6.

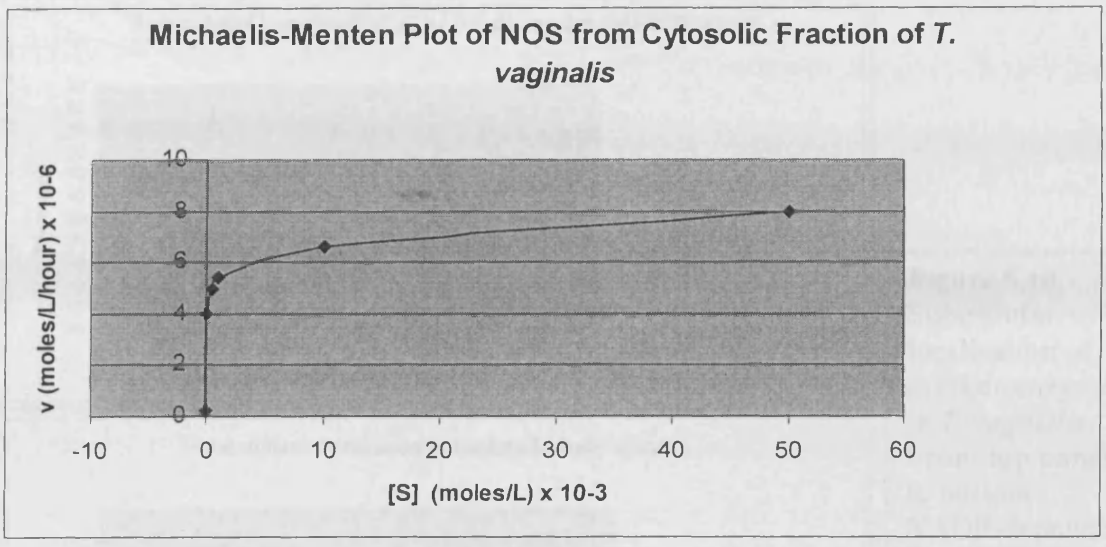

Figure 5.8: Apparent velocity of NOS from the cytosolic fraction at varying substrate concentrations. All points are mean values of six replicates.

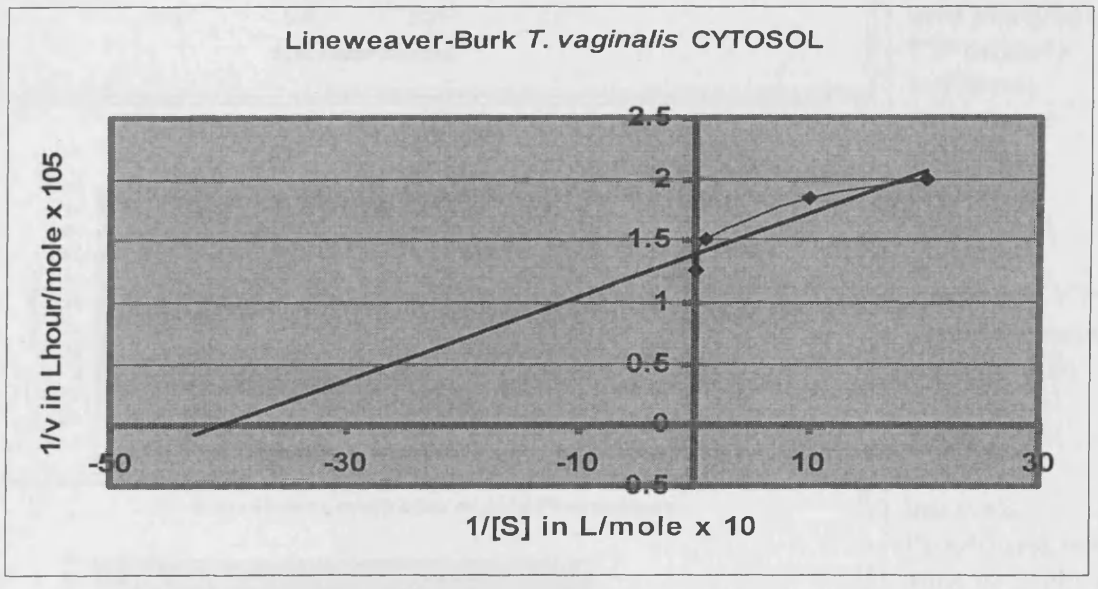

Figure 5.9: Reciprocals of the values found in Fig 4b were plotted in order to determine the apparent K_M and apparent V_{max} values for the cytosolic NOS. All points are mean values of six replicates. The cytosolic NOS apparent K_M was determined to be 2.5×10^{-4} moles/L while the apparent V_{max} was 7.3×10^{-6} moles/L/h.

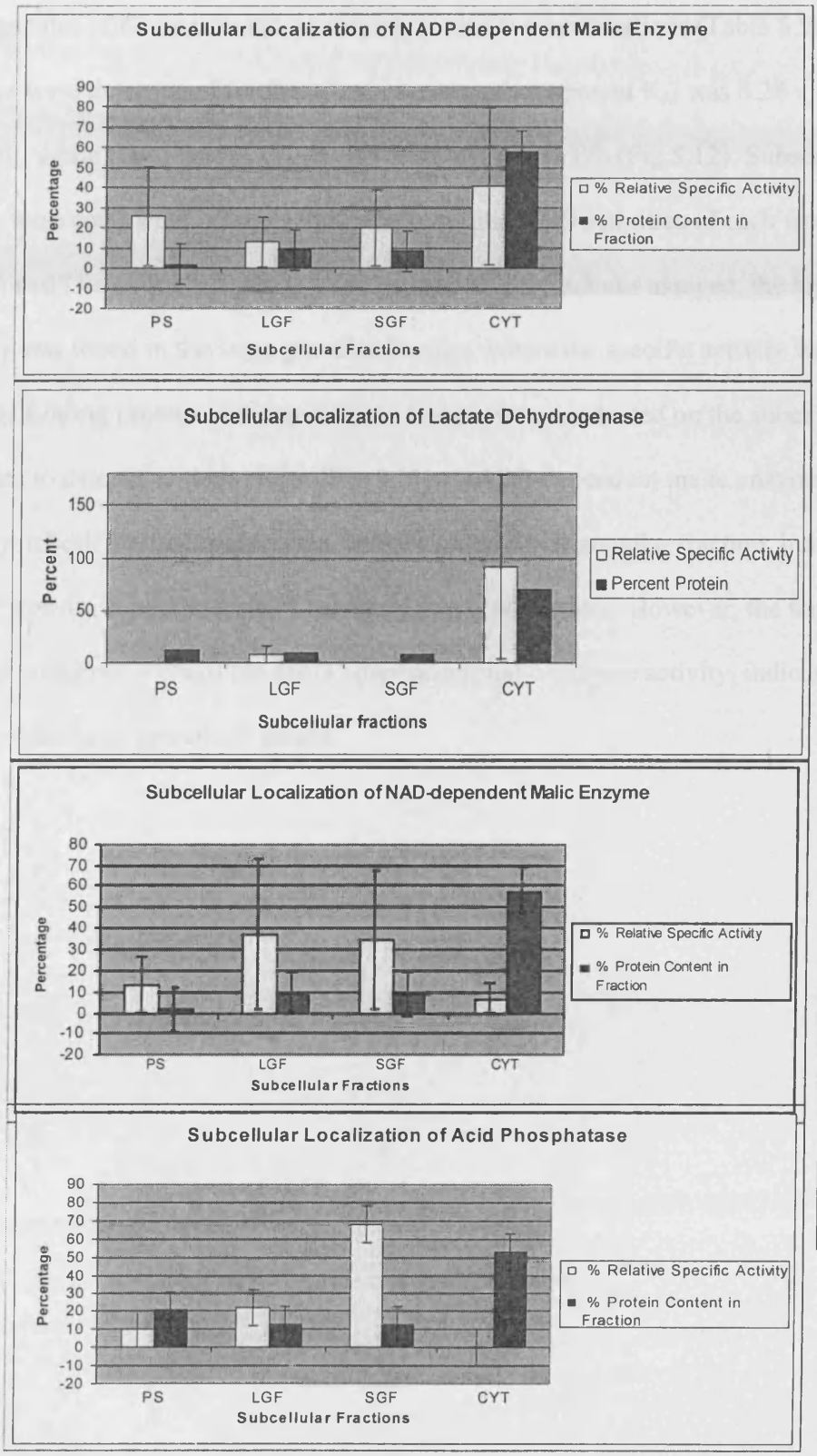

Figure 5.10. Subcellular localization of marker enzymes in *T. vaginalis*. From top panel to bottom: NADP-dependent malic enzyme, lactate dehydrogenase, NAD+-dependent malic enzyme, acid phosphatase. PS=primary sediment; LGF=large granular fraction; SGF=small granular fraction; CYT= non-sedimentable fraction. The error bars display 95% confidence intervals. Procedures were done in triplicate.

5.4g. NO-synthase assays in *G. intestinalis*. Assays were conducted on homogenates of *G. intestinalis*, at varying substrate concentrations (Table 5.9). The kinetics were determined for these homogenates; the apparent K_M was 8.28×10^{-3} moles/L, while the apparent V_{max} was 5.91×10^{-3} moles/L/h (Fig 5.12). Subsequent assays were conducted on subcellular fractions and NOS activities of each fraction were determined (Table 5.10; Fig 5.11). Of the subcellular fractions assayed, the highest NOS activity was found in the large granular fraction, where the specific activity was 5.6 μmoles/ L/h/mg protein. Marker enzyme assays were conducted on the subcellular fractions to determine their purity (Fig 5.11). NADP-dependent malic enzyme displayed activity in both the final supernatant as well as the small granular fraction, indicating some cytosolic contamination of the small granular fraction. However, the large granular fraction contained 97% of the NAD^+-dependent malic enzyme activity, indicating the purity of the large granular fraction.

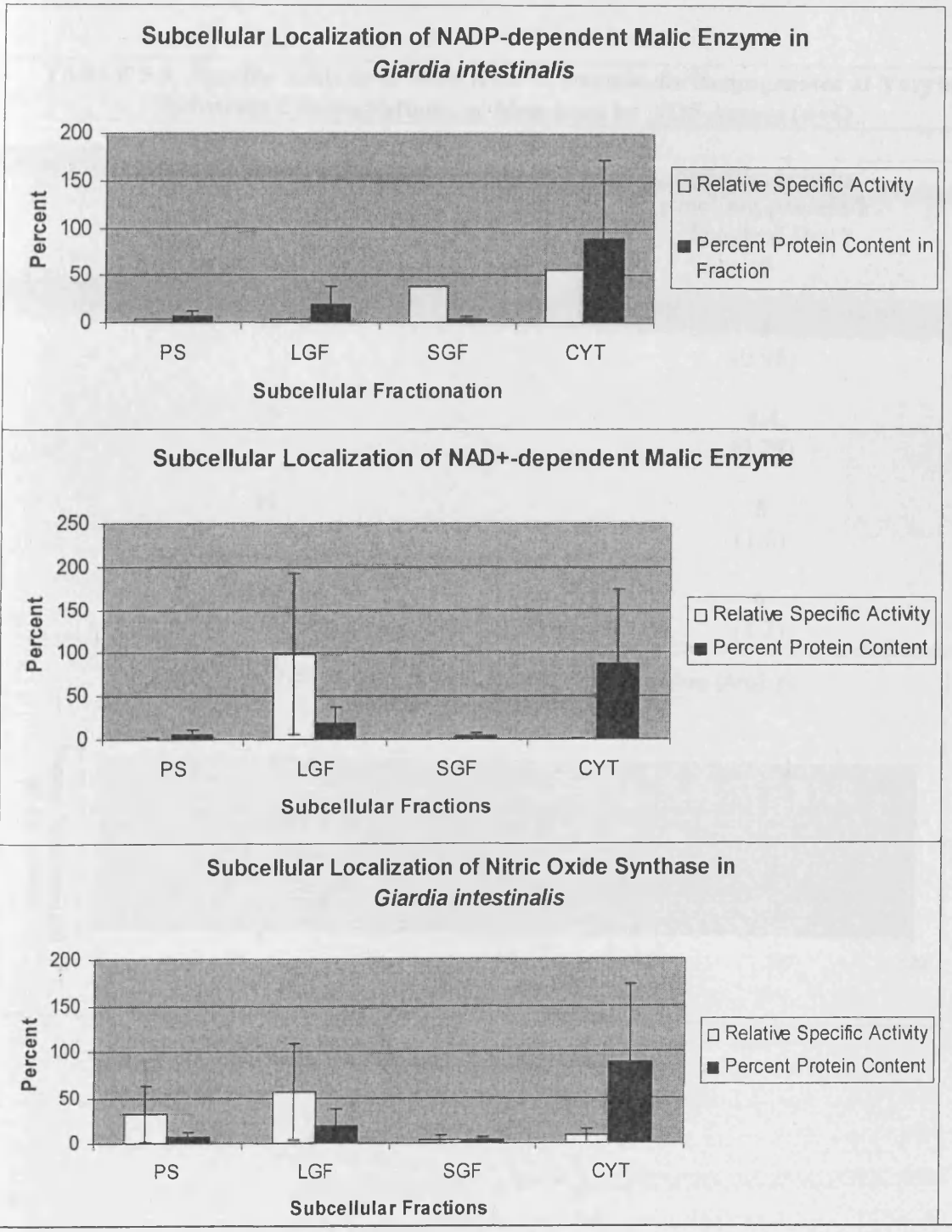

Figure 5.11. Enzyme activities in *Giardia intestinalis*. The top panel displays NADP-dependent malic enzyme (cytosolic marker – i.e non-sedimentable fraction), while the middle panel is the NAD^+-dependent malic enzyme (mitochondrial/hydrogenosomal marker), and the bottom panel displays NOS activities. Error bars represent 95% confidence intervals.
PS = primary sediment; LGF = large granular fraction; SGF = small granular fraction; CYT = non-sedimentable fraction. Marker enzyme procedures: N=3. NOS assays: N=6.

TABLE 5.9: Specific Activity of NOS from *G. intestinalis* Homogenates at Varying Substrate Concentrations, as Measured by NOS Assays (n=6)

Arginine Concentration (mM)	Specific Activity µmol/mg protein/h (Standard Dev.)
5	0
10	4 (0.98)
25	4.4 (0.79)
50	5 (1.6)
100	6 (1.2)

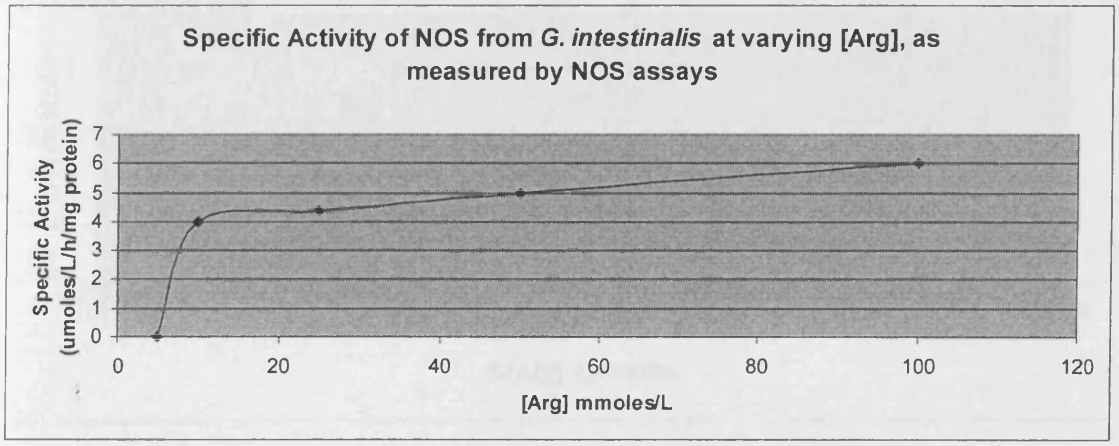

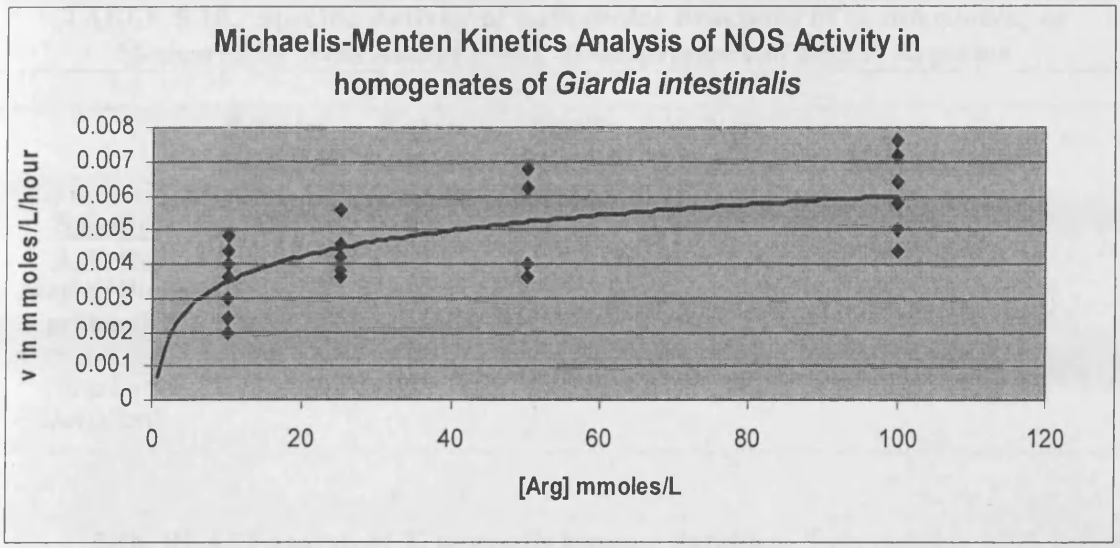

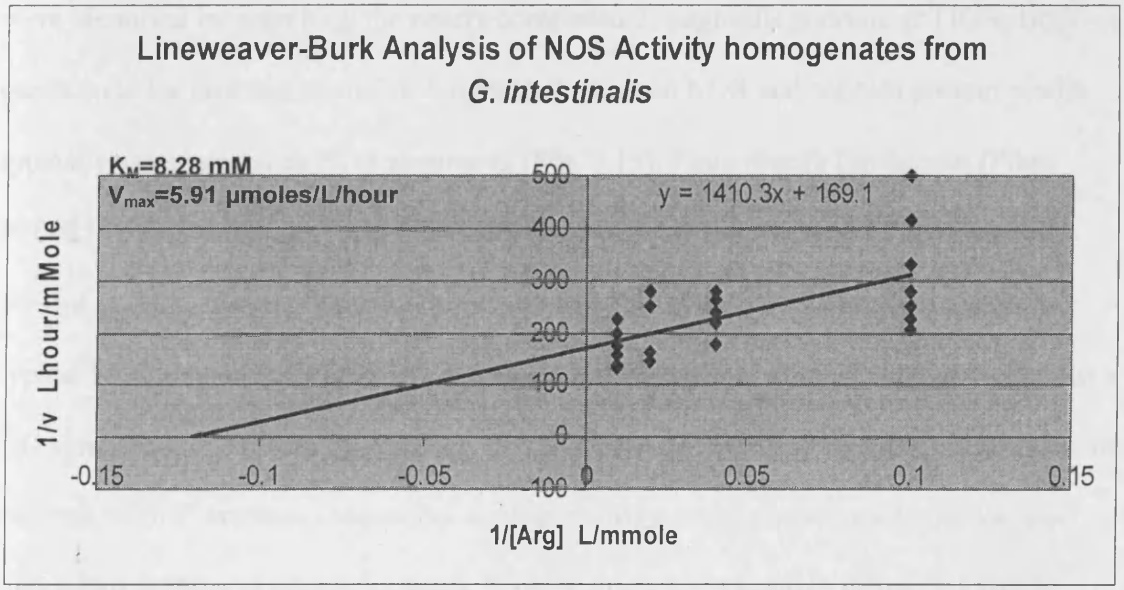

Figure 5.12. Top panel: Michaelis-Menten analysis of NOS assays, varying [Arg]. Bottom panel: Lineweaver-Burk Kinetics of NOS in homogenates of *Giardia intestinalis*, as calculated using NOS assay results. Note that these were based on rates of 1 h, while the NO electrode rates were per min.

TABLE 5.10.: Specific Activity of Subcellular Fractions of *G. intestinalis*, as Measured by NOS Assays (n=6), in the presence of 10mM Arginine					
	Primary Sediment	**Large Granular Fraction**	**Small Granular Fraction**	**Non-Sedimentable**	**Homogenates**
Specific Activity nmoleNO/mg protein/h	**2.6**	**5.6**	**0.4**	**0.4**	**4**
(Standard Deviation)	(1.8)	(1.9)	(0.3)	(0.35)	(0.98)

5.4h. BLAST search of *T. vaginalis* genome database. Two putative NOS genes were identified by searching the nearly completed *T. vaginalis* genome at TIGR. Both genes code for proteins of similar length to the human NOS and contain protein motifs typically associated with NOS sequences (Fig. 5.13). Pfam motifs flavodoxin (Pfam PF00258), FAD binding (Pfam PF00667) and NAD binding (Pfam PF00175) are all present in the C-terminal domain of the putative *T. vaginalis* NOS proteins, similar to typical NOS sequences (Fig. 5.13). However, the N-terminal domain normally contains a NO synthase motif (Pfam PF02898) which is absent from both *T. vaginalis* sequences. In contrast, both *T. vaginalis* sequences contain motifs normally associated with various iron sulfur proteins (Fe-hydrogenase). In order to clarify the nature of the N-terminal domain of these *T. vaginalis* proteins, further nr Genbank database BLASTp searches were conducted using both the N- and C-terminal halves independently. The C-terminal halves of the sequences returned sequences similar to NADPH:P450 reductases as expected for normal NOS sequences. On the other hand, the N-terminal halves of the sequences returned hits to NADH dehydrogenase/NADH ubiquinone oxidoreductase.

This protein is a subunit of Complex I, which, or at least components of this complex, has recently been discovered in *T. vaginalis* (Dyall *et al.*, 2004, Hrdý *et al.*, 2004).

5.4i. BLAST/Gene identification. The gene annotated in the *G. intestinalis* genome as iNOS (accession #AACB01000174) was found to have a high level of homology with iNOS amino acid sequences from *Rattus norvegicus* (accession #AAC13747, $E=4e^{-17}$), *Homo sapiens* (accession #AAC83553, $E=7e^{-17}$), as well as several other *Rattus norvegicus* proteins. A smaller, but still significant, amount of homology was found with *Mus musculus* (accession #NP_035057, $E=1e^{-14}$), *Meriones unguiculatus* (accession #BAD67165, $E=2e^{-13}$), and *Mesocricetus auratus* (accession #ABC96767, E=7e-13), all mammalian organisms. Only the C-terminal domain is conserved in *Giardia intestinalis*, while *T. vaginalis* seems to have swapped the oxidase domain with a NADH dehydrogenase part (Fig 5.13). The terminal three domains of the *Giardia*, *T. vaginalis*, and *Homo sapiens* gene all lined up, although the *G. intestinalis* NAD-binding domain seems to be missing, while the remainder of the protein does not seem to have been conserved in *G. intestinalis*.

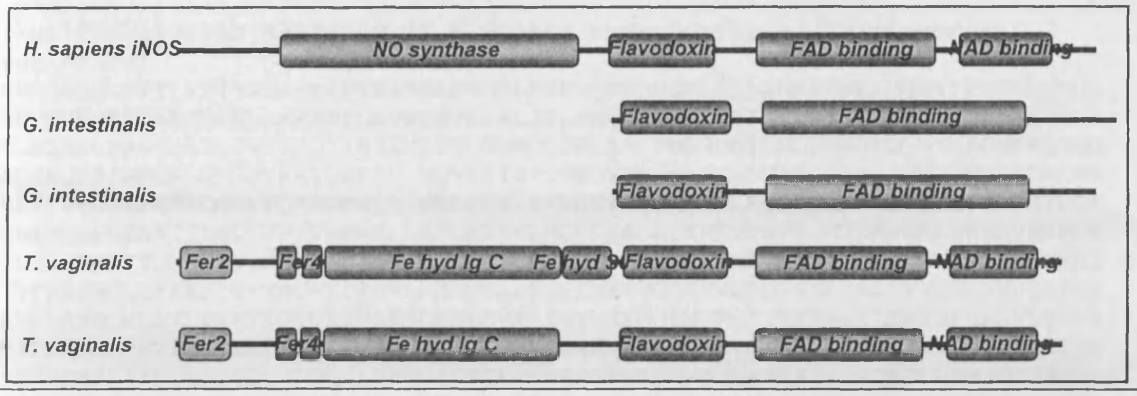

Figure 5.13: Domains of NOS proteins in three organisms: *Homo sapiens*, *Giardia intestinalis*, and *Trichomonas vaginalis*. Note the similarity of the terminal domains. Primary sequence features of the human NO synthase, two putative NO synthases identified on the *T. vaginalis* genome, and one putative NO synthase located in the *G. intestinalis* genome.. Schematic comparison of the *T. vaginalis* and *G. intestinalis* protein sequences with a human NOS indicating the positions and sizes of Pfam (www.sanger.ac.uk/Software/Pfam/) signature motifs PF02898 (NO synthase), PF00258 (flavodoxin), PF00667 (FAD binding) and PF00175 (NAD binding) on the characterized human iNOS sequence. Instead of the typical N-terminal NO synthase motif, the *T. vaginalis* sequences contain the following motifs which could potentially perform the NO releasing chemistry in a haem-protein-deficient organism; PF00111 (Fer2), PF00037 (Fer4), PF02906 (Fe hyd Ig C) and PF02256 (Fe hyd SSU).

5.4j. Motif-searching in genome database of *T. vaginalis*. Two nitrosylation sites were located in the glycogen phosphorylase gene of *T. vaginalis*, and one was located in a protein in the glycogen phosphorylase family (Fig 5.14). These sites constitute four amino acid matches with the motif for nitrosylation. Other matches were found with three amino acid matches (sequences not shown) in pyruvate:ferredoxin oxidoreductase, iron hydrogenase, lactate dehydrogenase isozyme, pyridoxyl-dependent decarboxylase, and pyruvate kinase family protein.

;>gi|18031895|gb|AAL23579.1| glycogen phosphorylase [*Trichomonas vaginalis*]
MSKQAQKLHPTIRPFYPDAKPIPTEAKNASLNTLSHKVQESQGEDLEQARHNLLWKLMGEYIPAEKDSVQL
SFVNHMEYTLARSRFNLDAFSSYLAVSYSVRDRLIELFNDTQEYFISSKAKQVYYVSAEFLVGRFLRNALL
NLELEDLYRKSLAELDVSLDQIYNEEYDPGLGNGGLGRLAACFMDSLATLNLPGWGYGLMYSFGMFKQIIG
ADGSQLEIPDYWLNFGDPWRIQKPTVCHQVHFYGRCENGVWKPSLTINAVANDFLIPGFGTDNTLALRLWS
SKPTVELDEEKFRGGDYFQAITMKQRCENLTSVLYPNDNTYEGKEMRLMQEYFMSSASLQDIIRRLKTHQK
QDIRQLPKYAAIQLNDTHPTVMVAECLRILMDEEDMGLLEALEITRKVFSYTCHTLMPEALEKWDVPMFQN
MLPRHLEIIYQLNQYYLDDVRAKYHVTDDVIRNLSIIEESNPKKVRMANLAVIGSHMVNGVAAIHSELMKI
YVFKDFAQLEPKKFINKTNGVTIRRWLHHCNPALSQIINRVVGDEKWALNAEGLTALTKKQDDRNFIAEWE
AVKLANKQHLAELVKKTTGVELNPEKQLFDIQVKRIHEYKRQQLNIFSIIYRYLNILEMTPAERAKLVPRA
MIFGGKAAPGYYAAKKLIKLINNVAKVVNADKNIGDLLKVVYIPNYNVSAAEIIIPGTDVCEQISTAGTEA
SGTSNMKFAFNGGLIIGTHDGANIEIGDAIGNENVFFFGEVAENVDTYRAAAEHPIPAGLRRVFDTIRTGL
FGDVNEYECLIYPVEHGDNYLVAKDFEDYLDAQRRCDEAYKNKEEWTKMSIASTANMARFSSDRTITEYAN
EVWGIHECKLPVVEPIEASGVQQMGVGSIGGSLRRHQSAAFAEQAPSSNGPTLSKGTYGSLSRKSQIPVPA
AQPVQDSKNDDHDGEIEIDYN

;>101083.m00008|glycogen/starch/alpha-glucan phosphorylases family ;protein|950|Identical to: TigrScan, GlimmerHMM gene predictions
MQNARQKRPTIRPYYPDVKVAPRGVFNSTISSLQRNISKAEGPEHEEARHDLLWKLMGNYIPADKNAIQQS
FVNHFEYTIARSRFNYDSFSAYLAASYSIRDRLIELFNDTQEFFVSSRAKQVYYVSAEFLVGRFLRNALLN
LELEDLYRDSLAELDVSLDDIYNEEYDPGLGNGGLGRLAACFMDSLATLNLPGWGYGLMYSFGMFKQKIAA
DGSQIEIPDYWLNFGDPWRIRKDTITHQVQFYGRTENGVWKPSLTVNAVANDFLIPGFGTDNTLALRLWSS
KPTIELDEEKFRGGDYYDAISMKQRCENLTSVLYPNDNTYEGKEMRLMQEYFMSSASLQDIIRRIKNNYKA
DIHDFPKYAAIQLNDTHPAIMVAELLRILIDQEKIPFIEALDITKQVFSYTCHTLMPEALEKWEIPLFQNM
LPRHLEIIYELNQYFLDDIRSRYRFPVEVIRNLSIIEESNPKKVRMANLAVIGSHMVNGVAAIHTELMKQN
VFKDFYTLEPRKFVNKTNGVTVRRWLHHCNPALSAIITRVCGNESWALNAEGLTELRNKVDDLNFLREWQS
IKLSNKLKLAELVQKTTGIQLDPENQLFDIQVKRIHEYKRQQLNIFSIIYRYISLLELSPEERQNIVPRAM
IFGGKAAPGYWAAKKLLKLINNVANVINNDSRIGNLLKIVFIPNYNVSAAEVIIPGTDVCEQISTAGTEAS
GTSNMKFAFNGALIIGTHDGANIEIGDAIGNENVFFFGELAENVDSYRSSPNKPIPQGLRRVFDLIRTGIF
GERNEYECLIYPIENGDNYLVAKDFDDYIDAQRRCDDVFRSKDEWTRMCITSTANMARFSSDRTISEYAEE
VWNIKEHKLPIVASPDEIATIPTFGIGSISGSLRRHQTAQMKPGEVMATGGYVPKKGSFGSLTKRDKNTKV
VIGVPSTLTPIKESDSEQDDEIPIDFN

Figure 5.14. Nitrosylation Motifs in Glycogen Phosphorylases from *T. vaginalis.* Top panel: Glycogen phosphorylase has two (four amino acids) nitrosylation motifs, labeled in red. One is located at amino acids 248-255, and the other at amino acids 309-312. Bottom panel: glycogen/startch.alpha-glucan phosphorylase has one nitrosylation site at amino acids 309-312.

DISCUSSION

This study has provided evidence of NO production by *T. vaginalis* and *G. intestinalis* trophozoites. The heterogeneity of the confocal images of *T. vaginalis* stained with DAF-FM provides evidence that the level of nitric oxide present in the organisms may be related to cell cycle. Future work will include synchronization of cultures to determine if this is indeed the case. When *T. vaginalis* cultures were incubated in Doran's

Buffer, without carbohydrate or arginine sources, a higher concentration of NO was detected by the NO electrode than with freshly harvested cultures. Perhaps the production of nitric oxide increases as glycolysis substrates become sparse. These results appear to indicate a relationship between NO production and CO_2 liberation in the absence of an exogenous carbohydrate supply (Harris *et al.*, unpublished data). This indicates that NO production activates glycogen phosphorylase activity. Under starvation conditions, *T. vaginalis* produces 800 nmole CO_2/h/10^6 cells (Harris *et al.*, unpublished). However, when organisms under the same conditions were given 5 mM arginine, CO_2 production increased to 2.5 μmoles/h/10^6 cells. Organisms that had been grown with DFMO in the absence of arginine, a potent inhibitor of ornithine decarboxylase, showed diminished CO_2 production to approximately the levels found in controls without arginine present. This observation was confirmed by the elevated nitric oxide production during starvation.

The localization of nitric oxide to the hydrogenosomes of *Trichomonas vaginalis* in many organisms viewed by confocal microscopy supports the conclusions that at some point in the *T. vaginalis* cell cycle, nitric oxide production is localized within the hydrogenosomes. Absence of hydrogenosomal marker enzyme activity in the non-sedimentable fraction suggests only minimal organellar breakage as an explanation of NOS activity in the cytosol. This was confirmed by monitoring hydrogenosome-rich fractions with the NO electrode. The aerobic production of nitric oxide by the hydrogenosomes, together with the images obtained from confocal microscopy indicating a localization of NO production in these organelles, was further confirmed by finding a proportional (%) NOS activity with the majority present in the large granular fraction. Therefore, this evidence supports the presence of two NOS enzymes: one in the cytosol

and another in the hydrogenosomes. Further evidence of their sensitivity to L-NAME, a typical NOS inhibitor, supports the evidence for their existence in *T. vaginalis*. Their insensitivity to L-NNA, another NOS inhibitor has been discovered in this study, and will provide further evidence as to the structure of this particular NOS.

The organellar composition of *G. intestinalis* has been the topic of many studies over the past several decades. Subpellicular bodies present in this organism were originally thought to be mitochondria (Cheissen, 1965). In a study of the organellar components of *G. intestinalis*, a very simplified picture of the organellar composition of this microaerophile was reported (Lindmark, 1980). This study involved the use of harsh conventional techniques of cell breakage, which were later replaced with a more delicate approach (Ellis *et al.*, 1993), at which time a granular fraction was isolated and marker enzyme activity within the fraction located, making subcellular fractionation possible. The subsequent discovery of a redox-generating organelle (Lloyd *et al.*, 2002), followed by the discovery of the mitosome (Tovar *et al.*, 2003) promoted discussions about the possible presence of redox-generating organelles in *Giardia intestinalis* with similarities to both hydrogenosomes and mitochondria.

In the current study, membrane potential-containing organelles were observed on the periphery of the cytosol of *G. intestinalis* when viewed by confocal microscopy after incubation with TMRE, confirming work done in a previous study (Lloyd *et al.*, 2002). Upon conducting marker enzyme assays on subcellular fractions of the organism, it was shown that the activity of NAD^+-dependent malic enzyme predominated in the large granular fraction. Does *G. intestinalis* contain redox balancing organelles? If so, considering the recent finding that these organisms produce hydrogen (Lloyd *et al.*,

2002), and the fact that hydrogenosomes have also been found to produce NO (Harris *et al.*, 2006), it may be that these the redox balancing organelles in *G. intestinalis* are a type of hydrogenosome. Fluorescent antibodies prepared from hydrogenosomal proteins have been incubated in *G. intestinalis*, but no specific interaction with a particular organelle was observed (Lloyd *et al.*, 2002). This negative result may be an indication that the proteins in hydrogenosomes from *T. vaginalis* are too different from those in any organelle in *G. intestinalis* for antibodies to bind.

The production of NO by the large granular fraction of *G. intestinalis* supports the presence of a redox-generating organelle. The heterogeneity of the confocal images stained with DAF-FM led us to believe that the level of nitric oxide present in the organisms may be related to cell cycle. The localization of nitric oxide to the periphery of the organism in many of the organisms viewed, which is where the redox balancing organelles of *G. intestinalis* were observed in our study as well as one previous study (Lloyd *et al.*, 2002), allowed us to conclude that at some point in the organism's cell cycle nitric oxide production was localized within these organelles. This was confirmed by monitoring the large granular fraction with the NO electrode. The production of nitric oxide by these redox-balancing organelles in *G. intestinalis*, together with the images obtained from confocal microscopy indicating a localization of NO production within these organelles, suggested that NOS activity would be found primarily in the large granular fraction; this was confirmed by the results obtained from NOS activity assays.

When the *T. vaginalis* genome, currently being sequenced at TIGR (http://www.tigr.org/tdb/e2k1/tvg/), was searched using a human NOS, two potential NOS encoding genes were identified. To validate their potential NOS status, both

sequences were used to search the nr GenBank databases; in each case, NOS sequences were retrieved as significant hits. However, in contrast to classical NOS, the trichomonad sequences seemed to have exchanged their N-terminal domain for another protein (Fig 5.13). Normally, the N-terminal domain of NOS, in conjunction with heme proteins, encodes the NO-producing protein (Alderton *et al.*, 2001). In the case of the *T. vaginalis* sequences, the N-terminal domain is similar to NADH dehydrogenase/NADH ubiquinone oxidoreductases and Fe-hydrogenases. Domain-swapping is relatively common and has been observed before in iron sulfur proteins such as, for example, a putative Fe-hydrogenase in the hydrogenosome-containing ciliate *Nyctotherus ovalis*; there the Fe-hydrogenase is fused at the C-terminus to mitochondrial complex I subunit domains (Akhmanova *et al.*, 1998). Since two similar sequences were identified in the *T. vaginalis* genome, originating from different contigs, I am confident these sequences are not sequence artifacts but genuine open reading frames.

If one had to 'invent' a potential protein domain which would have been capable of taking over the role of the usual N-terminal domain in NOS in an organism that does not contain heme proteins, then the two genes identified are in line with one that could be created based on mechanistic theories. The di-iron center of the H-cluster found in Fe-hydrogenases (Fig 5.13) could be capable of performing the kind of chemistry required to produce NO. Although hydrogenases are typically inactivated by oxygen, diiron centers are capable of activating oxygen in a similar manner to heme, and are employed to do such in ribonucleotide reductases and other enzymes. Thus, proteins containing a diiron/Fe-S site similar to that of the Fe-only hydrogenases would bear the only cofactor known to be able to duplicate the heme-based chemistry of NOS. It has to be said that no

such mechanism has been detected or studied before. Further studies will be required to understand this novel protein and how the mechanism of NO release operates. A possible function for the nitric oxide produced by this NOS may be as the missing effector in regulating carbohydrate metabolism. This theory is supported by the presence of nitrosylation sites in the glycogen phosphorylase as well as a glycogen/starch alpha-glucan phosphorylase of *T. vaginalis*. Further work must be done to determine whether these nitrosylation sites function in this way, and whether the other proteins with possible nitrosylation sites (with only three amino acid matches) may also be regulated by NO.

The gene for an inducible NO-synthase (iNOS) in the published genome of *Giardia intestinalis* (accession # AACB01000174) was found to have homology with several NOS genes from mammalian organisms, including several conserved domains with *Homo sapiens* (Fig 6.7). Mitochondria have NOS activity, and have been shown to produce nitric oxide (Ghafourifar & Richter, 1997). The fact that redox-generating organelles from *G. intestinalis* produce NO and contain an active NOS, just like mitochondria in eukarytotic organisms, suggests that these organisms are not 'primitive', but are in fact more complex than originally thought, and may have evolved from organisms containing mitochondria which adapted to living in anaerobic environments, as has been postulated by several other groups (Biagini *et al.*, 1997; van der Giezen *et al.*, 2005). Future work will include the determination of whether all three of the genes located in these organisms contain mitochondrial leader sequences, which would help to determine and further confirm their location in the respective organism. In addition, primers will be created, and recombinant proteins produced using an expression system

to create antibodies. Western Blotting will determine the viability of this protein as a NOS.

Interestingly, mammalian ornithine decarboxylase cysteine (360) in the active site is nitrosylated, resulting in the inhibition of enzyme activity (Bauer *et al.*, 2001). This specific cysteine residue is also responsible for binding DFMO, the irreversible competitive inhibitor of ornithine decarboxylase (Bauer *et al.*, 2001). This cysteine residue is also conserved in the *Trichomonas vaginalis* ornithine decarboxylase, suggesting that nitric oxide may regulate ornithine decarboxylase activity in this species via *S*-nitrosylation as well.

NO synthases are traditionally associated with a guanalyl cyclase which is tightly associated with a heme group. This guanalyl cyclase is induced when NO binds to the heme group and activates cGMP production. Since *G. intestinalis* lacks the heme proteins necessary for NOS enzymes to function, it is clear that the mechanism of the NOS in *G. intestinalis* differs from those in other eukaryotic cells. This is not unprecedented, as plant cells have been found to contain NOS enzyme activity, cross-reactivity with mammalian NOS antibodies. Although sensitivity to mammalian NOS inhibitors have been detected in these plant cells, no gene or protein was found with sequence similarity to a known mammalian-type NOS. This suggests that plants contain a completely different NOS enzyme (Garcia-Mata *et al.*, 2003; Butt *et al.*, 2003). The levels of homology of the NOS in *G. intestinalis* with NOS genes from mammalian organisms supports the theory that *G. intestinalis* should be allocated a new, higher taxonomic crown, and is not 'primitive', as it has often been asserted.

Mitochondria display NOS activity, and have been shown to produce nitric oxide (Ghafourifar & Richter, 1997; Giulivi *et al.*, 1998; Nisoli *et al.*, 2006; Kato *et al.*, 2006). The fact that hydrogenosomes from *T. vaginalis* and the granular fraction from *G. intestinalis* produce NO and contain an active NOS, supports their similarities to mitochondria in mammals and other organisms. This suggests that *T. vaginalis* and *G. intestinalis* evolved from a lineage which has witnessed the mitochondrial endosymbiosis (Biagini *et al.*, 1997; van der Giezen *et al.*, 2005; Richards & van der Giezen, 2006). Whilst the NOS in mitochondria was originally thought to be an inducible NOS (iNOS) or a neuronal NOS (nNOS), it has most recently been shown to have a structure unique from the other known NOS enzymes (Lacza *et al.*, 2003).

The presence of an active NO-synthase in this parasitic protozoan, along with other studies that have shown the presence of NOS activity in *Entamoeba histolytica* (Hernandez-Campos *et al.*, 2003), *Trypanosoma cruzi* (Paveto *et al.*, 1995), and *Leismania* (Genestra *et al.*, 2003) suggests that parasitic protozoa, in general, may produce nitric oxide. There are many reasons why these parasites would find it beneficial to produce nitric oxide. It has been shown that nitric oxide has the ability induce apoptósis in HL-60 cells (Wang *et al.*, 2006); the parasite could be using the gas as a defense mechanism against the host's immune response. Furthermore, nitric oxide, a potent vasodilator, may be responsible for a rush of nutrients from the blood vessels of the host, thereby facilitiating parasite survival, especially when near-starvation has resulted in depletion of its amino acid pools. Another possibility is that the parasite may be producing nitric oxide to induce its own apoptosis mechanism; if this was the case, this would be an indication that these organisms function as a community.

CHAPTER 6: Phospholipids of the microaerophilic protozoal flagellate, *Trichomonas vaginalis*

6.1 Summary.

Lipid composition of the sexually transmitted flagellate protist, *Trichomonas vaginalis*, showed the following (% total) distribution of polar lipids: phosphatidyl-ethanolamine (30%), phosphatidylcholine (9%), phosphatidylglycerol (7%), phosphatidylserine (7%), phoshpatidic acid (3%), dimethyl-phosphatidylethanolamine (2%), and phosphatidylinositol (9%). Two unusual constituents were acylphosphatidylglycerol (26%) and ceramide phosphorylethanolamine (7%). The two unusual lipids were subjected to both single-stage electrospray ionization mass spectrometry (ESI-MS) and tandem ESI-MS for structural analysis. For acylphosphatidylglycerol, the peak at m/z 1013 gave fragments at m/z 281, 283, and 255 representing stearic, oleic and palmitic acids, respectively. A fragment ion at 749 corresponded to 16:0/18:1 phosphatidylglycerol, and those at 757 and 729 indicated neutral losses of palmitic and stearic acids, respectively. For ceramide phosphoryl-ethanolamine (m/z 661), palmitic acid was the amide-linked fatty acid of the phosphoceramide (m/z 617), whereas stearic acid and ethanolamine were the other fragments detected. The structure finally assigned corresponded to N-(hexadecanoyl)-sphing-4-enine-1-phosphoethanolamine. Cardiolipin was not detected on thin layer chromatography (TLC) plates, nor by ESI-MS of total lipid eluates from TLC plates, although an authentic standard gave the expected negative ion $(M-H)^-$ at m/z 1470. These data are discussed in relation to the unusual lifestyle of the organism and its phylogenetic status.

6.2. Introduction.

Hydrogenosomes from *T. vaginalis*, now realized to be evolved forms of mitochondria (Biagini *et al.*, 1997), rely solely on substrate-level phosphorylation to produce energy, and do not perform oxidative phosphorylation, the major characteristic of mitochondria (Chance & Williams, 1956). Cardiolipin (CL) (diphosphatidylglycerol) is a key constituent of the inner mitochondrial membrane, where it is essential for normal mitochondrial function, e.g. electron transport and oxidative phosphorylation. Since cardiolipin binds nonyl acridine orange, this fluorophore has been widely used as a marker when studying structural and physiological characteristics of mitochondria (Septinus *et al.*, 1983; Jacobson *et al.*, 2002).

The presence or absence of cardiolipin in hydrogenosomes of trichomonads has been a debate for several decades. Čerkasovová and co-workers reported identification of this lipid in hydrogenosomes isolated from the cattle parasite *Tritrichomonas foetus* (Čerkasovová *et al.*, 1976), although subsequently this could not be confirmed (Paltauf & Meingassner, 1982). In this second study, an analysis of lipids of cell homogenates and hydrogenosome-enriched fractions from *T. vaginalis* and *T. foetus* by using one- and two-dimensional thin-layer chromatography determined that cardiolipin was not detectable. However, the presence of an unusual phosphoglycerolipid was noted which may have been misidentified as cardiolipin in the previous study. It was suggested that this unusual phosphoglycerolipid was O-acylphosphatidylglycerol (Acyl-PG), and its structure was later confirmed by negative-ion liquid secondary ionization mass spectrometry (Costello *et al.*, 2001). Recently another research group claimed to have shown that *Tritrichomonas foetus* contains cardiolipin (de Andrade Rosa *et al.*, 2006). Since fully functional

mitochondria characteristically contain cardiolipin (McMillin & Dowhan, 2002), if mitochondria-like organelles from *T. vaginalis* were also found to contain this lipid, the evolutionary relationship between mitochondria and hydrogenosomes would be clarified.

Trichomonads have developed unique metabolic pathways that allow them to survive and multiply in reproductive tracts by scavenging nutrients from their hosts (Smith, 1993; Das *et al.*, 2002). Experiments using [U-^{14}C] glucose labelled choline-containing lipids in *T. vaginalis*, with phosphatidylethanolamine again being heavily labeled, indicated the extent of precursor scavenging (Beach *et al.*, 1991). They concluded that biosynthesis of PE proceeds totally, whereas that of PC as well as phosphatidylinositol, PS, PG and Acyl-PG showed a major deficiency. Moreover, only a limited potential for exchange reactions and turnover was shown for labeled phosphoglycerides incorporated directly from the environment. Thus trichomonads probably lack many of the enzymes involved in complex phosphoglyceride metabolism (Beach *et al.*, 1991).

However, trichomonads can synthesize glycolipids and glycophosphosphingolipids *de novo* (Singh *et al.*, 1991). Two major ethanolamine phosphate-substituted inositol phosphosphingolipids have been identified in the unsaponifiable acidic fractions of *T. foetus* and *T. vaginalis* by a combination of MS-MS and nuclear magnetic resonance (NMR) (Costello *et al.*, 1993). The authors suggested that these glycosphingolipids may represent metabolic intermediates for new types of membrane anchors for surface glycopeptides or glycolipids that mediate the host-parasite relationship of these trichomonads (Costello *et al.*, 1993).

The aim of the present work was to use state-of-the-art techniques to analyze the lipid composition of extracts from *T. vaginalis* in order to resolve the conflicting claims of previous work regarding the presence of cardiolipin. This constituent was not detected. However an unusual lipid, N-(hexadecanoyl)-sphing-4-enine-1-phosphoethanolamine, was characterized.

6.3. Materials and Methods.

6.3a. Confocal microscopy.

Living *T. vaginalis,* stained with 5μM nonyl-acridine orange (NAO) and immobilized with 2% (w/v) methyl cellulose, were applied to poly-L-lysine-coated slides. Fluorescent signals from NAO were collected on a Zeiss Pascal confocal microscope through a Plan-Apochromat 63x 1.4 N.A. water objective. Excitation of NAO was performed using an argon ion laser at 488 nm. Emitted light was reflected through a 505–550-nm band pass filter from a 540-nm dichroic mirror.

6.4. Results.

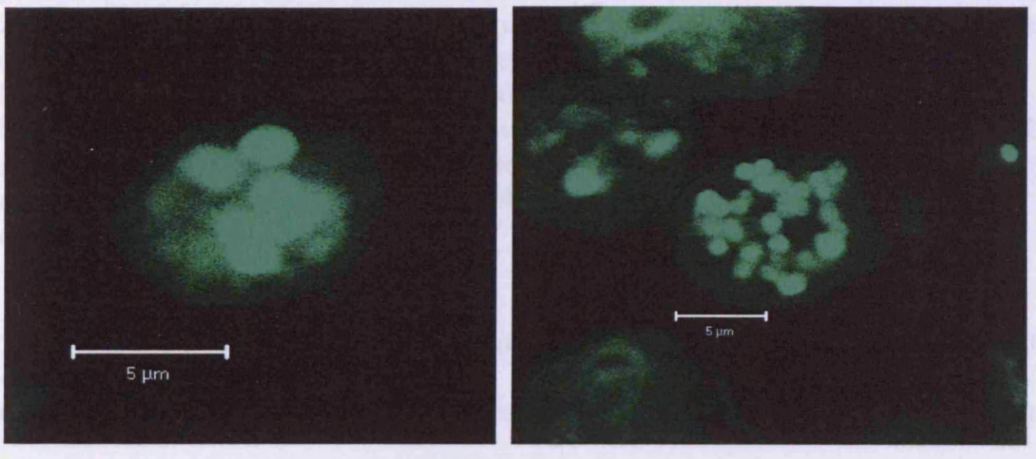

Figure 6.1. Images of *T. vaginalis* after incubation with NAO, a fluorophore known to specifically congregate in mitochondria by associating with cardiolipin, showed a localization of the fluorophore in the hydrogenosomes.

6.4a. Confocal microscopy. When viewed by confocal microscopy *T. vaginalis* organisms incubated with 5μM nonyl-acridine orange (NAO), a fluorophore which accumulates within mitochondria by binding to cardiolipin, showed a localization in the hydrogenosomes (Fig 6.1). This evidence alone would suggest the presence of cardiolipin in this redox-balancing organelle, but only if one can assume absolute specificity of this fluorophore's interaction. Further analysis of the lipid composition fails to show this lipid in *T. vaginalis*, suggesting this fluorophore is not absolutely specific.

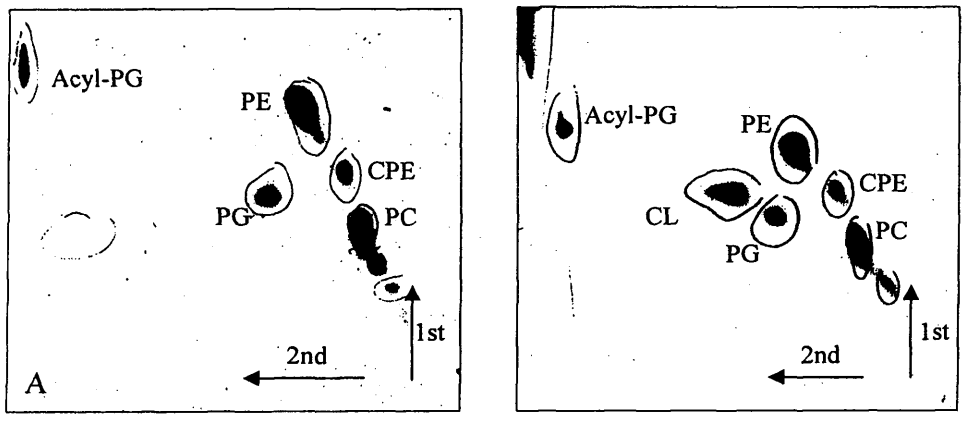

Figure 6.2. Two dimensional TLC-separation of total lipids from *T. vaginalis* (A) and total lipids from *T. vaginalis* plus cardiolipin (CL) standard added (B). A clear additional spot of cardiolipin appeared in B. Lipids were separated using chloroform/methanol/water (65:25:4, by vol.) in the first dimension and then chloroform/acetone/methanol/acetic acid/water (50:20:10:10:5, by vol.) in the second direction. Abbreviations: PE, phosphatidylethanolamine; PC, phosphatidylcholine; PG, phosphatidylglycerol; Acyl-PG, acylphosphatidylglycerol; CPE, ceramide phosphorylethanolamine; CL, cardiolipin.

6.4b. Lipid analysis. Analysis of individual polar lipids from *T. vaginalis* by two-dimensional thin-layer chromatography gave no evidence for the presence of cardiolipin in *T. vaginalis* (Fig 6.2). When a standard of cardiolipin was co-applied on a TLC-plate together with an aliquot of total lipid extract, it appeared distinctly separated from the

other lipids (PG and PE) (Fig 6.2B). In order to identify all polar lipids, TLC-plates were sprayed with various specific color reagents (Kates, 1986). Lipids containing phosphorus (PC, PE, PG, PI, PS, PA, DM-PE as well as two unusual lipids further identified as ceramide phosphorylethanolamine and Acyl-PG were identified by using Zinzade's reagent, which contains phospholipase DM. This will react with phospholipids (i.e. those lipids containing phosphorus) to produce a primary or secondary alcohol derivative. PC gave a positive reaction with the "Dragendorff" reagent, which is used to detect alkaloids and other nitrogen compounds. The presence of amino groups in PE, PS and ceramide phosphorylethanolamine was detected with the aid of a ninhydrin spray. All three of these sprays change color upon reacting with these specific structures. The quantitative analysis of these lipids are illustrated by Fig. 6.3. Similar to previous studies, PC and PE were the major polar lipids in *T. vaginalis*, although the amount of Acyl-PG was higher (26%) according to this study (Fig 6.3) than previously determined for this organism (about 6%) (Das *et al.*, 2002).

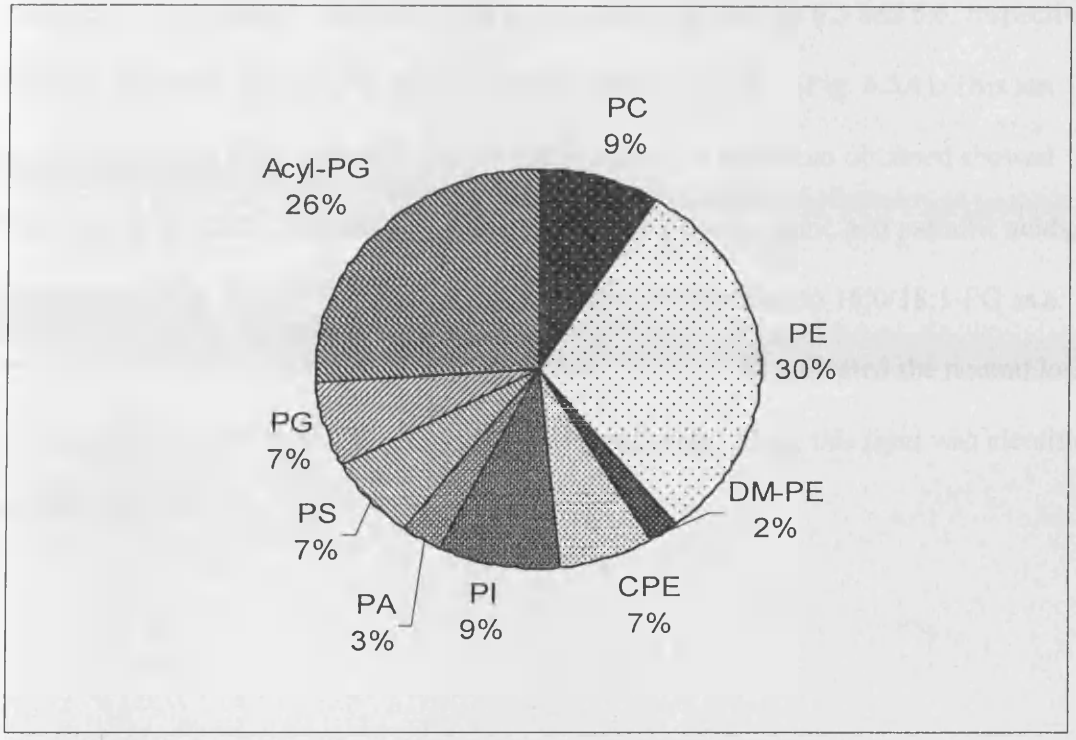

Figure 6.3. The relative (% of total) distribution of polar lipids from *T. vaginalis*. Abbreviations: PE, phosphatidylethanolamine; PC, phosphatidylcholine; PG, phosphatidylglycerol; Acyl-PG, acylphosphatidylglycerol; CPE, ceramide phosphorylethanolamine; DPG, diphosphatidylglycerol; PI, phosphatidylinositol; PS, phosphatidylserine; DM-PE, dimethyl-phosphatidylethanolamine; PA, phosphatidic acid.

In order to allow the precise structural identification of polar lipids found in *T. vaginalis*, ESI-MS and ESI-MS/MS analysis was used. By injecting an aliquot of total lipid extract into the ESI chamber, mass spectra obtained gave molecular weight information on all lipids present in *T. vaginalis* (Fig 6.4B). As expected from TLC data, no signal corresponded to that obtained by a cardiolipin standard (*m/z* 1470 $(M-H)^-$) (Fig 6.4A). Moreover, none of the individual lipids (which were eluted from TLC plates and analyzed separately in the same manner, in the single stage MS mode) showed a peak corresponding to cardiolipin (data are not shown).

Single-stage ESI-MS and tandem ESI-MS analysis were used to characterize the structure of two uncommon lipids found in *T. vaginalis*. Negative ion mass spectra from

ESI-MS for these lipids, Acyl-PG and Cer-PE, are given in Figs 6.5 and 6.6, respectively. ESI-MS spectrum of Acyl-PG showed a base peak at *m/z* 1013 (Fig. 6.5A). This ion signal was further fragmented in ESI-MS/MS mode. The spectrum obtained showed fragments at *m/z* 281, 283 and 255 which represented stearic, oleic and palmitic acids, respectively (Fig. 6.5B). The fragment ion at 749 corresponded to 16:0/18:1-PG as a structural part of the molecule. The fragments at 757 and 729 indicated the neutral losses of 256 (palmitic acid) and 284 (stearic acid), respectively. Thus, this lipid was identified as Acyl-PG.

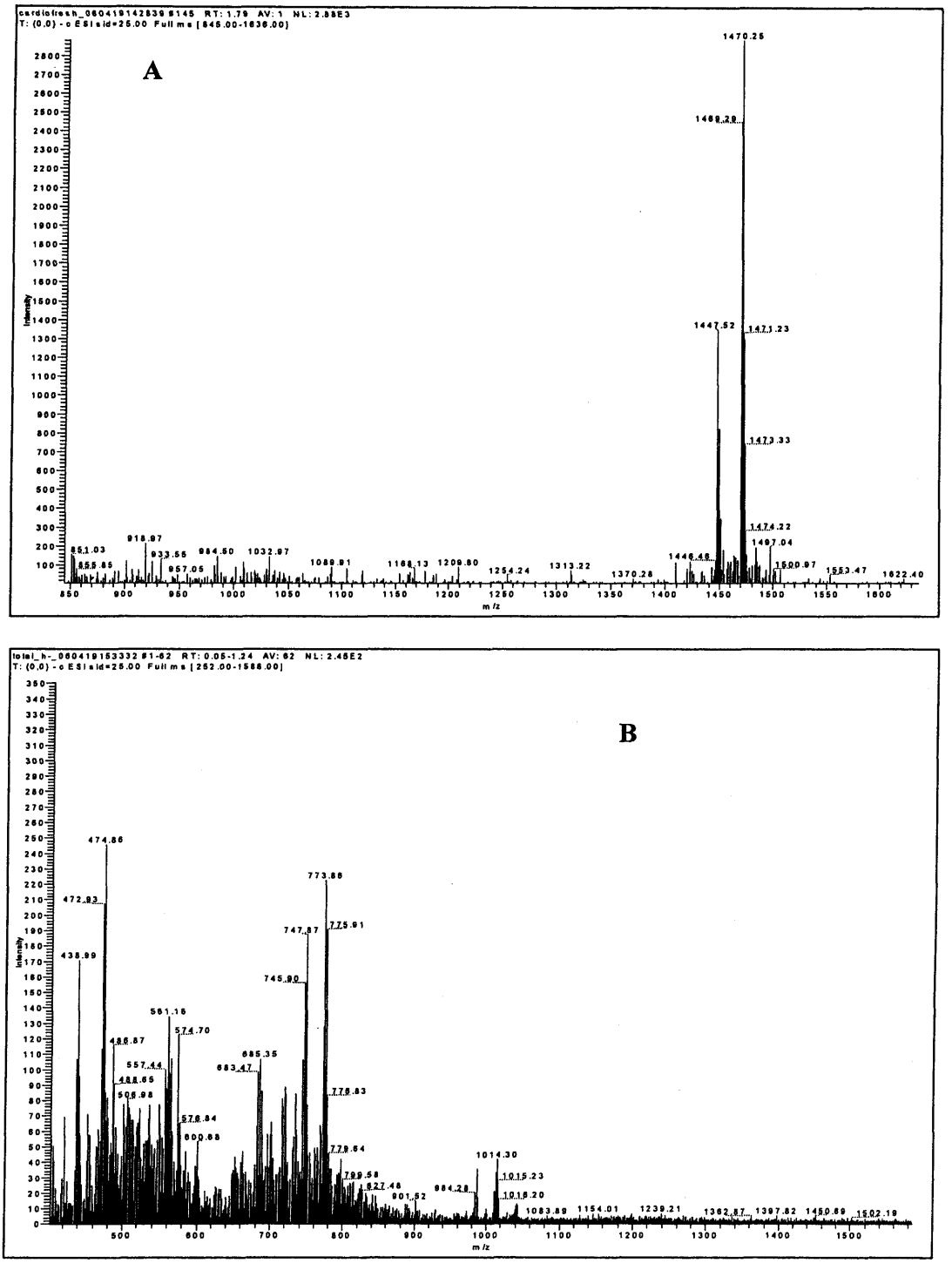

Figure 6.4. Negative ion ESI-MS spectrum of cardiolipin standard (A) and total lipid extract from *T. vaginalis* (B).

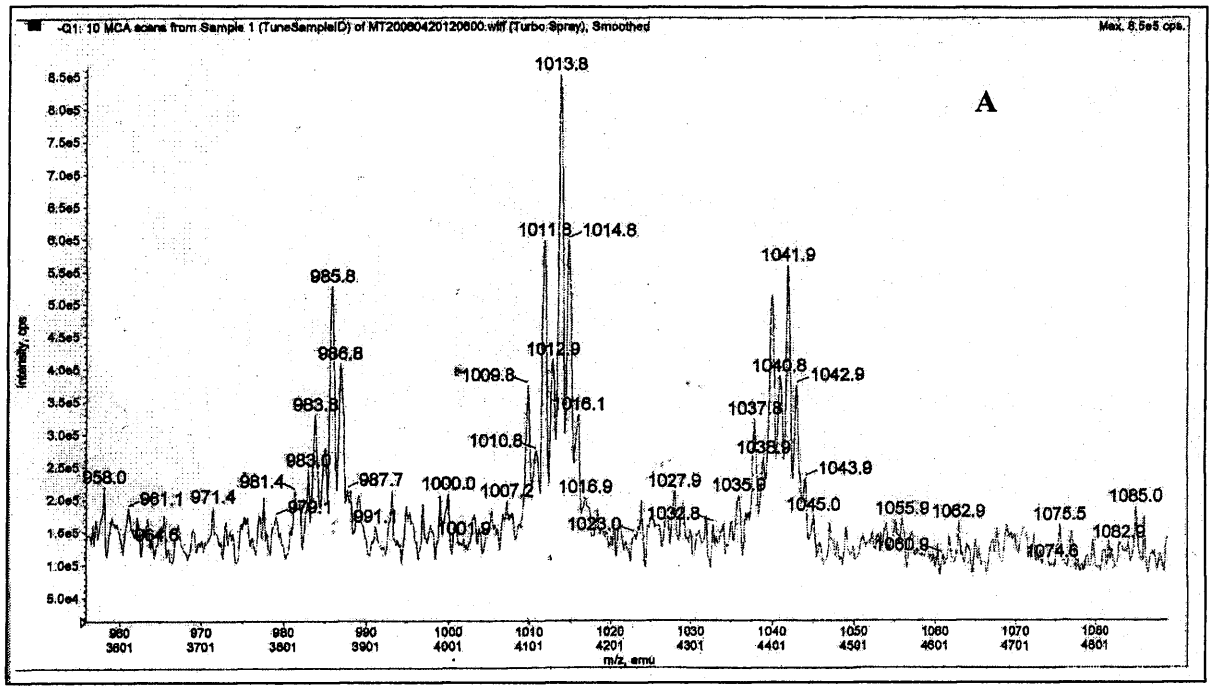

Figure 6.5. Negative-ion ESI-MS (A) and ESI-MS/MS (B) spectrum from the precursor ion at *m/z* 1013 of Acyl-PG from *T. vaginalis*. For product ion assignment, see the text.

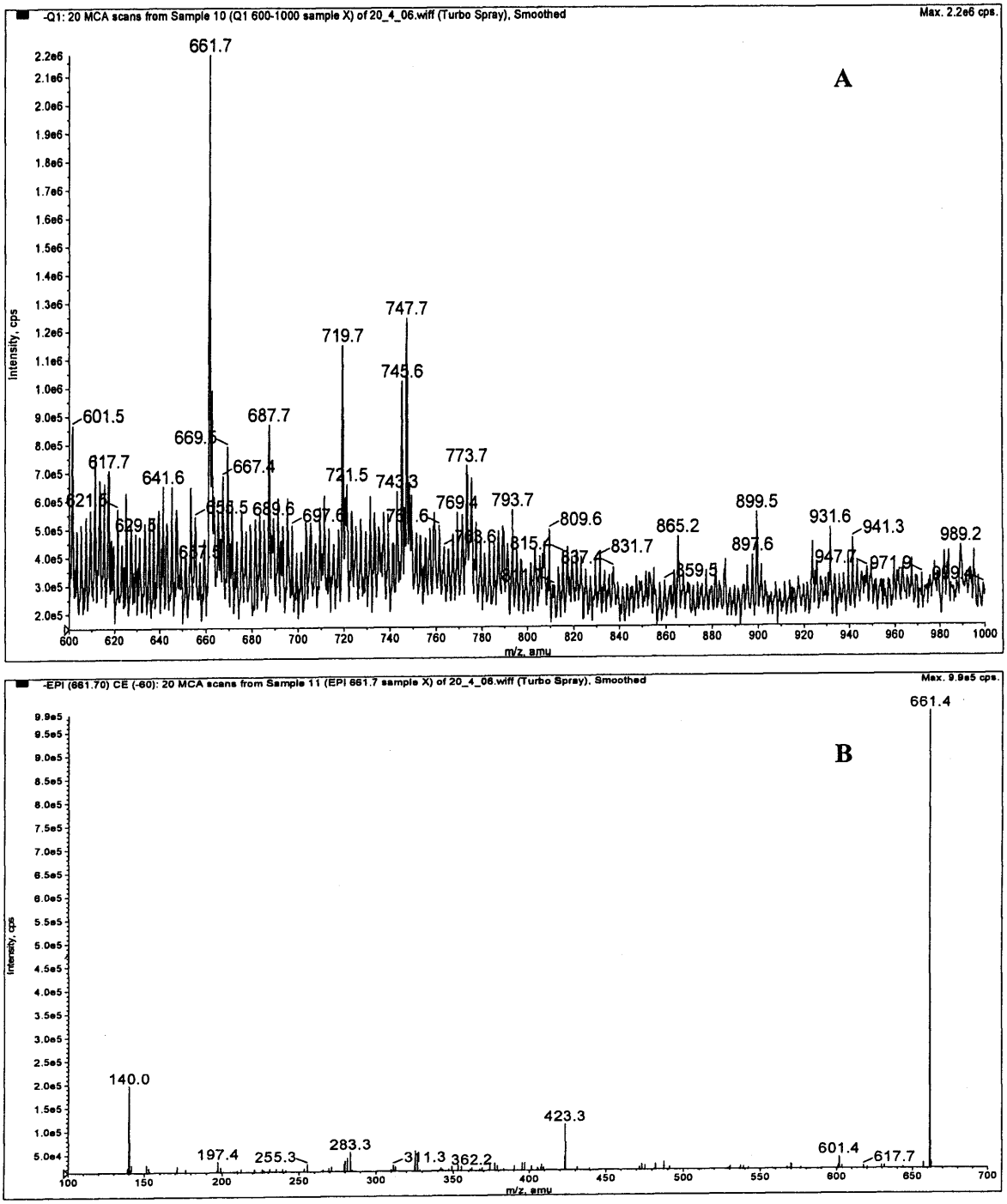

Figure 6.6. Negative-ion ESI-MS (A) and ESI-MS/MS from the precursor ion at *m/z* 661 (B) spectra of ceramide phosphorylethanolamine from *T. vaginalis*. For product ion assignment, see the text.

Only one major base peak at *m/z* 661 was detected when another unknown lipid, Cer-PE, was analyzed in a single-stage mode (Fig. 6.6A). The molecular mass of 661 corresponded to the suggested structure of this compound as ceramide phosphorylethanolamine with palmitic acid as the amide-linked fatty acid and a 18-carbon di-OH sphingoid base, and the further MS/MS fragmentation further confirmed this suggestion (Fig. 6.6B). The spectrum showed a phosphoceramide fragment at *m/z* 617 indicating a neutral loss of 44 (ethanolamine), a fragment at *m/z* 601 indicating a neutral loss of 60 (ethanolamine with an oxygen attached) as well as two fatty acid fragments at *m/z* 283 (stearic) and 255 (palmitic). A fragment ion at low mass, *m/z* 140, can be assigned to the phosphoethanolamine anion (Fig. 6.6B). The ion fragments at 423 indicate the neutral loss of 238 as a result of cleavage of long chain bases C(2) (carbon linked to amide group) – C(3) (carbon with hydroxyl group). Thus, based on data provided by tandem mass spectral analysis, the structure of this lipid was elucidated as N-(hexadecanoyl)-sphing-4-enine-1-phosphoethanolamine (Fig. 6.7).

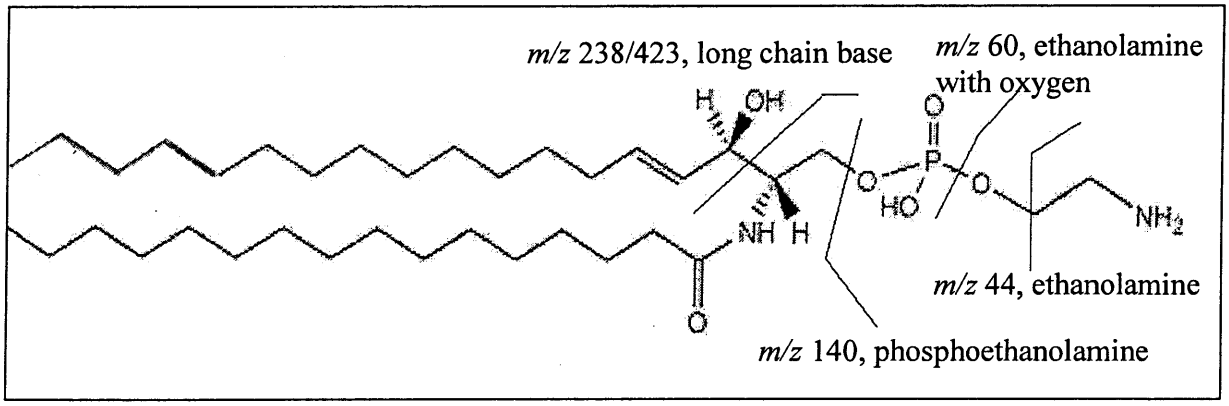

Figure 6.7. The major fragments derived from *m/z* 661 of ceramide phosphorylethanolamine (N-(hexadecanoyl)-sphing-4-enine-1-phosphoethanolamine).

7.5. Discussion.

Trichomonads have been regarded as early-branching eukaryotes, but much debate has ensued as a result of this classification. The origin of hydrogenosomes in *T. vaginalis* has been postulated to have occurred as the result of either an endosymbiosis of an anaerobic eubacterium with an eukaryotic host (Martin & Müller, 1998; Martin *et al.*, 2001) or the conversion of a mitochondrion to an anaerobic lifestyle (Biagini *et al.*, 1997; Embley *et al.*, 2003). The relationship of mitochondria to hydrogenosomes has been much studied and debated, but evidence has been presented to support both hypotheses. When *T. vaginalis* was incubated with nonyl acridine orange and viewed by confocal microscopy, the fluorophore accumulated within the hydrogenosomes, indicating the presence of cardiolipin in the organism. Other studies have concluded that NAO often binds non-specifically (Gohil *et al.*, 2005), suggesting that the binding of NAO to the hydrogenosomes may not have been due to the presence of cardiolipin.

Subsequent lipid analysis revealed that cardiolipin could not be detected in *T. vaginalis;* this tends to support the idea that fully functional mitochondria are not closely related to hydrogenosomes. However, the undetectability of cardiolipin alone does not invalidate the theory that hydrogenosomes are evolved forms of mitochondria. It is likely that the hydrogenosome no longer requires cardiolipin, as it lost many of its functional components (e.g. cytochromes and ATP synthases) (Lloyd *et al.*, 1979a & b) when the organisms adapted to microaerophilic conditions.

The presence of an unusual lipid, Acyl-PG, in *T. vaginalis* has already been verified by negative-ion liquid secondary ionization MS and collision-induced decomposition MS/MS (Paltauf & Meingassner, 1982). In this work, the presence of this rare lipid was

confirmed and its structure was proved by ESI-MS/MS. Moreover, this work showed that Acyl-PG accounted for 26% of total polar lipids and was, together with PE, PC and PI, one of the major lipid compounds in *T. vaginalis*. As mentioned in previous studies (Paltauf & Meingassner, 1982; Costello *et al.*, 2001), the presence of PG and Acyl-PG in *T. vaginalis* is rare in eukaryotes, and when they are present in other organisms their percentage in relation to a given organism's overall lipid composition is very small. Future work is required to establish their metabolic production and functions, and why such large quantities are present in *T. vaginalis*.

T. vaginalis are also unique in that they can synthesize glycophosphosphingolipids (Singh *et al.*, 1991). Two major ethanolamine phosphate-substituted inositol phosphosphingolipids have been identified in the unsaponifiable acidic lipid fraction of *T. vaginalis* (Costello *et al.*, 1993). It has been suggested that these lipids represent metabolic intermediates for new types of membrane anchors for surface glycopeptides or glycolipids that mediate the host-parasite relationship of this organism (Costello *et al.*, 1993). In the present study, another component representing a class of ceramides was identified: ceramide phosphorylethanolamine. This lipid, which is a sphingolipid analogue of phosphatidylethanolamine, was first discovered in the housefly, *Musca domestica* (Crone & Bridges, 1963). Shortly thereafter, it was identified in bacteria (*Bacteroides ruminicola* and *B. melanogenicus)* as well as in some protozoa, snails, marine bivalves, insects and also chicken and rat liver (Broad & Dawson, 1973). In recent studies, this lipid was isolated from three species of oomycete plant pathogens (Moreau *et al.*, 1998) and from several species of *Sphingobacterium* (Naka, 2003).

The physiological roles of sphingolipids in mammalian cells (as ubiquitous compounds of eukaryotic cell membranes) are well-known, and include involvement in cell differentiation, proliferation and receptor-mediated endocytosis (Minamino *et al.*, 2003). Ceramides have been shown to be important second messengers in intracellular signal transduction systems, and also play a crucial role in the induction of apoptosis (Minamino *et al.*, 2003). Further investigation is needed to reveal the specific role of these lipids in *T. vaginalis*, especially in order to discover whether Cer-PE plays a role in trichomonad-host interactions.

CHAPTER 7

DISCUSSION

7.1 DFMO as an inhibitor of polyamine synthesis in *T. vaginalis.*

This work has shown the importance of the pathways of polyamine synthesis for maintenance of full functionality in *Trichomonas vaginalis*. When organisms were grown overnight in the presence of 5mM DFMO: voltage-sensitive dye uptake into hydrogenosomes decreased, electron-dense inclusions appeared in greater numbers in hydrogenosomes, and the oxygen consumption rates of hydrogenosomes increased by approximately two-fold. In short, hydrogenosomal function was affected by the inhibition of the polyamine synthesis pathway. The experimental use of 5mM DFMO was not based on therapeutic concentrations used for treatment of patients, but rather used as a tool for this study of polyamine metabolism. Examining differences between organisms with a functional ODC and those without provided information on the bioenergetics of the organism that may be used for future drug treatments, although that was not the primary goal of this study. Quantification of the electron-dense inclusions and altered membrane potentials of hydrogenosomes will require more TEM and confocal images depicting multiple organisms in the same field of view for better comparison. Direct membrane potential measurements will require patch clamp technique, not yet used on these highly motile organisms. This technique presents many challenges, and has never before been used on these organisms.

Polyamine depletion by DFMO, due to inhibition of ODC, also caused inhibition of the arginine dihydrolase pathway. This reduction in enzymatic activity could have serious implications for the organism, not only with respect to polyamine synthesis, but

perhaps more importantly would result in reduced ATP formation. Anabolic ornithine carbamyltransferase activity, on the other hand, increased, indicating the importance of citrulline production under these conditions. Citrulline condensation with aspartate can form arginosuccinate, and this product can then be cleaved to fumarate and arginine by arginosuccinate lyase. The arginine could then also be converted to citrulline by arginine deiminase. Fumarate can be further metabolized to succinate and malate, which could be further metabolized in the hydrogenosome. Although a fumarase gene has been found in *T. vaginalis*, its expression has not yet been shown (Gerbod *et al.*, 2001).

The various detrimental effects resulting from the depletion of polyamines from this organism reinforces the case for the importance of this pathway to the parasite, and therefore its possible use as a target for chemotherapy. These studies also pose several additional questions about the regulation of the polyamine pathway and under which conditions it is utilized most. Does the arginine dihydrolase pathway function simultaneously with other energy-generating pathways (e.g. glycolysis) or only when substrates for the other bioenergetic pathways are absent? How is the arginine dihydrolase pathway controlled? Is signaling taking place to induce one pathway while the other is arrested in the absence of its substrate?

Upon adding exogenous sources of spermine or spermidine, various effects inflicted by the presence of DFMO were virtually reversed. This evidence led us to question the existence of a spermine:spermidine antiport in *T. vaginalis* (Yarlett *et al.*, 2000). If such an antiport existed, the irreversible inhibition of ornithine decarboxylase by DFMO would prevent putrescine from being produced, thereby preventing the uptake of spermine or spermidine (Yarlett & Bacchi, 1988). Based on the results presented in

this work, both spermine and spermidine entered the DFMO-grown organism and stabilized the membrane potential, as was the case in a previous study (Yarlett & Bacchi, 1988). If putrescine was not being produced due to the inhibition of ODC, how were spermine and spermidine entering the organism, if not through a spermine:putrescine antiport? Experiments must be done to confirm the low level of putrescine present, and were not included in this work. Although further work is necessary to confirm the absence of this type of antiport and determine the transport system in its place, evidence from this work questions the functioning of the spermine:spermidine antiport as it has been published, where putrescine is said to be counter-transported with spermine or spermidine (Yarlett *et al.*, 2000). Future work must be done to determine if this is indeed the case in *T. vaginalis*.

7.2 Nitric oxide production in *T. vaginalis*.

Evidence presented in this work extends the view that *T. vaginalis* hydrogenosomes possess a significant similarity to mitochondria: they contain the enzyme nitric oxide synthase (NOS) and produce nitric oxide (Bates *et al.*, 1996). The roles of nitric oxide (NO) in *T. vaginalis*, particularly as it relates to the role of the arginine dihydrolyase pathway of arginine metabolism and the production of NO, have been the focus of this study. The metabolism of arginine was initially examined with an NO electrode combined with a Clark O_2 electrode, and the organism was found to produce NO under aerobic conditions. After a granular fraction enriched with hydrogenosomes was monitored by the NO electrode, hydrogenosomes were also found to produce NO, suggesting this NO-producing reaction takes place in the

hydrogenosome, the mitochondria-like organelle primarily responsible for redox balancing and ATP production. The method used for isolating hydrogenosomes resulted in a large granular fraction rich in hydrogenosomes, although other membrane-bounded organelles, including lysosomes and microsomes, were also present. In future studies, *T. vaginalis* hydrogenosomes could be further purified using a Percoll gradient fractionation in order to definitively confirm the presence of NOS activities in the hydrogenosomes and not the other organelles present in the fraction.

Confocal microscopy of *T. vaginalis* incubated with DAF-FM, a NO-specific probe, showed areas of nitric oxide production localized in specific organelles in some organisms, and in the cytosol in others. In the future, co-localization of the signal obtained by DAF-FM will be assessed with antibodies to one of many hydrogenosomal marker proteins available. This procedure presents challenges as the DAF-FM requires the organisms be alive, while the antibody requires fixation. Preliminary attempts to colocalize these two elements have been unsuccessful. Current data show varying levels of NO present in individual organisms of the *T. vaginalis* population by DAF-FM staining. Although some organisms show organelles with intense fluorescence, many of the cells also contain non-fluorescent organelles. These problems underscore the necessity for the co-localization experiments in order to confirm the production of NO by hydrogenosomes. Images taken with synchronized organisms would help to answer the question whether the localization of NO production to the hydrogenosomes may be dependent on cell cycle. Nevertheless, subsequent enzyme assays confirmed the presence of NO synthase activity in both the cytosolic and hydrogenosome-enriched fractions from *T. vaginalis,* suggesting the presence of two NO synthases. Bioinformatic searches also

confirmed the presence of two different and unique NOS genes in the *T. vaginalis* genome.

The presence of two novel NOS enzymes in *T. vaginalis*, and one NOS in *G. intestinalis*, both organisms without heme proteins, is significant because these enzymes must utilize an unusual mechanism for nitric oxide production. Although labeling these proteins as putative NOS proteins is speculative, plans for future work include showing biochemically that they act as NOS proteins. The bioinformatic searches done in this study provide clues as to how this novel production of NO might be achieved. It is likely that the flavodoxin takes the place of the heme protein in the production of NO, much like the mechanism in *Arabidopsis*, which also does not contain heme proteins (Garcia-Mata *et al.*, 2003; Butt *et al.*, 2003). The existence of a new mechanism for nitric oxide production is not unprecedented. Certain plant cells have been found to contain NOS enzyme activity, cross-reactivity with mammalian NOS antibodies, and sensitivity to mammalian NOS inhibitors, although no gene or protein was found with sequence similarity to a known mammalian-type NOS. This suggests that these plants contain a completely different NOS enzyme (Garcia-Mata et al., 2003; Butt et al., 2003; Yamasaki & Cohen, 2006). The discovery of NOS in *T. vaginalis* is also important because its carbohydrate metabolism has been the topic of numerous studies, and yet no regulatory signaling has been discovered. Organisms exposed to starvation conditions (no exogenous glucose in Doran's buffer) displayed increased rates of nitric oxide production. Could NO be the missing effector controlling carbohydrate metabolism in *T. vaginalis*?

7.3 Nitric oxide production in *G. intestinalis*.

The production of nitric oxide by the large granular fraction of *G. intestinalis* supports the presence of a redox-generating organelle (not the mitosome, which would be too small to sediment in the large granular fraction at 10,000 x g). The heterogeneity of the confocal images stained with DAF-FM led us to believe that the level of nitric oxide present in the organisms may be related to cell cycle, although more images must be obtained at lower magnification to show the varied nature of the presence of fluorescence. Obtaining images of more organisms would also allow us to make more quanititative observations about the relative percentages of organisms that take up the fluorogen, as well as how many show a localization of NO in the periphery of the cell. This accumulation of nitric oxide to the periphery of the organism in many of those viewed, is where the redox balancing organelles of *G. intestinalis* were observed in this study as well as one previous study (Lloyd et al., 2002). This leads us to believe that, at some point in the organism's cell cycle, nitric oxide production is localized within these organelles.

The gene for an inducible NO-synthase (iNOS) in the published genome of *Giardia intestinalis* (accession # AACB01000174) was found to have homology with several NOS genes from mammalian organisms, including several conserved domains with *Homo sapiens* and *Trichomonas vaginalis*. Mitochondria have NOS activity, and have been shown to produce nitric oxide (Ghafourifar & Richter, 1997). The fact that mitochondria-like organelles from *G. intestinalis* produce NO and contain an active NOS, just like mitochondria in eukarytotic organisms, suggests that these organisms are not

'primitive', but in fact have evolved from organisms containing mitochondria which adapted to living in anaerobic environments, as has been postulated by several other groups (Biagini *et al.*, 1997; van der Giezen *et al.*, 2005).

7.4 Possible control mechanisms for energy-yielding pathways in micraerophilic protists.

Data from this study suggests that a regulatory control mechanism exists for energy-generating pathways. This regulatory mechanism seems to control the switching from carbohydrates to amino acids as substrates for the bioenergetic pathways in *T. vaginalis*. It has been shown that nitrosylation is a means for cellular control of enzymatic activity by nitrosylating specific cysteine motifs in the active site of specific key proteins (Broillet 1999, Bauer *et al.*, 2001). BLAST analysis of the *T. vaginalis* genome has resulted in the location of a cysteine with a nitrosylation motif in the active site of the ornithine decarboxylase (ODC), like the motif identified by Bauer for mammalian ODC (Bauer *et al.*, 2001). Further, Bauer showed that when the NOS gene was transfected into NIH 3T3 cells and expressed, the active site specific cysteine (cys360) was nitrosylated and this inhibited proliferation of 3T3 cells (Bauer *et al.*, 2001). More bioinformatic searches for nitrosylation sites will be performed in the future to obtain more evidence about the role of nitric oxide production in *T. vaginalis* and *G. intestinalis*.

The presence of unique NOS enzymes in *T. vaginalis* and *G. intestinalis* poses interesting evolutionary as well as functional questions. Firstly, as mentioned above, how do these unique NOS enzymes function without heme? A novel mechanism for this NOS

must exist, and would be the first of its kind found in a non-plant eukaryote. Since this is the case, what are the evolutionary implications of the presence of this enzyme in *T. vaginalis* and *G. intestinalis*? Do other eukaryotes contain these novel NOS enzymes? The presence of NOS enzymes in both the hydrogenosomes of *T. vaginalis* and the redox-generating organelles of *G. intestinalis* presents more evidence in support of these organelles having evolved from mitochondria.

7.5 Phospholipids in *T. vaginalis* and *G. intestinalis*.

Despite evidence to the contrary (Paltauf & Meingassner, 1982), the recent assertion that cardiolipin is present in *Tritrichomonas foetus* (de Andrade Rosa *et al.*, 2006) and an abstract stating the same for *Giardia intestinalis* (Lloyd *et al.*, 2005) led us to explore this question further. Since fully-functional mitochondria contain cardiolipin (McMillin & Dowhan, 2002), if mitochondria-like organelles from *T. vaginalis* and *G. intestinalis* were also found to contain this lipid, the evolutionary relationship between mitochondria and mitochondria-like organelles would be clarified. *G. intestinalis* was deemed part of a "simple and primitive, ancient amitochondriate lineage" (Cavalier-Smith, 1987). Many studies have challenged this notion (Embley & Hirt, 1998; Biagini *et al.*, 1997; Richards & van der Giezen, 2006). Results obtained in this work showed the absence of cardiolipin from both *T. vaginalis* and *G. intestinalis* (details not included in this thesis); this tends to support the idea that mitochondria are not closely related to hydrogenosomes or mitochondria-like organelles. However, the absence of cardiolipin alone does not disprove the theory that hydrogenosomes are evolved forms of mitochondria. It is possible that the hydrogenosome no longer requires cardiolipin; this

loss could have occurred when the mitochondria adapted to microaerophilic conditions. While the absence of cardiolipin from both of these organisms is significant, its absence alone does not prove or disprove either theory put forth to this point about the taxa to which these organisms have been assigned. In general, overwhelming evidence supports the theory that hydrogenosomes evolved from mitochondria.

The presence of a sphingolipid, N-hexadeconoyl sphinganine-1-phosphoethanolamine, in *T. vaginalis* but not in *G. intestinalis* is of interest because sphingolipids function in adhesion (Radin, 2006; Masserini & Ravasi, 2001). *T. vaginalis* burrows into the vaginal epithelial wall, which could be aided by this sphingolipid. *G. intestinalis* has an alternative mechanism; it is known to use its ventral disc to attach to the intestinal epithelial wall.

The subcellular distribution of the N-hexadeconoyl sphinganine-1-phosphoethanolamine in *T. vaginalis* suggests no association of this lipid with one particular organelle or membrane within the organism, but instead the data supports the presence of this lipid in various areas of the organism. This is surprising as it is such an important component of plasma membranes in other cells. This lack of localization to one organelle leads us to believe that during the subcellular fractionation, various portions of the plasma membrane containing this lipid were fragmented and distributed in the various fractions. In the future, cytological localization using a labeled antibody and a gradient must be used to further purify the subcellular fractions in order to determine if there is, in fact, a localization of this lipid to the plasma membrane. The lipid's purpose and function is still unclear, and its presence in *T. vaginalis* but absence in *G. intestinalis* is another point that must be explored.

7.6. Future work.

The data presented in this work indicates the existence of a regulatory control mechanism for energy-generating pathways in *T. vaginalis*. Evidence suggests this regulatory mechanism controls the switching from carbohydrates to amino acids as substrates for these bioenergetic pathways. It has been shown that nitrosylation is a means for cellular control of enzymatic activity by nitrosylating specific cysteine motifs in the active site of specific key proteins (Broillet 1999, Bauer *et al.*, 2001). BLAST analysis of the *T. vaginalis* genome resulted in the location of a cysteine with a nitrosylation motif in the active site of ornithine decarboxylase (ODC), like the motif identified by Bauer (Bauer *et al.*, 2001) for mammalian ODC.

(1). How does NO produced by the NO synthases affect activities of bioenergetic metabolic pathways that utilize carbohydrates or keto acids derived from amino acids to produce ATP by substrate-level phosphorylation?

This study **hypothesizes** that the binding of NO to specific proteins forms a regulatory connection between carbohydrate, arginine-polyamine and keto acid metabolism to generate ATP by substrate-level phosphorylation. *T. vaginalis* is 15% glycogen, by dry weight, and rapidly activates glycogen phosphorylase to make glucose available for carbohydrate metabolism. *Trichomonas* has a very high intracellular alanine pool. Alanine levels in plasma are found to reach concentration of 10^{-3}M. Alanine can be a source of pyruvate through transamination reactions. Lowe & Rowe (1986) previously reported that there is an alanine aminotransferase which reacts with α-ketoglutarate (2-oxoglutarate) to produce glutamate. Furthermore, Turner & Lushbaugh (1988) have shown that *T. vaginalis* has an NADP-dependent glutamate dehydrogenase

that would regenerate α-ketoglutarate. Alanine and arginine are important sources of keto acids to drive ATP synthesis in the absence of glucose.

(2). To clone both of these genes, express the proteins and characterize both NO synthase proteins.

This study **hypothesizes** that *T. vaginalis* has two very unique NOS proteins, with a unique Fe and enzymatic mechanism that are possible targets for chemotherapy. *T. vaginalis* contains hydrogenosomes, which carry out the redox reactions necessary for energy production and substrate-level phoshorylation. This organelle contains pyruvate ferridoxin oxireductase (PFOR) and several Fe-hydrogenases that produce H_2 as an end-product. Oxygen is utilized by several specific oxidases when O_2 is present. These oxidases oxidize NADH and NADPH to cycle nicotinamide nucleotides so as to maintain the cellular redox state.

REFERENCES

Adam, R.D. 2001. Biology of *Giardia lamblia. Clinical Microbiology.* **14**:447-75.

Albina, J.E. & Reichner, J.S. 1998. Role of Nitric Oxide in Mediation of Macrophage Cytotoxicity and Apoptosis. *Cancer and Metastis Reviews.* **17**:39-53.

Akhmanova, A., Voncken, F., van Alen, A.T., van Hoek, H.A., Boxma, B., Vogels, G., Veenhuis, M., and Hackstein, J.H. 1998. A hydrogenosome with a genome. *Nature.* **396**: 527-528.

Alderton, W.K., Cooper, C.E., and Knowles, R.G. 2001. Nitric oxide synthases: structure, function and inhibition. *Biochemical Journal.* 357: 593-615.

Ang L.H. 2003. Outbreak of giardiasis in a daycare nursery. *Communicable Diseases and Public Health.* **3**:212-3.

Arisue, N., Sanchez, L.B., Weiss, L.M., Muller, M., Hashimoto, T. 2002. Mitochondrial-type hsp70 genes of the amitochondriate protists *Giardia intestinalis, Entamoeba histolytica* and two microsporidians. *Parasitology International.* **51**:9-16.

Bacchi, C.J., Nathan, H.C., Hutner, S.H., McCann, P.P., Sjoerdsma, A. 1980. Polyamine metabolism: a potential therapeutic target in trypanosomes. *Science.* **210**:332-4.

Bacchi, C.J., Yarlett, N. 1993. Effects of antagonists of polyamine metabolism on African trypanosomes. *Acta Tropica.* **54**:225-36.

Barwick, R.S., Levy, D.A., Craun, G.F., Beach, M.J., Calderon, R.L. 2000. Surveillance for waterborne disease outbreaks – United States, 1997-1998. *CDC Surveillance Summaries.* **49**:1-35.

Bascal, Z. A., Cunningham, J. M., Holden-Dye, L., O'Shea, M., Walker, R. J. 2001. Characterization of a putative nitric oxide synthase in the neuromuscular system of the parasitic nematode *Ascaris suum*. *Parasitology*. **122**:219-31.

Basu N. K., Kole L., Ghosh A., Das P. K. 1996. Isolation of a nitric oxide synthase from the protozoan parasite, *Leishmania donovani*. *FEMS Microbiology Letters*. **156**:40-44.

Bates T. E., Loesch A., Burnstock G., Clark J. B. 1996. Mitochondrial nitric oxide synthase: a ubiquitous regulator of oxidative phosphorylation? *Biochemistry Biophysics Research Community*. **218**:40-44.

Bauer, P.M., Buga, G.M., Fukuto, J.M., Pegg, A.E., Ignarro, L.J. 2001. Nitric oxide inhibits ornithine decarboxylase via S-nitrosylation of cysteine 360 in the active site of the enzyme. *Journal of Biological Chemistry*. **276**:34458-64.

Beach, D.H., Holz, Jr., G.G., Singh, B.N., Lindmark, D.G. 1991. Phospholipid metabolism of cultured *Trichomonas vaginalis* and *Tritrichomonas foetus*. *Molecular and Biochemical Parasitology*. **44**:97-108.

Benchimol, M., Johnson, P.J., de Souza, W. 1996. Morphogenesis of the hydrogenosome: an ultrastructural study. *Biology of the Cell*. **87**:197-205.

Benchimol, M. 2004. Participation of the adhesive disc during karyokinesis in *Giardia lamblia*. *Biology of the Cell*. **96**:291-301.

Bendesky, A., Menendez, D., Ostrosky-Wegman, P. 2002. Is metronidazole carcinogenic? *Mutation Research*. **511**:133-44.

Bergmeier, H.U. 1970. Methoden der enzymatischen Analyse. 2. Auflage, Akademie Verlag, Berlin.

Bernander, R., Palm, J.E.D., Svärd, S.G. 2001. Genome ploidy in different stages of the *Giardia lamblia* life cycle. *Cellular Microbiology.* **3**:55–62.

Biagini, G. A., Finlay, B. J., Lloyd, D. 1997. Evolution of the hydrogenosome. *FEMS Microbiology Letters.* **155**:133-140.

Bitonti, A. J., Bacchi, C. J., McCann, P. P., Sjoerdsma, A. 1985. Catalytic irreversible inhibition of *Trypanosoma brucei* ornithine decarboxylase by substrate and product analogs and their effects on murine trypanosomiasis. *Biochemical Pharmacology.* **34**:1773-1777.

Bockman, D.E. & Winborn, W.B. 1968. Electron microscopic localization of exogenous ferritin within vacuoles of *Giardia muris. Journal of Protozoology.* **15**:26-30.

Bogdan, C. 2001. Nitric oxide and the immune response. *Nature Immunology.* **2**:907 916.

Bogdan, C. 2001. Nitric oxide and the regulation of gene expression. *Trends in Cell Biology.* **11**:66-75.

Broad, T.E. & Dawson, R.M.C. 1973. Formation of ceramide phosphorylethanolamine from phosphatidylethanolamine in the rumen protozoon *Entodinium caudatum. Biochemical Journal.* **134**:659-662.

Broillet, M. C. 1999. S-Nitrosylation of proteins. *Cellular and Molecular Life Sciences.* **55**:1036-1042.

Bui, E.T., Bradley, P.J., Johnson, P.J. 1996. A common evolutionary origin for mitochondria and hydrogenosomes. *Proceedings of the National Academy of Sciences USA.* **93**:9651-6.

Bui, E.T., Johnson, P.J. 1996. Identification and characterization of [Fe]-hydrogenases in the hydrogenosome of *Trichomonas vaginalis. Mol Biochem Parasitol.* **76**:305-10.

Butt, Y.K., Lum, J.H., Lo, S.C. 2003. Proteomic identification of plant proteins probed by mammalian nitric oxide synthase antibodies. *Planta.* **216**:762-71.

Cavalier-Smith, T. 1987. Eukaryotes with no mitochondria. *Nature.* **326**:332-3.

Cavalier-Smith, T. 1987. The simultaneous symbiotic origin of mitochondria, chloroplasts, and microbodies. *Annual New York Academy of Science - Biology.* **503**:55-71.

Cerkasóv, J, Cerkasovova, A, Kulda, J, Vilhelmova, D. 1978. Respiration of hydrogenosomes of *Tritrichomonas foetus*. I. ADP-dependent oxidation of malate and pyruvate. *Journal of Biological Chemistry.* **253**:1207-1214.

Cerkasovova, A., Cerkasov, J., Kulda, J., Reischig, J. 1976. Circular DNA and cardiolipin in hydrogenosomes, microbody-like organelles of trichomonads. *Folia Parasitology (Praha).* **23**:33-37.

Chance, B. & Williams, G. R. 1956. Respiratory enzymes in oxidative phosphorylation. VI. Theeffects of adenosine diphosphate on azide-treated mitochondria. *Journal of Biological Chemistry.* **221**:477-489.

Chapman, A., Hann, A. C., Linstead, D., Lloyd, D. 1985. Energy-dispersive X-ray microanalysis of membrane-associated inclusions in hydrogenosomes isolated from *Trichomonas vaginalis. Journal of General Microbiology.* **131**: 2933-9.

Cheissen, E.M. 1965. Ultrastructure of *Giardia duodenalis*. 2. The locomotory apparatus, axial rod and other organelles. *Archiv fur Protistenkunde.* **108**: 8-18.

Chen, K.C., Amsel, R., Eschenbach, D.A., Holmes, K.K. 1982. Biochemical diagnosis of vaginitis: determination of diamines in vaginal fluid. *Journal of Infectious Diseases.* **145**:337-345.

Costello, C. E., Beach, D. H. and Singh, B. N. 2001. Acidic glycerol lipids of *Trichomonas vaginalis* and *Tritrichomonas foetus. Journal of Biological Chemistry.* **382**:275-281.

Costello, C. E., Glushka, J., van Halbeek, H. and Singh, B. N. 1993. Structural characterization of novel inositol phosphosphingolipids of *Tritrichomonas foetus* and *Trichomonas vaginalis. Glycobiology.* **3**:261-269.

Crone, H.D. and Bridges, R.G. 1963. The phospholipids of the housefly, *Musca domestica. Biochemical Journal.* **89**:11-21.

Das, S., Stevens, T., Castillo, C., Villasenor, A., Arrendondo, H., Reddy, K. 2002. Lipid metabolism in mucous-dwelling amitochondriate protozoa. *International Journal of Parasitology.* **32**:655-675.

Davidson, R.A. 1984. Issues in clinical parasitology: the treatment of giardiasis. *American Journal of Gastroenterology.* **79**:256-61.

de Andrade Rosa, I., Einkicker-Lamas, M., Roney Bernardo, R., Previatto, L. M., Mohana-Borges, R., Morgado-Diaz, J. A. and Benchimol, M. 2006. Cardiolipin in hydrogenosomes: evidence of symbiotic origin. *Eukaryotic Cell.* **5**:784-787.

de Duve, C. & Berthet, J. 1953. Reproducibility of differential centrifugation experiments in tissue fractionation. *Nature.* **172**:1142.

de Duve, C., Pressman, B.C., Gianetto, R., Wattiaux, R., Appelmans, F. 1955. Tissue fractionation studies. In: intracellular distribution of enzymes in rat liver tissue. *Biochemical Journal.* **6**:604-617.

de Duve, C. 1964. Principles of tissue fractionation. *Jounral of Theoretical Biology.* **6**:33-59.

Diamond, L. S. 1957. The establishment of various trichomonads of animals and man in axenic cultures. *Journal of Parasitology.* **3**:488-490.

Drmota, T., Proost, P., Van Ranst, M., Weyda, F., Kulda, J. Tachezy, J. 1996. Iron ascorbate cleavable malic enzyme from hydrogenosomes of *Trichomonas vaginalis*: purification and characterization. *Molecular and Biochemical Parasitology.* **83**:221-34.

Dunne, R.L., Dunn, L.A., Upcroft, P., O'Donooghue, P.J., Upcroft, J.A. 2003. Drug resistance in the sexually transmitted protozoan *Trichomonas vaginalis. Cell Research.* **13**:239-249.

Dyall, S. D., Yan, W., Delgadillo-Correa, M. G., Lunceford, A., Loo, J. A., Clarke, C. F., Johnson, P. J. 2004. Non-mitochondrial complex I proteins in a hydrogenosomal oxidoreductase complex. *Nature.* **431**:1103-1107.

Edwards, M.R., Gilroy, F.V., Jimenez, B.M., O'Sullivan, W.J. 1989. Alanine is a major end product of metabolism by *Giardia lamblia*: a proton nuclear magnetic resonance study. *Molecular and Biochemical Parasitology.* **37**:19-26.

Ellis, J.E., Williams, R., Cole, D., Cammack, R., Lloyd, D. 1993. Electron transport components of the parasitic protozoon *Giardia lamblia. FEBS Letters.* **325**:196-200.

Elmendorf, H.G., Dawson, S.C., McCaffery, J.M. 2003. The cytoskeleton of *Giardia lamblia*. *International Journal of Parasitology*. **33**:3-28.

Embley, T.M. & Hirt, R.P. 1998. Early branching eukaryotes? *Current Opinion in Genetic Development*. **8**:624-629.

Embley, T. M., van der Giezen, M., Horner, D. A., Hirt, R. P., Dyal, P. L., Bell, S., Foster, P. G. 2003. Hydrogenosomes, mitochondria and early eukaryotic evolution. *International Union of Biochemistry and Molecular Biology (IUBMB) Life*. **55**:387-35.

Fernandez-Cancio M., Fernandez-Vitos E. M., Centelles J. J., Imperial S. 2001. Sources of interference in the use of 2,3-diaminonaphthalene for the fluorimetric determination of nitric oxide synthase activity in biological samples. *Clinica Chimica Acta*. **312**:205-12.

Fiori, P.L., Rappelli, P., Addis, M.F. 1999. The flagellated parasite *Trichomonas vaginalis*: new insights into cytopathogenicity mechanisms. *Microbes and Infection*. **1**:149-56.

Forsgren, A. & Forssman, L. 1979. Metronidazole-resistant *Trichomonas vaginalis*. *British Journal of Venereal Diseases*. **55**:351-3.

Garbus, J., Deluca, H.F., Loomans, M.E., Strong F.M. 1963. The rapid incorporation of phosphate into mitochondrial lipids. *Journal of Biological Chemistry*. **238**:59-63.

Garcia, A.F., Benchimol, M., Alderete, J.F. 2005. *Trichomonas vaginalis* polyamine metabolism is linked to host cell adherence and cytotoxicity. *Infection and Immunity*. **73**:2602-10.

Garcia-Mata, C. & Lamattina, L. 2003. Abscisic acid, nitric oxide and stomatal closure – is nitrate reductase one of the missing links? *Trends in Plant Science.* **8**:20-26.

Gaston, B. & Stamler, J.S. 1999. Biochemistry of nitric oxide. Nitric Oxide and Infection (ed. Fang, F.C.). Kluwer/Plenum, New York. pp. 37-55.

Genestra, M., Cysne-Finkelstein, L., Guedes-Silva, D., Leon, L.L. 2003. Effect of L-arginine analogs and a calcium chelator on nitric oxide (NO) production by Leishmania sp. *Journal of Enzyme Inhibition and Medical Chemistry.* **18**:445-452.

Gerbod, D., Edgcomb, V.P., Noel, C., Vanacova, S., Wintjens, R., Tachezy, J., Sogin, M.L., Viscogliosi, E. 2001. Phylogenetic relationships of class II fumarase genes from trichomonad species. *Molecular Biology and Evolution.* **18**:1574-1584.

Ghafourifar, P., Richter, C. 1997. Nitric oxide synthase activity in mitochondria. *FEBS Letters.* **418**:291-6.

The *Giardia lamblia* Genome Database (www.mbl.edu/Giardia)

Gillin, F.D., Reiner, D.S., McCann, P.P. 1984. Inhibition of growth of *Giardia lamblia* by difluoromethylornithine, a specific inhibitor of polyamine biosynthesis. *Journal of Protozoology.* **31**:161-3.

Giulivi, C., Poderoso, J. J., Boveris, A. 1998. Production of nitric oxide by mitochondria. *Journal of Biological Chemistry.* **273**:11038-11043.

Gohil, V.M., Gvozdenovic-Jeremic, J., Schlame, M., Greenberg, M.L. 2005. Binding of 10-N-nonyl acridine orange to cardiolipin-deficient yeast cells: implications for assay of cardiolipin. *Analytical Biochemistry.* **343**:350-352.

Green, L. C., Wagner D. A., Glogowski, J., Skipper, P. L., Wishnok, J. S., Tannenbaum, S. R. 1982. Analysis of nitrate, nitrite, and [^{15}N] nitrate in biological fluids. *Analytical Biochemistry.* **126**:131-138.

Gustafsson, M. K., Lindholm, A. M., Terenina, N. B., Reuter, M. 1996. NO nerves in a tapeworm. NADPH-diaphorase histochemistry in adult *Hymenolepis diminuta. Parasitology.* **113**:559-565.

Harris, J.C., Plummer, S., Lloyd, D. 2001. Antigiardial drugs. *Applied Microbiology Biotechnology.* **57**:614-9.

Harris, K.M., Goldberg, B., Biagini, G.A., Lloyd, D. 2006. *Trichomonas vaginalis* and *Giardia intestinalis* produce nitric oxide and display NO-synthase activity. *Journal of Eukaryotic Microbiology.* **53**:182-183.

Harris, K.M., Lloyd, D., Goldberg, B. In preparation. Glycogen metabolism and other bioenergetic pathways: does NO facilitate the switching between these pathways?

Hashimoto, T., Sanchez, L.B., Shirakura, T., Muller, M. & Hasegawa, M. 1998. Secondary absence of mitochondria in *Giardia lamblia* and *Trichomonas vaginalis* revealed by valyl-tRNA synthetase phylogeny. *Proceedings of the National Academy of Sciences USA.* **95**:6860-6865.

Hernandez-Campos M. E., Campos-Rodriguez R., Tsutsumi V., Shibayama M., Garcia Latorre E., Castillo-Henkel C., Valencia-Hernandez I. 2003. Nitric oxide synthase in *Entamoeba histolytica*: its effect on rat aortic rings. *Experimental Parasitology.* **104**:87-95.

Hess, D.T., Matumoto, A., Kim, S.O., Marshall, H.E., Stamler, J.S. 2005. Protein S-nitrosylation purview and parameters. *Nature Reviews. Molecular Cell Biology.* **6**:150-166.

Hlavsa, M.C., Watson, J.C., Beach, M.J. 2005. Giardiasis surveillance – United States, 1998-2002. *Surveillance Summaries: Morbidity and Mortality Weekly Report.* **54**:9-16.

Holberton, D.V. 1974. Attachment of *Giardia* – A Hydrodynamic Model Based on Flagellar Activity. *Journal of Experimental Biology.* **60**:207-221.

Honigberg, B.M., editor. 1990. Trichomonads parasitic in humans. Springer Publishing Company, New York, NY.

Honigberg B.M., Brugerolle G. 1990. Structure. In BM Honigberg, *Trichomonads Parasitics in Humans,* Springer-Verlag, New York, pp. 5-35.

Hrdý, I. & Mertens, E. 1993. Purification and partial characterization of malate dehydrogenase (decarboxylating) from *Tritrichomonas foetus* hydrogenosomes. *Parasitology.* **107**:379-385.

Hrdý, I. & Müller, M. 1995. Primary structure and eubacterial relationships of the pyruvate:ferredoxin oxidoreductase of the amitochondriate eukaryote *Trichomonas vaginalis*. *Journal of Molecular Evolution.* **41**:388-396.

Hrdý, I., Hirt, R.P., Dolezal, P., Bardonová, L., Foster, P.G., Tachezy, G., Embley, T.M. 2004. *Trichomonas* hydrogenosomes contain the NADH hydrogenase module of mitochondrial complex I. *Nature.* **432**:618-22.

Humphreys, M. J., Allman, R. & Lloyd, D. 1994. Determination of the viability of *Trichomonas vaginalis* using flow cytometry. *Cytometry* **15**:343-348.

Humphreys, M.J., Ralphs, J., Durrant, L., Lloyd, D. 1994. Hydrogenosomes in trichomonads are calcium stores and have a transmembrane electrochemical potential. *Biochemical Society Transactions.* **22**:324S.

Inge, P.M., Edson, C.M., Farthing, M.J. 1988. Attachment of *Giardia lamblia* to rat intestinal epithelial cells. *Gut.* **29**:795-801.

Jacobson, J., Duchen, M.R. and Heales, S.J. 2002. Intracellular distribution of the fluorescent dye Nonyl acridine orange responds to the mitochondrial membrane potential: implications for assays of cardiolipin and mitochondrial mass. *Journal of Neurochemistry.* **82**:224-233.

Kabnick, K.S. & Peattie, D.A. 1990. *In situ* analyses reveal that the two nuclei of *Giardia lamblia* are equivalent. *Journal of Cell Science.* **95**:353-360.

Kappus K.D., Lundgren R.G., Juranek D.D., Roberts J.M., Spencer H.C. 1994. Intestinal parasitism in the United States: update on a continuing problem. *American Journal of Tropical Medicine and Hygiene.* **50**:705-13.

Kates, M. 1986. Techniques in Lipidology, 2nd edition. Elsevier, Amsterdam.

Kato, K. & Giulivi, C. 2006. Critical overview of mitochondrial nitric oxide synthase. *Frontiers in Bioscience.* **11**:12725-38.

Keeling, P. J. 1998. A kingdom's progress: Archezoa and the origin of eukaryotes. *BioEssays.* **20**:87–95.

Keister D. B. 1983. Axenic culture of *Giardia lamblia* in TYI-S-33 medium supplemented with bile. *Transactions of the Royal Society of Tropical Medicine and Hygiene.* 77:487-8.

Keithly, J.S. 1989. Ornithine decarboxylase and trypanothione reductase genes in *Leishmania braziliensis guyanensis*. *Journal of Protozoology.* **36**:498-501.

Keithly, J.S., Zhu, G., Upton, S.J., Woods, K.M., Martinez, M.P., Yarlett, N. 1997. Polyamine biosynthesis in *Cryptosporidium parvum* and its implications for chemotherapy. *Molecular and Biochemical Parasitology.* **88**:35-42.

Kohn, A. B., Moroz, L. L., Lea, J. M., Greenberg, R. M. 2001. Distribution of nitric oxide synthase immunoreactivity in the nervous system and peripheral tissues of *Schistosoma mansoni*. *Parasitology.* **122**:87-92.

Kramer, M.H., Herwaldt, B.L., Craun, G.F., Calderon, R.L., Juranek, D.D. 1996. Surveillance for waterborne-disease outbreaks – United States, 1993-1994. *CDC Surveillance Summaries.* **45**:1-33.

Kulda, J. 1999. Trichomonads, hydrogenosomes and drug resistance. *International Journal of Parasitology.* **29**:199-212.

Lacza, Z., Snipes, J. A., Zhang, J., Horvath, E. M., Figueroa, J. P., Szabo, C., Busija, D.W. 2003. Mitochondrial nitric oxide synthase is not eNOS, nNOS or iNOS. *Free Radical Biology and Medicine.* **35**:1217-1228.

Lee, S.H., Levy, D.A., Craun, G.F., Beach, M.J., Calderon, R.L. 2002. Surveillance for waterborne-disease outbreaks – United States, 1999-2000. *CDC Surveillance Summaries.* **51**:1-48.

Lehker, M.W. & Alderete, J.F. 2000. Biology of trichomonosis. *Current Opinion in Infectious Disease.* **13**:37-45.

Letunic, I., Copley, R.R., Pils, B., Pinkert, S., Schultz, J., and Bork, P. 2006. SMART 5: domains in the context of genomes and networks. *Nucleic Acids Research.* **34**: D257-260.

Levy, D.A., Bens, M.S., Craun, G.F., Calderon, R.L., Herwaldt, B.L. 1998. Surveillance for waterborne-disease outbreaks – United States, 1995-1996. *CDC Surveillance Summaries.* **47**:1-34.

Lindholm, A. M., Reuter, M., Gustafsson, M. K. 1998. The NADPH-diaphorase staining reaction in relation to the aminergic and peptidergic nervous system and the musculature of adult *Diphyllobothrium dentriticum. Parasitology.* **117**:283-92.

Lindmark, D.G. 1980. Energy metabolism of the anaerobic protozoon *Giardia lamblia. Molecular and Biochemical Parasitology.* **1**:1-12.

Lindmark, D.G. & Müller, M. 1973. Hydrogenosome, a Cytoplasmic Organelle of the Anaerobic Flagellate *Tritrichomonas foetus*, and Its Role in Pyruvate Metabolism. *Journal of Biological Chemistry.* **248**:7724-7728.

Lindmark, D. G. & Müller, M. 1975. Hydrogenosomes in *Trichomonas vaginalis. Journal of Parasitology.* **61**:552–552.

Linstead, D. & Cranshaw, M.A. 1983. The pathway of arginine catabolism in the parasitic flagellate *Trichomonas vaginalis. Molecular and Biochemical Parasitology.* **8**:241-52.

Lloyd, D., Harris, J.C., Maroulis, S., Wadley, R., Ralphs, J.R., Hann, A.C., Turner, M.P., Edwards, M.R. 2002. The "primitive" microaerophile *Giardia intestinalis* (syn. *lamblia, duodenalis*) has specialized membranes with electron transport and membrane-potential-generating functions. *Microbiology.* **148**:1349-1354.

Lloyd, D. & Hayes, A. J. 1995. Vigour, Vitality and Viability of Microorganisms. *FEMS Microbiology Letters.* **133**:1-7.

Lloyd, D., Lindmark, D. G., Müller, M. 1979. Adenosine triphosphatase activity of *Tritrichomonas foetus. Journal of General Microbiology.* **115**:301--307.

Lloyd, D., Ralphs, J.R., Harris, J.C. 2002. Hydrogen production in *Giardia intestinalis*, a eukaryote with no hydrogenosomes. *Trends in Parasitology.* **18**:155-6.

Lopes, L.C., Ribeiro, K.C., Benchimol, M. 2001. Immunolocalization of tubulin isoforms and post-translational modifications in the protists *Tritrichomonas foetus* and *Trichomonas vaginalis. Histochemistry and Cell Biology.* **116**:17-29.

Lowry, O.H., Rosebrough, N.J., Farr, A.L., Randall, R.J. 1951. Protein measurement with the Folin phenol reagent. *Journal of Biological Chemistry.* **193**:265-275.

Lujan, H.D., Marotta, A., Mowatt, M.R., Sciaky, N., Lippincott-Schwartz, J., Nash, T.E. 1995. Developmental Induction of Golgi Structure and Function in the Primitive Eukaryote *Giardia lamblia. Journal of Biological Chemistry.* **270**:4612-4618.

MacMicking, J., Xie, Q.W. & Nathan, C. 1997. Nitric oxide and macrophage function. *Annual Review of Immunology.* **15**:323-350.

Magne, D., Favennec, L., Chochillon, C., Gorenflot, A., Meillet, D., Kapel, N., Raichvarg, D., Savel, J., Gobert, J.G. 1991. Role of cytoskeleton and surface lectins in *Giardia duodenalis* attachment to Caco2 cells. *Parasitology Research.* 77:659-662.

Mammen-Tobin, A. & Wilson, J.D. 2005. Management of metronidazole-resistant *Trichomonas vaginalis*--a new approach. *International Journal of STD & AIDS.* **16**:488-490.

Martin, W., Hoffmeister, M., Rotte, C., Henze, K. 2001. An overview of endosymbiotic models for the origins of eukaryotes, their ATP-producing organelles (mitochondria and hydrogenosomes), and their heterotrophic lifestyle. *Journal of Biological Chemistry.* **382**: 1521-1539.

Martin, W. & Müller, M. 1998. The hydrogen hypothesis for the first eukaryote. *Nature.* **392**:37-41.

Marton, L.J. & Pegg, A.E. 1995. Polyamines as targets for therapeutic intervention. *Annual Review of Pharmacology & Toxicology.* **35**:55-91.

Masetti, M., Locci, T., Cecchettini, A., Lucchesi, P., Magi, M., Malvadi, G., Bruschi, F. 2004. Nitric oxide synthase immunoreactivity in the nematode *Trichinella britovi*. Evidence for nitric oxide production by the parasite. *International Journal of Parasitology.* **34**:715-21.

Mason, D.J., Lopez-Amoros, R., Allman, R., Stark, J.M., Lloyd, D. 1995. The ability of membrane potential dyes and calcafluor white to distinguish between viable and non-viable bacteria. *Journal of Applied Bacteriology.* **78**:309-15.

Masserini, M. & Ravasi, D. 2001. Role of sphingolipids in the biogenesis of membrane domains. *Biochimica et Biophysica Acta.* **1532**:149-61.

McCabe, R.E., Yu, G.S., Conteas, C., Morrill, P.R., McMorrow, B. 1991. *In vitro* model of attachment of Giardia intestinalis trophozoites to IEC-6 cells, an intestinal cell line. *Antimicrobial Agents & Chemotherapy.* **35**:29-35.

McCann, P.P., Bacchi, C.J., Clarkson, A.B. Jr., Seed, J.R., Nathan, H.C., Amole, B.O., Hunter, S.H., Sjoerdsma, A. 1981. Further Studies of Difluoromethylornithine in African Trypanosomes. *Medical Biology.* **59**:434-40.

McFarland, L.V. 2000. Normal flora: diversity and functions. *Microbial Ecology in Health & Disease.* **12**:193-207.

McMillin, J. B. and Dowhan, W. 2002. Cardiolipin and apoptosis. *Biochimica et Biophysica Acta.* **1585**:97-107.

Minamino, M., Sakaguchi, I., Naka, T., Ikeda, N., Kato, Y., Tomiyasu, I., Yano, I., Kobayashi, K. 2003. Bacterial ceramides and sphingophospholipids induce apoptosis of human leukaemic cell. *Microbiology.* **149**:2071-2081.

Minotto, L., Tutticci, E.A., Bagnara, A.S., Schofield, P.J., Edwards, M.R. 1999. Characterization and expression of the carbamate kinase gene from *Giardia intestinalis. Molecular Biochemical Parasitology.* **98**:43-51.

Moore, A.C., Herwaldt, B.L., Craun, G.F., Calderon, R.L., Highsmith, A.K., Juranek, D.D. 1993. Surveillance for waterborne-disease outbreaks – United States, 1991-1992. *CDC Surveillance Summaries.* **42**:1-22.

Moreau, R.A., Young, D.H., Danis, P.O, Powell, M.J., Quinn, C.J., Beshah, K., Slawecki, R.A. and Dilliplane, R.L. 1998. Identification ceramide phosphorylethanolamine in oomycete plant pathogens: *Pythium ultimum, Phytophthora infestans,* and *Phytophthora capsici. Lipids.* **33**:307-317.

Morrison, H.G., Roger, A.J., Nystul, T.G., Gillin, F.D., Sogin, M.L. 2001. *Giardia lamblia* expresses a proteobacterial-like DNA K homolog. *Molecular Biology & Evolution.* **18**:530-541.

Müller, M. 1992. Energy metabolism of ancestral eukaryotes: a hypothesis based on the biochemistry of amitochondriate parasitic protists. *Biosystems*. **28**:33-40.

Müller, M. & Lindmark, D. G. 1978. Respiration of hydrogenosomes of *Tritrichomonas foetus*. II. Effect of CoA on pyruvate oxidation. *Journal of Biological Chemistry*. **253**:1215-1218.

Müller, M., Meingassner, J. G., Miller, W. A., Ledger, W. J. 1980. Three metronidazole-resistant strains of *Trichomonas vaginalis* from the United States. *American Journal of Obstetrics & Gynecology*. **138**:808-812.

Naka, T., Fujiwara, N., Yana, I., Maeda, S., Doe, M., Minamino, M., Ikeda, N., Kato, Y., Watabe, K., Kumazawa, Y., Tomiyasu., I. and Kobayashi, K. 2003. Structural analysis of sphingophospholipids derived from *Sphingobacterium spiritivorum,* the type species of genus *Sphingobacterium. Biochimica et Biophysica Acta.* **1635**:83-92.

Nathan, C. 1992. Nitric oxide as a secretory product of mammalian cells. *FASEB Journal*. **6**:3051-3064.

Nielsen, M.H. 1974. Fine structural localization of nucleoside triphosphatase and acid phosphatase activity in *Trichomonas vaginalis* Donne. *Cell Tissue Research.* **151**:269-280.

Nisoli, E. & Carruba, M.O. 2006. Nitric oxide and mitochondrial biogenesis. *Journal of Cell Science* **119**:2855-62.

North, M. J., Lockwood, B. C., Bremner, A. F., Coombs, G. H. 1986. Polyamine biosynthesis in trichomonads. *Molecular & Biochemical Parasitology*. **19**:241 249.

Oredsson, S. M., Friend, D. S., Marton, L. J. 1983. Changes in mitochondrial structure and function in 9l rat brain tumor cells treated in vitro with alpha difluoromethylornithine, a polyamine biosynthesis inhibitor. *Proceedings of the National Academy of Sciences U.S.A.* **80**:780-784.

Padh, H., Lavasa, M., Steck, T.L. 1989. Prelysosomal acidic vacuoles in Dictyostelium discoideum. *Journal of Cell Biology.* **108**:865-874.

Paget, T.A., Jarroll, E.L., Manning, P., Lindmark, D.G., Lloyd, D. 1989. Respiration in the cysts and trophozoites of *Giardia muris*. *Journal of General Microbiology.* **135**:145-54.

Paget, T.A., Kelly, M.L., Jarroll, E.L., Lindmark, D.G., Lloyd, D. 1993. The effects of oxygen on fermentation in *Giardia lamblia. Molecular & Biochemical Parasitology.* **57**:65-71.

Paget, T. A. & Lloyd, D. 1990. *Trichomonas vaginalis* requires traces of oxygen and high concentrations of carbon dioxide for optimal growth. *Molecular & Biochemical Parasitology.* **41**:65--72.

Paget, T.A., Raynor, M.H., Shipp, D.W., Lloyd, D. 1990. *Giardia lamblia* produces alanine anaerobically but not in the presence of oxygen. *Molecular & Biochemical Parasitology.* **42**:63-67.

Palm, D., Weiland, M., McArthur, A.G., Winiecka-Krusnell, J., Cipriano, M.J., Birkeland, S.R., Pacocha, S.E., Davids, B., Gillin, F., Linder, E., Svard, S. 2005. Developmental changes in the adhesive disk during Giardia differentiation. *Molecular & Biochemical Parasitology.* **141**:199-207.

Paltauf, F. & Meingassner, J.G. 1982. The absence of cardiolipin in hydrogenosomes of *Trichomonas vaginalis* and *Tritrichomonas foetus. Journal of Parasitology.* **68**:949-950.

Paveto C., Pereira C., Espinosa J., Montagna A. E., Farber M., Esteva M., Flawia M. M., Torres H. N. 1995. The nitric oxide transduction pathway in *Trypanosoma cruzi. Journal of Biological Chemistry.* **270**:16576-9.

Petrin, D., Delgaty, K., Bhatt, R., Garber, G. 1998. Clinical and microbiological aspects of *Trichomonas vaginalis. Clinical Microbiology Reviews.* **11**:300-17.

Pfarr, K.M. & Fuhrman, J. A. 2000. *Burgia malayi*: localization of nitric oxide synthase in a lymphatic filariid. *Experimental Parasitology.* **94**:92-98.

Quick, R., Paugh, K., Addiss, D., Kobayashi, J., Baron, R. 1992. Restaurant associated outbreak of giardiasis. *Journal of Infectious Diseases.* **166**:673--6.

Rahmatullah M. & Boyd T.R. 1980. Optimizaion of conditions for the colorimetric determination of citrulline, using diacetyl monoxime. *Analytical Biochemistry.* **107**:424-31.

Rasoloson, D., Vanacova, S., Tomkova, E., Razga, J., Hrdy, I., Tachezy, J., Kulda, J 2002. Mechanism of in vitro development of resistanct to metronidazole in *Trichomonas vaginalis. Microbiology.* **148**:2467-2477.

Regoes, A., Zourmpanou, D., Leon-Avila, G., van der Giezen, M., Tovar, J., Hehl, A.B. 2005. Protein import, replication, and inheritance of a vestigial mitochondrion. *Journal of Biological Chemistry.* **280**:30557-63.

Reguera, R.M., Tekwani, B.L., Balana-Fouce, R. 2005. Polyamine transport in parasites: a potential target for new antiparasitic drug development. *Comparative Biochemistry and Physiology. Toxicology and Pharmacology.* **140**:151-164.

Rein, M.F. 1990. Clinical manifestations of urogenital trichomoniasis in women. In *Trichomonads Parasitic in Humans*, ed. Honigberg, B.M. New York: Springer Verlag. pp. 225-273.

Reis, I. A., Martinez, M. P., Yarlett, N., Johnson, P. J., Silva-Filho, F. C., Vannier Santos, M. A. 1999. Inhibition of polyamine synthesis arrests trichomonad growth and induces destruction of hydrogenosomes. *Antimicrobial Agents & Chemotherapy.* **43**:1919-1923.

Rendtorff R.C. 1954. The experimental transmission of human intestinal protozoan parasites. II. *Giardia lamblia* cysts given in capsules. *American Journal of Hygiene.* **59**:209-20.

Reynolds, E. S. 1963. The use of lead citrate at high pH as an electron-opaque stain in electron microscopy. *Journal of Cell Biology.* **17**:208-212.

Rhyan JC, Stackhouse LL, Quinn WJ. 1988. Fetal and placental lesions in bovine abortion due to *Tritrichomonas foetus. Veterinary Pathology.* **25**:350-355.

Richards, T.A., and van der Giezen, M. 2006. Evolution of the Isd11/IscS complex reveals a single α-proteobacterial endosymbiosis for all eukaryotes. *Moecular Biology & Evolution.* **23**:1341-1344.

Roger, A.J. 1998. A mitochondrial-like chaperonin 60 gene in Giardia lamblia: evidence that diplomonads once harbored an endosymbiont related to the progenitor of mitochondria. *Proceedings of the National Academy of Sciences USA.* **95**:229-234.

Samuelson, J. 1999. Why metronidazole is active against both bacteria and parasites. *Antimicrobial Agents & Chemotherapy.* **43**:1533-1541.

Sarti, P., Fiori, P. L., Forte, E., Rappelli, P., Teixeira, M., Mastronicola, D., Sanciu, G., Giuffre, A., Brunori, M. 2004. *Trichomonas vaginalis* degrades nitric oxide and expresses a flavorubredoxin-like protein: a new pathogenic mechanism? *Cellular and Molecular Life Sciences.* **61**:618-23.

Scaduto, R. C. Jr. & Grotyohann, L. W. 1999. Measurement of mitochondrial membrane potential using fluorescent rhodamine derivatives. *Biophysics Journal.* **76**:469-477.

Septinus, M., Seiffert, W., Zimmermann, H. W. 1983. Hydrophobic acridine dyes for fluorescence staining of mitochondria in living cells. Thermodynamic and spectroscopic properties of 10-n-alkylacridine orange chlorides. *Histochemistry.* **79**:443-456.

Singh, B. N., Costello, C. E. and Beach, D. H. 1991. Structures of glycophosphosphingolipids of *Tritrichomonas foetus*: a novel glycophosphosphingolipid. *Archives of Biochemistry and Biophysics.* **286**:409 418.

Smith, J. D. 1993. Phospholipid Biosynthesis in Protozoa. *Progress in Lipid Research.* **32**:47-60.

Sogin, M.L. & Silberman, J.D. 1998. Evolution of the protists and protistan parasites from the perspective of molecular systematics. *International Journal of Parasitology.* **28**:11-20.

Soper, D. 2004. Trichomoniasis: under control or undercontrolled? *American Journal of Obstetrics and Gynecology.* **190**:281-290.

Sorvillo, F. & Kerndt, P. 1998. *Trichomonas vaginalis* and amplification of HIV-1 transmission. *Lancet.* **351**:213-214.

Sorvillo, F., Smith, L., Kerndt, P., Ash, L. 2001. *Trichomonas vaginalis*, HIV, and African-Americans. *Emerging Infectious Diseases.* 7:927-932.

Stuehr, D. Mammalian nitric oxide synthases. 1999. *Biochimica et Biophysica Acta.* **1411**:217-230.

Stevens, L. & McKinnon, I.M. 1977. The effect of 1,4 diaminobutanone on the stability of ornithine decarboxylase from *Aspergillus nidulans. Biochemical Journal.* **166**:635-637.

Swygard, H., Sena, A.C., Hobbs, M.M., Cohen, M.S. 2004. Trichomoniasis: clinical manifestations, diagnosis and management. *Sexually Transmitted Infection.* **80**:91-95.

Tachezy, J., Sanchez, L. B., Müller, M. 2001. Mitochondrial type iron-sulfur cluster assembly in the amitochondriate eukaryotes *Trichomonas vaginalis* and *Giardia intestinalis*, as indicated by the phylogeny of IscS. *Molecular Biology & Evolution.* **18**:1919-1928.

Tanabe M. 1979. *Trichomonas vaginalis*: NADH oxidase activity. *Experimental Parasitology.* **48**:135-143.

Thirion, J., Wattiaux, R., Jadot, M. 2003. The acid phosphatase positive organelles of the *Giardia lamblia* trophozoite contain a membrane bound cathepsin C activity. *Biology of the Cell.* **95**:99-105.

Thompson RC. 2000. Giardiasis as a re-emerging infectious disease and its zoonotic potential. *International Journal of Parasitology.* **30**:1259-1267.

Tovar, J., Leon-Avila, G., Sanchez, L.B., Sutak, R., Tachezy, J., van der Giezen, M., Hernandez, M., Muller, M., Lucocq, J.M. 2003. Mitochondrial remnant organelles of Giardia function in iron-sulphur protein maturation. *Nature.* **426**:172-6.

van der Giezen, M., Tovar, J., and Clark, C.G. 2005. Mitochondrion-derived organelles in protists and fungi. *International Review or Cytology.* **244**:175-225.

Vickerman, K. 1978. Antigenic variation in trypanosomes. *Nature.* **273**:613-617.

Visser, A.A. & Hundt, H.K. 1984. The pharmacokinetics of a single intravenous dose of metronidazole in pregnant patients. *Journal of Antimicrobial Chemotherapy.* **13**:279-283.

Wallace, H.M., Fraser, A.V., Hughes, A. 2003. A perspective of polyamine metabolism. *Biochemical Journal.* **376**:1-14.

Wang, X., Sun, H., Li, C. 2006. Nitric oxide induces promyelocytic cell growth arrest and apoptosis through deactivation of Akt pathway. *Leukemia Research.* Doi: 10.1016/j.leukres.2006.07.023.

White, E., Hart, D., Sanderson, B. E. 1983. Polyamines in *Trichomonas vaginalis*. *Molecular & Biochemical Parasitology.* **9**:309-18.

Wiesehahn, G.P., Jarroll, E.L., Lindmark, D.G., Meyer, E.A., Hallick, L.M. 1984. *Giardia lamblia*: autoradiographic analysis of nuclear replication. *Experimental Parasitology.* **58**:94-100.

World Health Organization. 2001. Global Prevalence and Incidence of Selected Curable Sexually Transmitted Infections Overview and Estimates. http://whqlibdoc.who.int/hq/2001/WHO_HIV_AIDS_2001, pp. 1-50.

Wright, J.M., Dunn, L.A., Upcroft, P., Upcroft, J.A. 2003. Efficacy of antigiardial drugs. *Expert Opinions on Drug Safety.* **2**:529-541.

Yamasaki, H. & Cohen, M.F. 2006. NO signal at the crossroads: polyamine-induced nitric oxide synthesis in plants? *Trends in Plant Science.* **11**:522-524.

Yarlett, N. & Bacchi, C.J. 1988. Effect of DL-alpha-difluoromethylornithine on polyamine synthesis and interconversion in *Trichomonas vaginalis* grown in a semi-defined medium. *Molecular & Biochemical Parasitology.* **31**:1-9.

Yarlett, N. & Bacchi, C.J. 1994. Parasite polyamine metabolism: targets for chemotherapy. *Biochemical Society Transactions.* **22**:875-879.

Yarlett, N., Goldberg, B., Moharrami, M.A., Bacchi, C.J. 1993. *Trichomonas vaginalis*: characterization of ornithine decarboxylase. *Biochemical Journal.* **293**: 487-493.

Yarlett, N., Lindmark, D. G., Goldberg, B., Moharrami, M. A., Bacchi, C. J. 1994. Subcellular localization of the enzymes of the arginine dihydrolase pathway in *Trichomonas vaginalis* and *Tritrichomonas foetus. Journal of Eukaryotic Microbiology.* **41**:554-559.

Yarlett, N., Martinez, M. P., Goldberg, B., Kramer, D. L., Porter, C. W. 2000. Dependence of *Trichomonas vaginalis* upon polyamine backconversion. *Microbiology.* **146**: 2715-2722.

Yarlett, N., Martinez, M. P., Moharrami, M. A., Tachezy, J. 1996. The contribution of the arginine dihydrolase pathway to energy metabolism by *Trichomonas vaginalis. Molecular & Biochemical Parasitology.* **78**:117-125.

Yu, L.Z., Birky, C.W. Jr., Adam, R.D. 2002. The two nuclei of *Giardia* each have complete copies of the genome and are partitioned equationally at cytokinesis. *Eukaryotic Cell.* 1:191-199.

APPENDIX: Microscopy of *T. vaginalis*

Scanning electron microscopy. Sedimented *T. vaginalis* organisms were fixed in a solution containing 2.5% (v/v) glutaraldehyde, 0.05M sodium cacodylate (pH 6.8), 2mM $CaCl_2$, and 0.2M sucrose, and incubated for 1 h. The samples were then dried on a platform surrounded by paper towels immersed in glutaraldehyde for 20 min. The filter paper was then put into tubes, and centrifuged on low speed (500 x g) for 2 min to completely dry the filter. The samples were subsequently incubated in 1.0% osmium tetroxide in 0.1M cacodylate buffer for 1 h. The samples were dehydrated at 20 °C by exposure to successive ethanol washes, each lasting 5 min: 30%, 50%, 70%, 90%, and finally three successive washes in 100% ethanol (% v/v). Samples were then plated with gold using a thirty min cycle. Samples were then viewed under the scanning electron microscope.

Transmission electron microscopy. All procedures were carried out at 4 °C, unless otherwise specified. Sedimented organisms or subcellular fractions were fixed in a solution containing 2.5% (v/v) glutaraldehyde, 0.05M sodium cacodylate (pH 6.8), 2mM $CaCl_2$, and 0.2M sucrose, and incubated for 1 h. The pellet was then washed in a buffer containing 0.1M calcium cacodylate, 2mM $CaCl_2$, and 0.2M sucrose, and incubated overnight. The samples were then incubated in 1.0% osmium tetroxide in 0.1M cacodylate buffer for 1 h. The samples were dehydrated at 20 °C by exposure to successive ethanol washes, each lasting 5 min: 30%, 50%, 70%, 90%, and finally three successive washes in 100% ethanol (% v/v). The samples were then incubated for 10 min in pure propylene oxide at 20 °C. Samples were subsequently incubated overnight in a 1:1 mixture of propylene dioxide and

araldite CY212 at 20 °C. The following day, samples were embedded into new resin and allowed to incubate at 60 °C for 48 h. Thin sections were then cut, stained for 10 min with 2% uranyl acetate (% w/v) and subsequently with lead citrate for 5 min (Reynolds, 1963), washed briefly and finally examined using a Philips Electron Microscope 208, operated at 80kV.

SCANNING ELECTRON MICROSCOPY: *Trichomonas vaginalis*

All scanning EM images (Fig. A1.1-A1.8) represent whole organisms, grown under control conditions. They have been fixed using the procedures outlined above.

Fig. A1.1: *T. vaginalis*

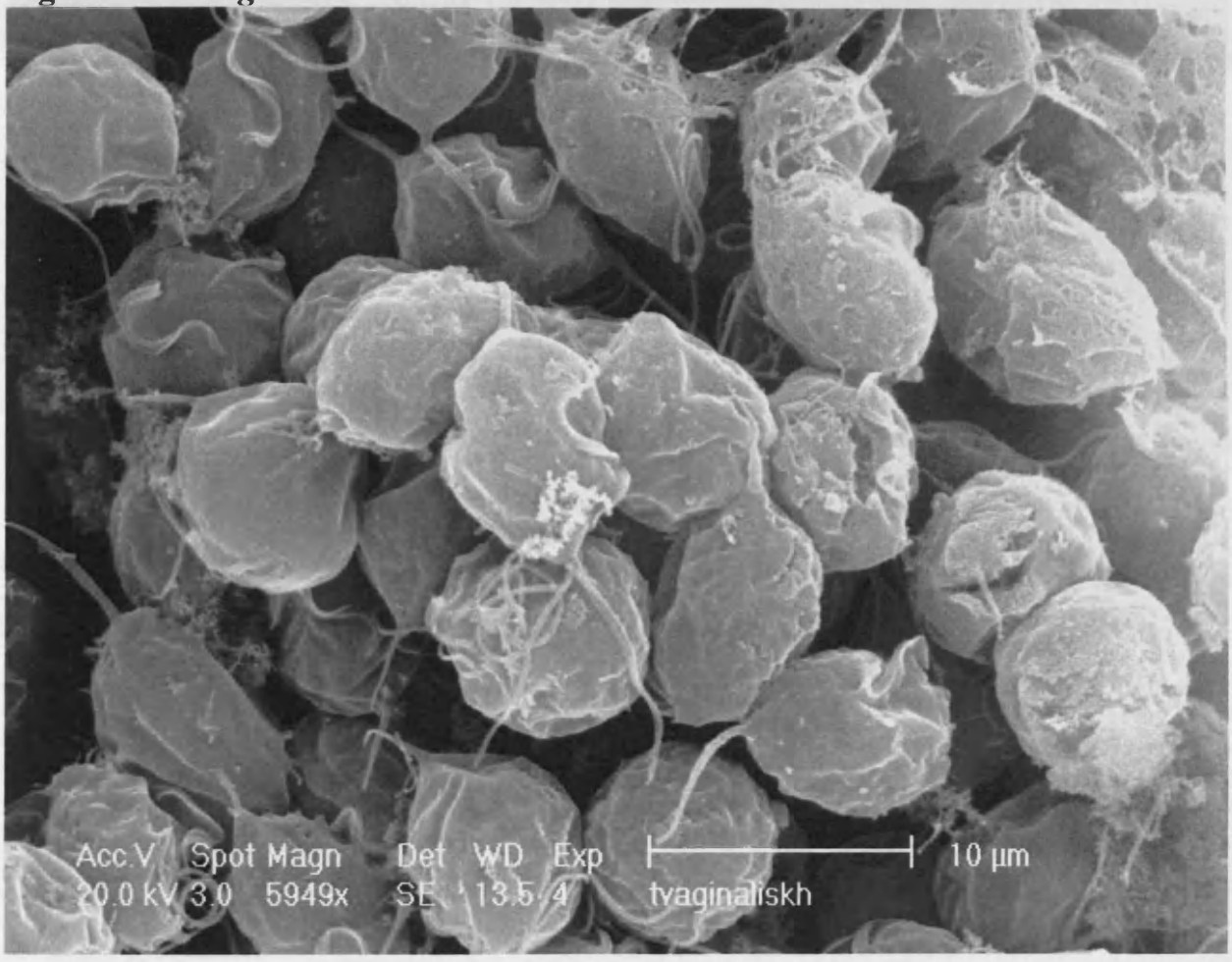

Fig. A1.2: *T. vaginalis*

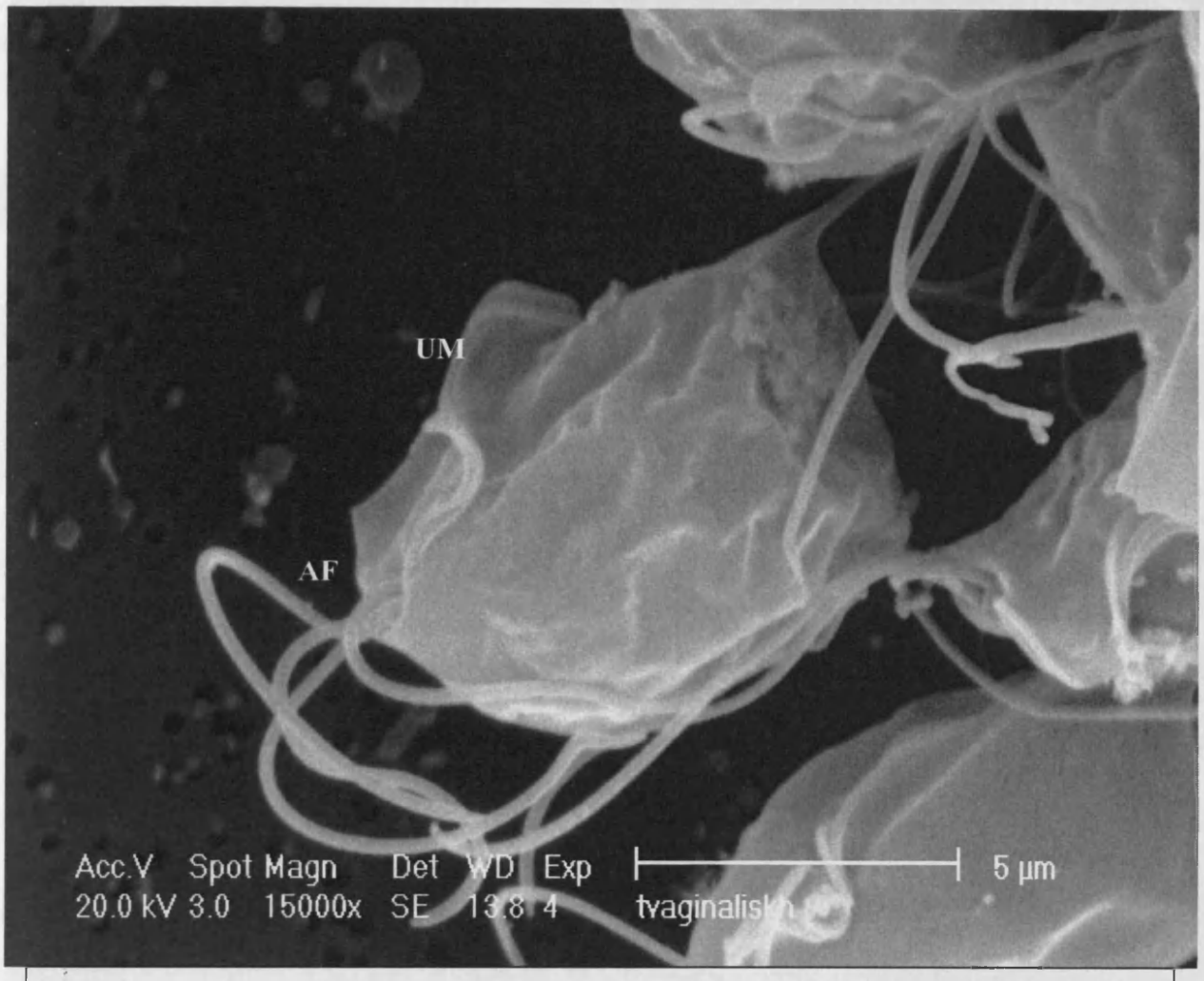

One *T. vaginalis* organism. UM = undulating membrane. AF = anterior flagella (note the presence of four, as expected).

Fig. A1.4: ***T. vaginalis***

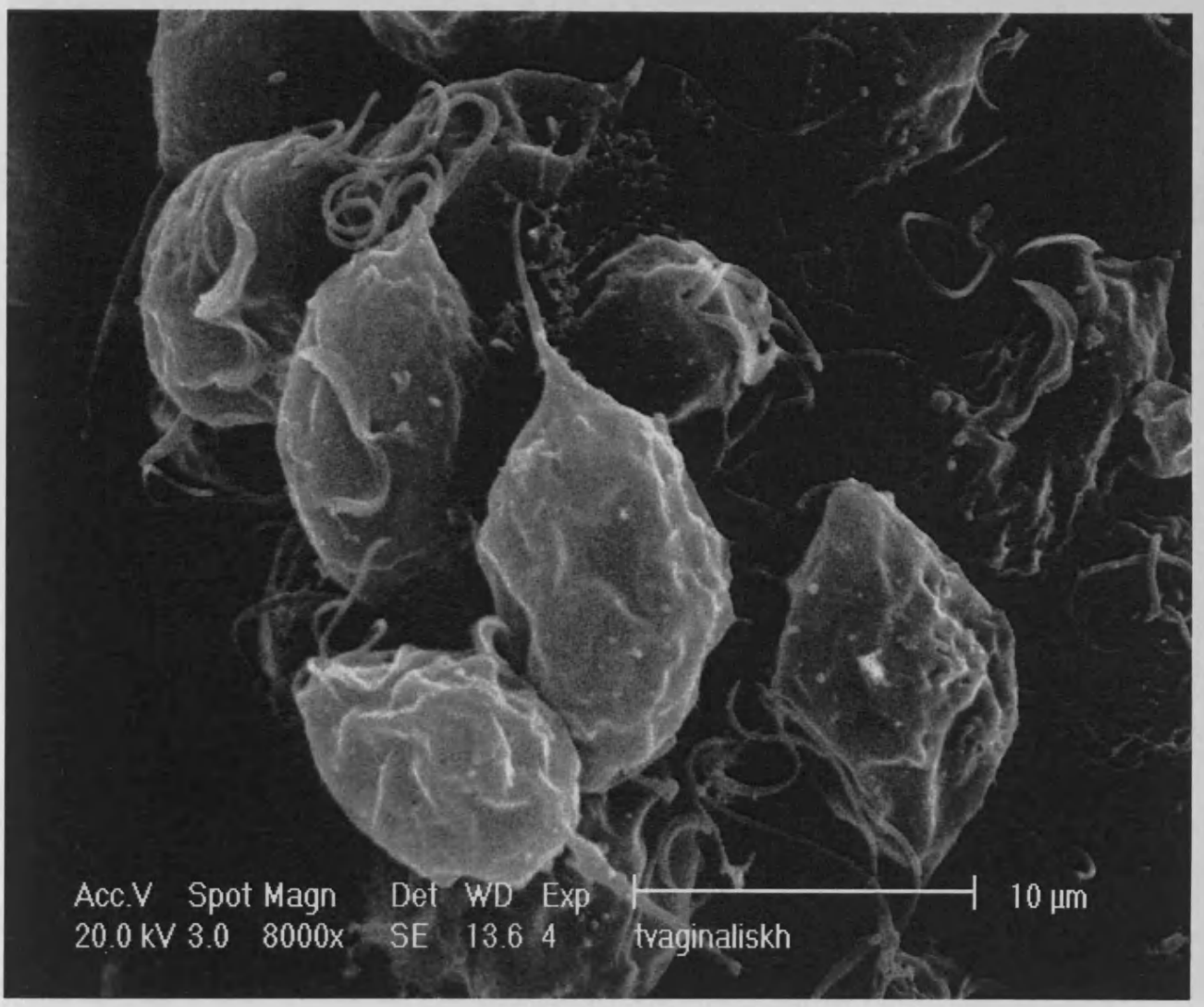

Fig. A1.5: *T. vaginalis*

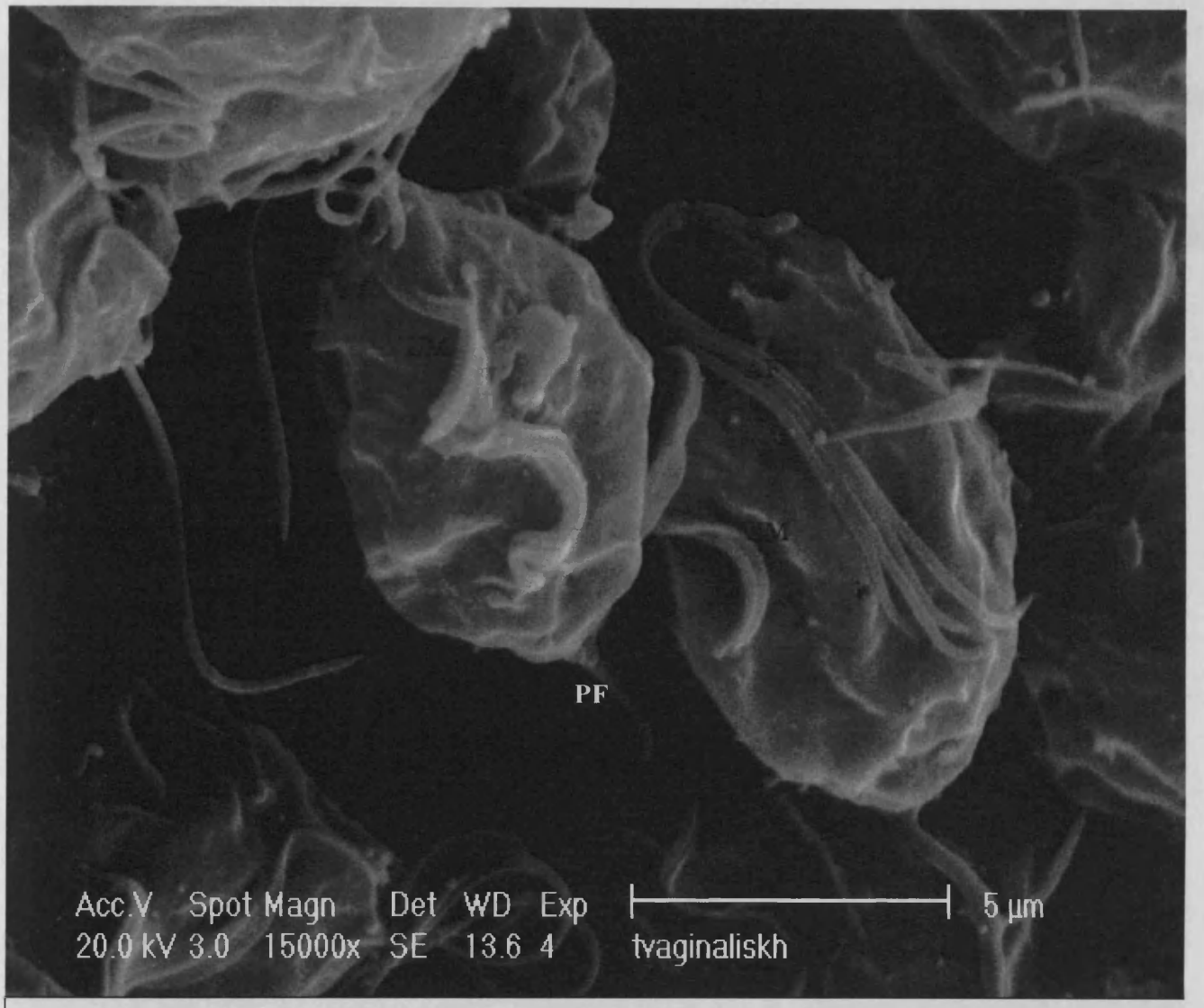

***T. vaginalis*. Note the presence of the unulating membrane (UM) and four anterior flagella (AF) as well as one posterior flagellum (PF)**

Fig. A1.6: *T. vaginalis*

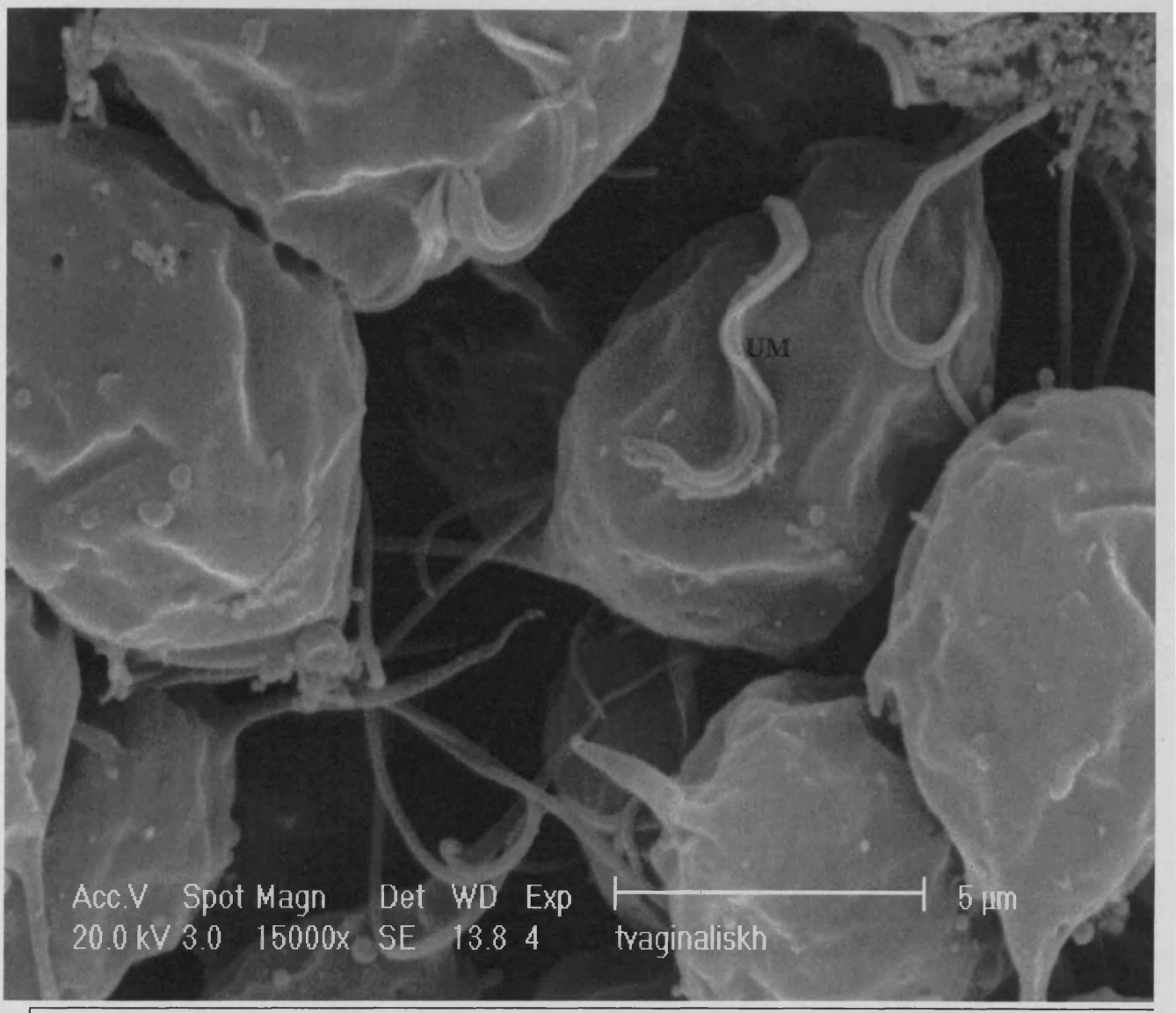

***T. vaginalis*. Note the presence of the unulating membrane (UM).**

Fig. A1.7: ***T. vaginalis***

Fig. A1.8: *T. vaginalis*

***T. vaginalis*. Note the presence of the unulating membrane (UM).**

TRANSMISSION ELECTRON MICROSCOPY

Fig. A2.1-A2.6 represent whole organisms, grown under control conditions. They have been fixed using the procedures outlined above.

Fig. A2.1: Control *T. vaginalis.* Scale bar=500nm

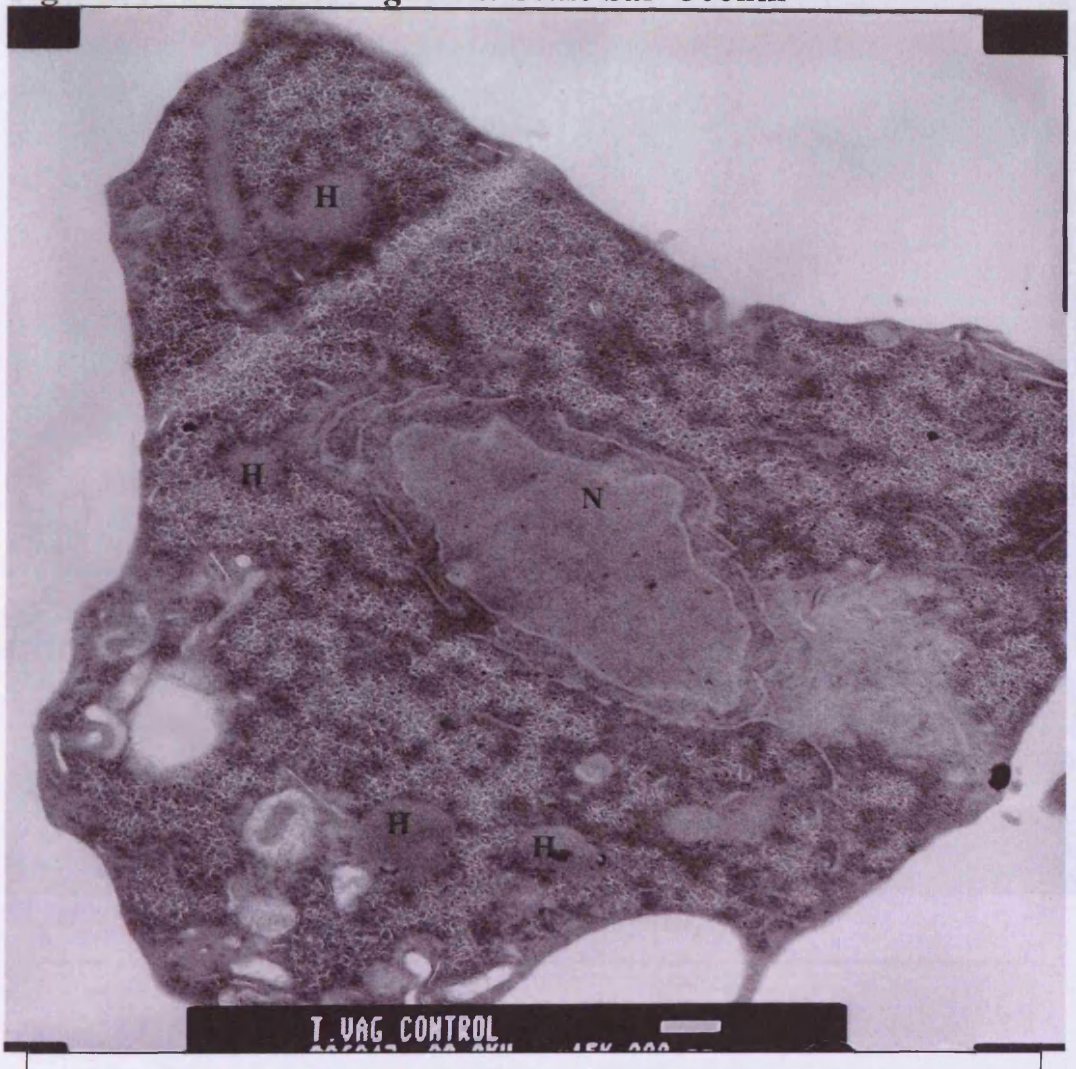

Section of *T. vaginalis.* N=nucleus, H=hydrogenosome

Fig. A2.2:Control *T. vaginalis.* Scale bar=500nm

Section of *T. vaginalis.* H=hydrogenosome

Fig. A2.3:Control *T. vaginalis.* Scale bar=100nm

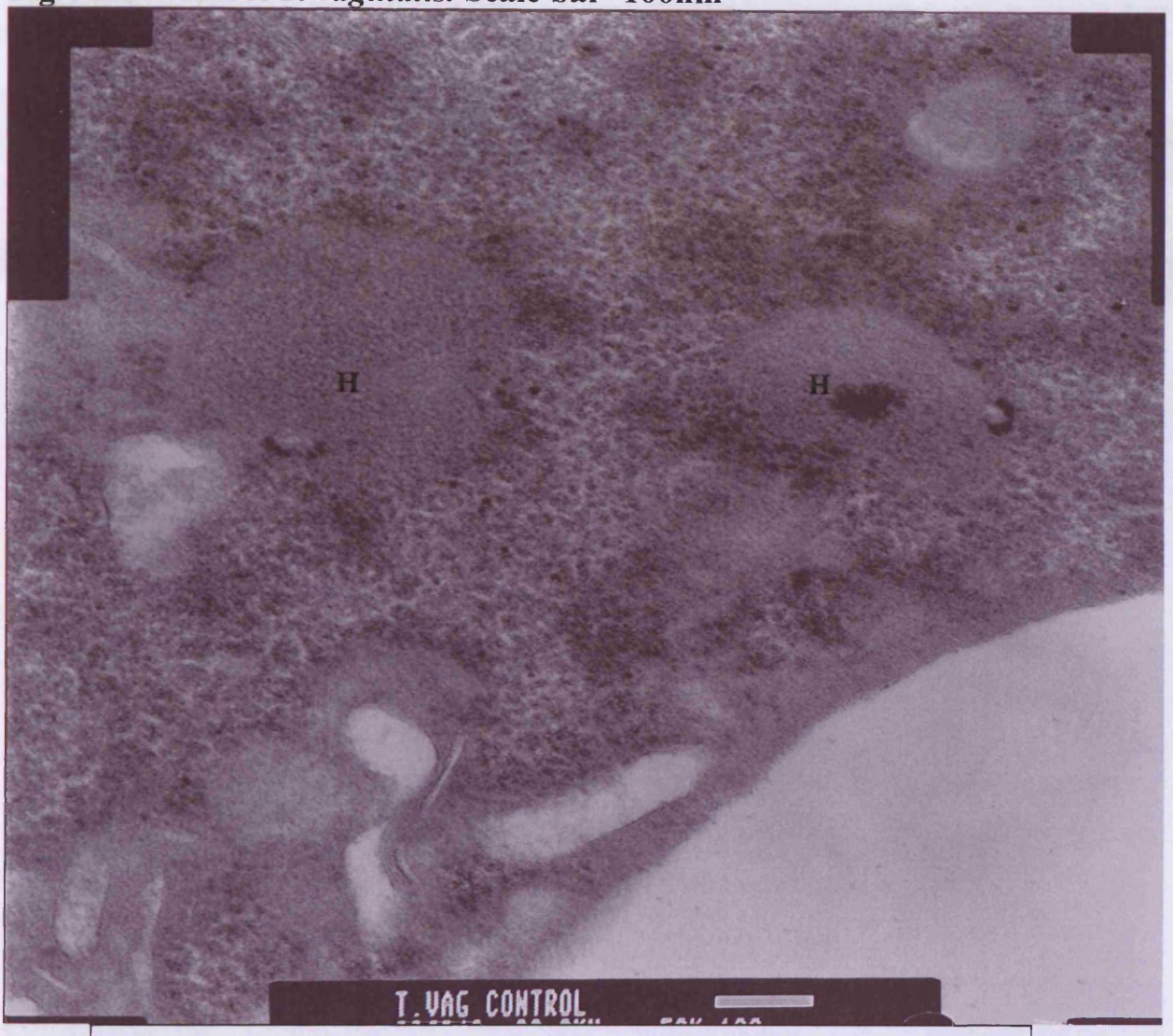

Section of *T. vaginalis* at increased magnification. H=hydrogenosome

Fig. A2.3: Control *T. vaginalis*

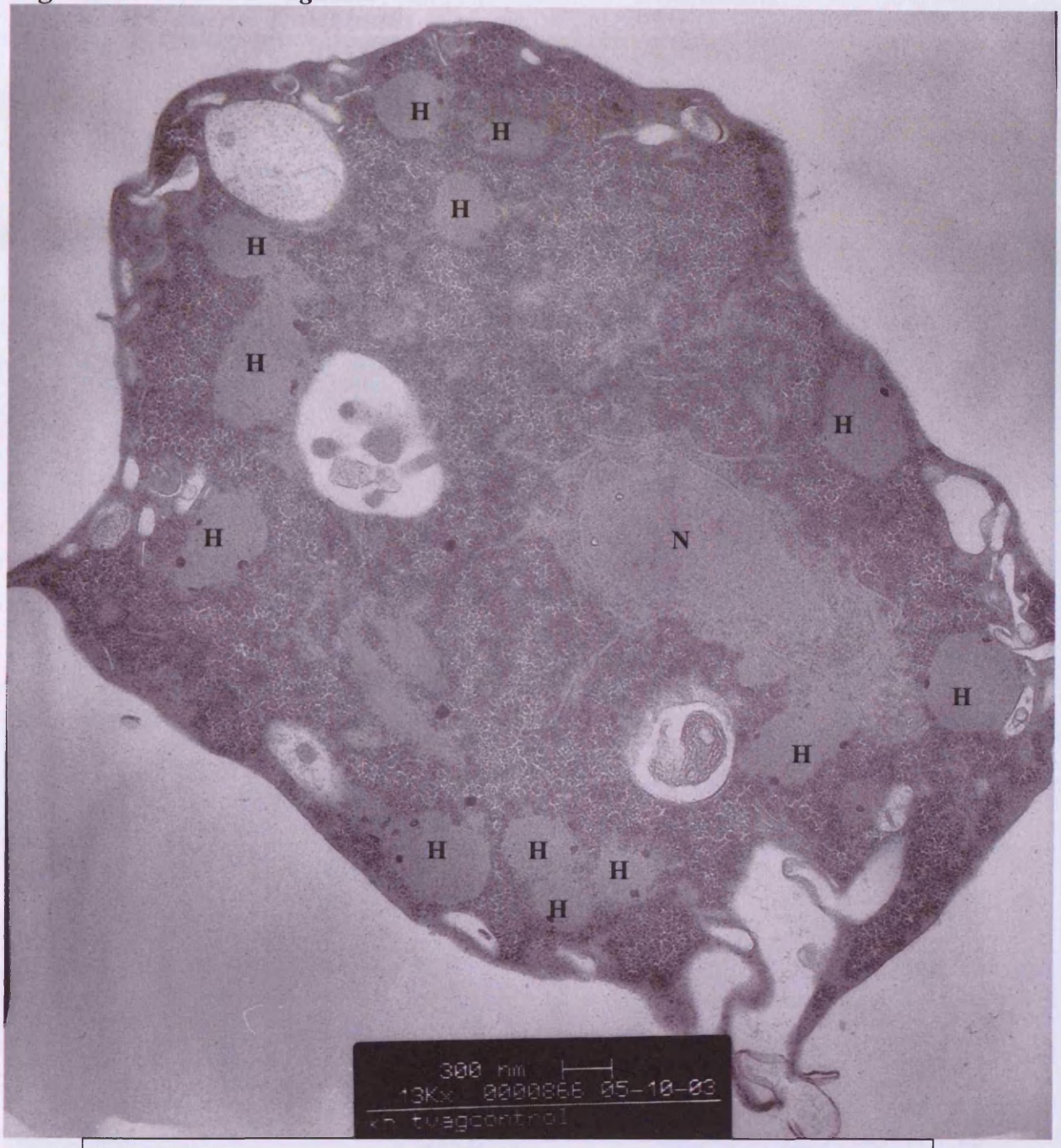

Section of *T. vaginalis*. N=nucleus, H=hydrogenosome

Fig. A2.4: Control *T. vaginalis*

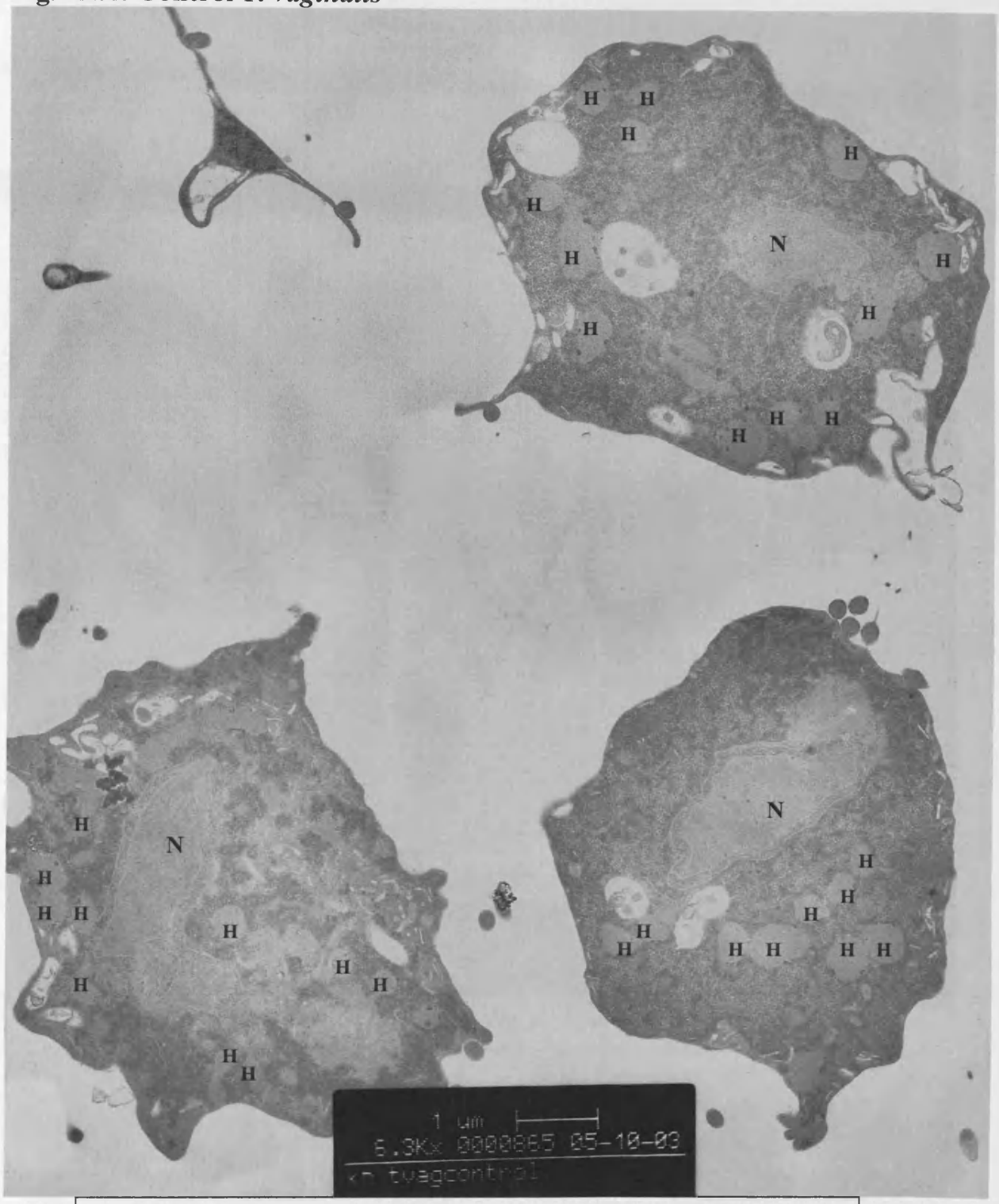

Section of three *T. vaginalis*. N=nucleus, H=hydrogenosome

Fig. A2.5: Control *T. vaginalis*

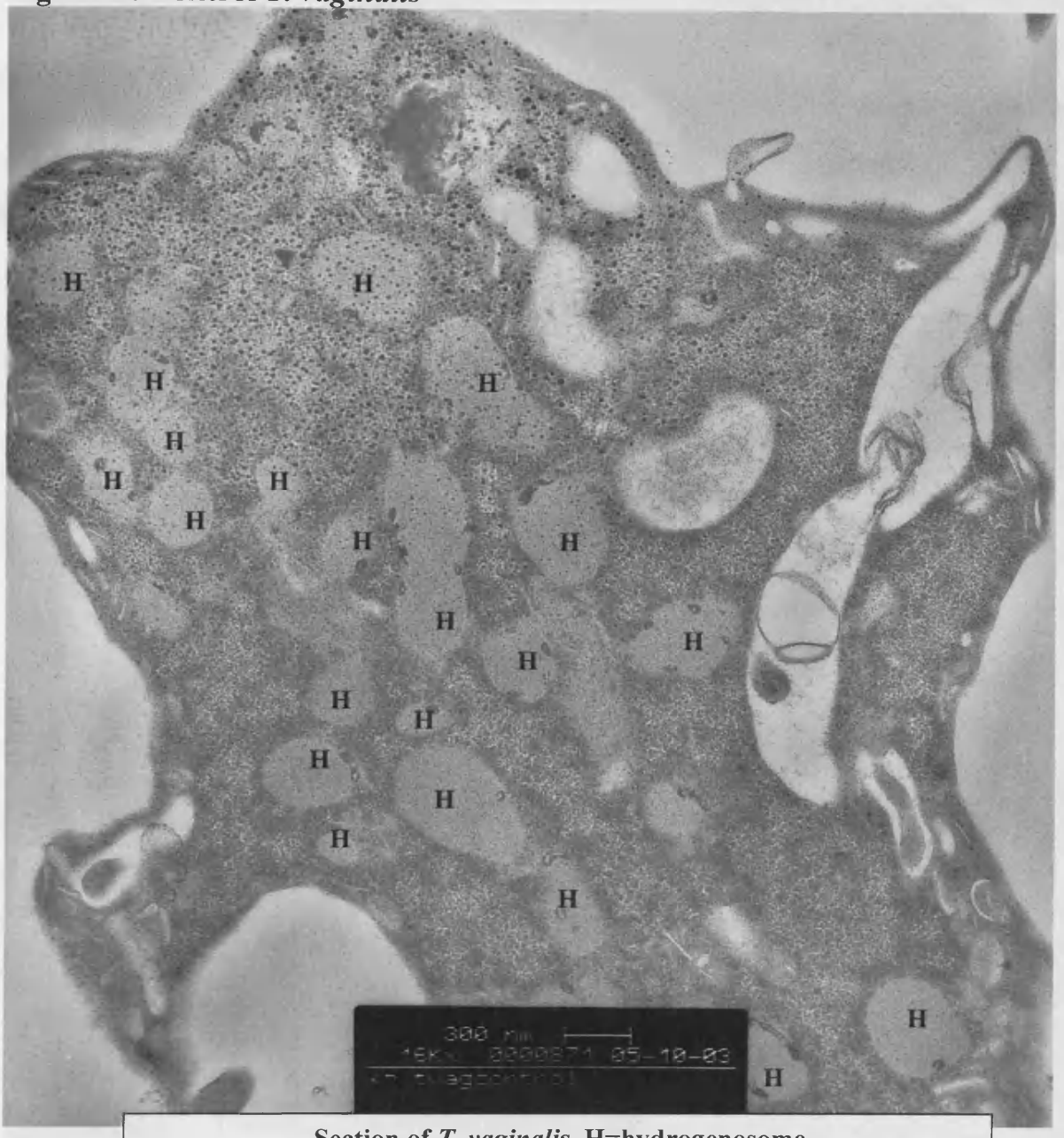

Section of *T. vaginalis*. H=hydrogenosome

Fig. A2.6: Control *T. vaginalis*

Section of *T. vaginalis*. N=nucleus, H=hydrogenosome

TRANSMISSION ELECTRON MICROSCOPY

Fig. A2.7-A2.8 represent whole organisms, grown in the presence of 5mM difluoromethylornithine (DFMO). They have been fixed using the procedures outlined above.

Fig. A2.7: DFMO-grown *T. vaginalis*:

Section of DFMO-grown *T. vaginalis*. H=hydrogenosome

Fig. A2.8: DFMO-grown *T. vaginalis*:

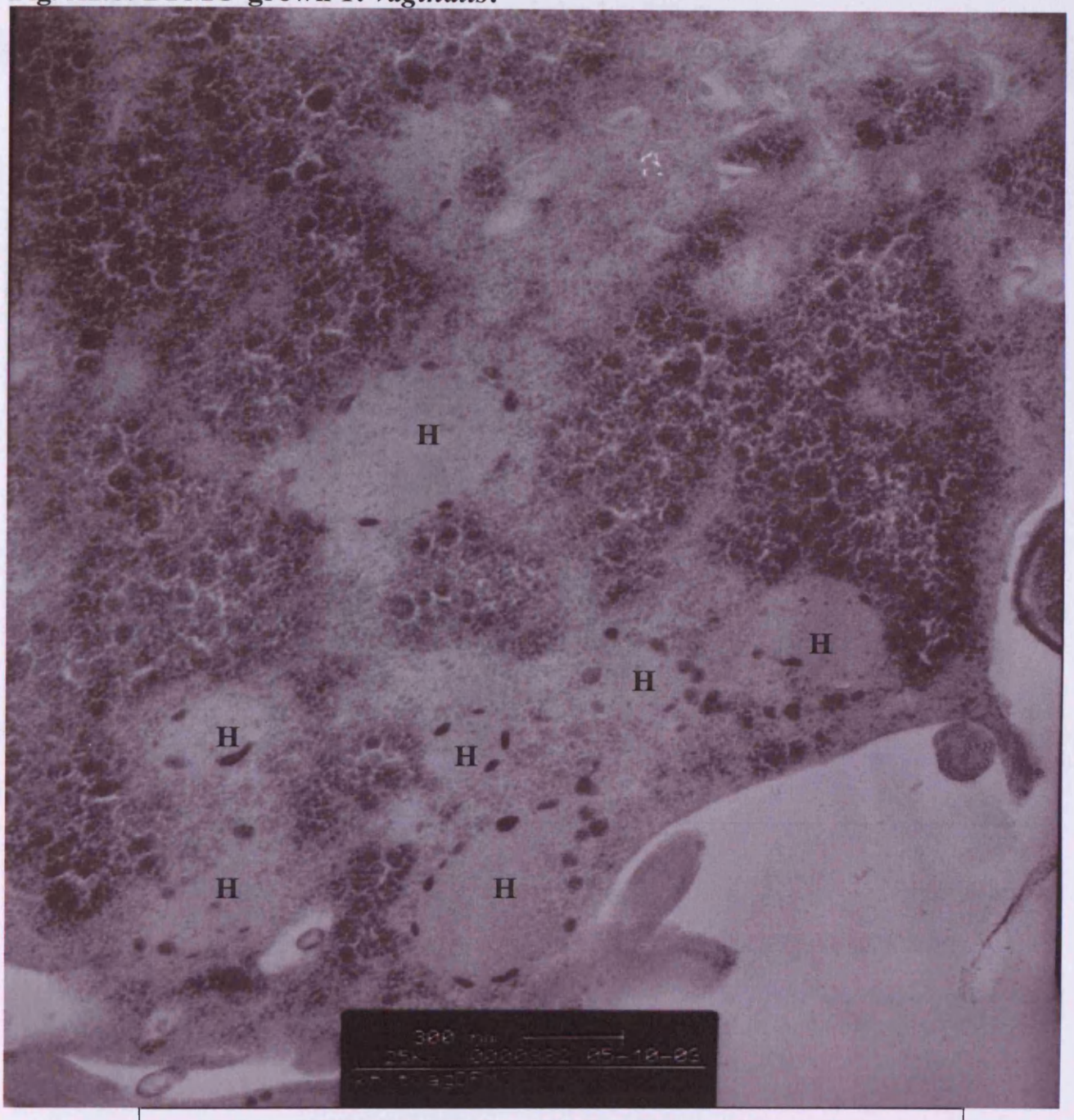

Section of DFMO-grown *T. vaginalis* at increased magnification. H=hydrogenosome

TRANSMISSION ELECTRON MICROSCOPY: ISOLATED HYDROGENOSOMES

Control hydrogenosomes (Appendix Fig. A3.1-A3.6) were isolated from cultures grown overnight in tryptose/yeast/maltose (TYM) medium and isolated using subcellular fractionation techniques (see Methods).

Fig. A3.1: Control hydrogenosome

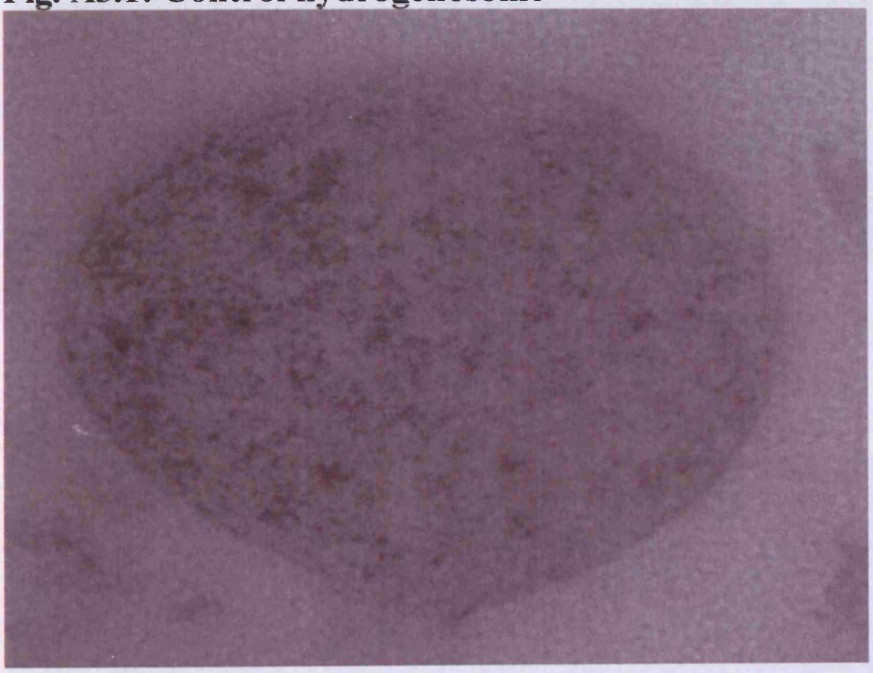

100nm

Fig. A3.2: Control hydrogenosome

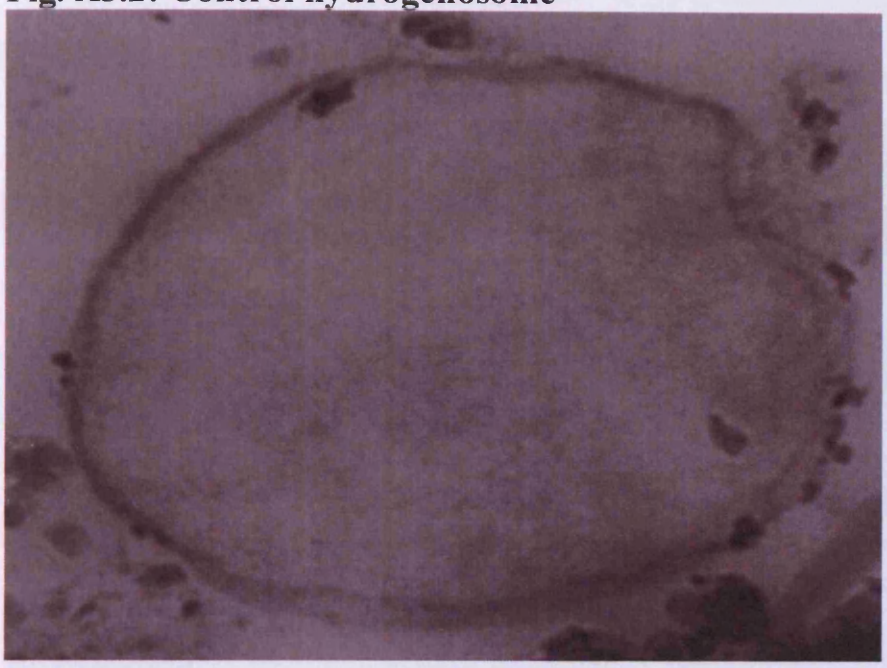

100nm

Fig. A3.3: Control hydrogenosome

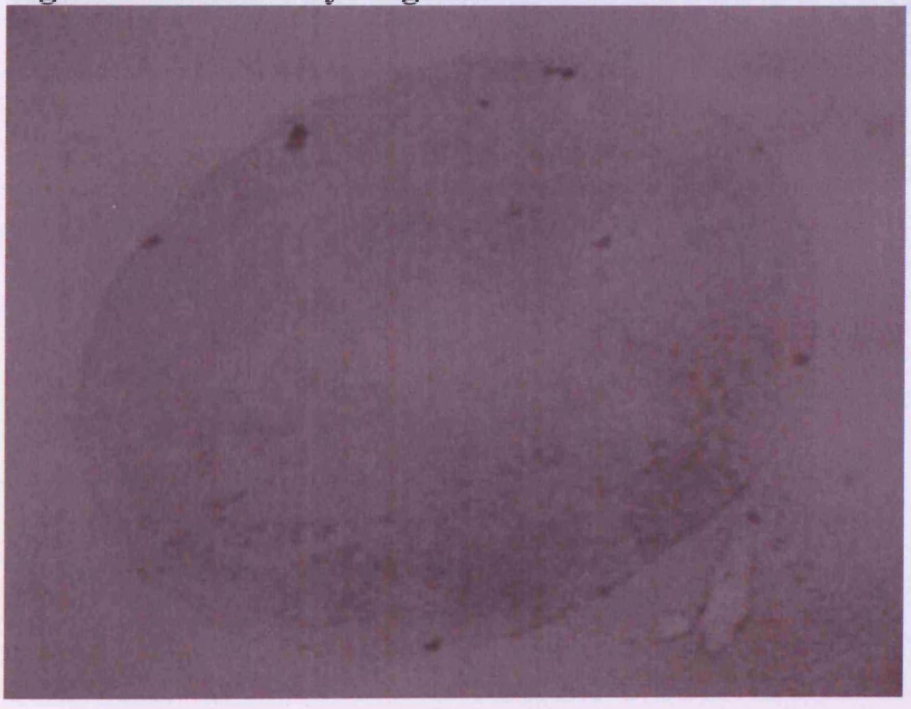

100nm

Fig. A3.4: Control hydrogenosome

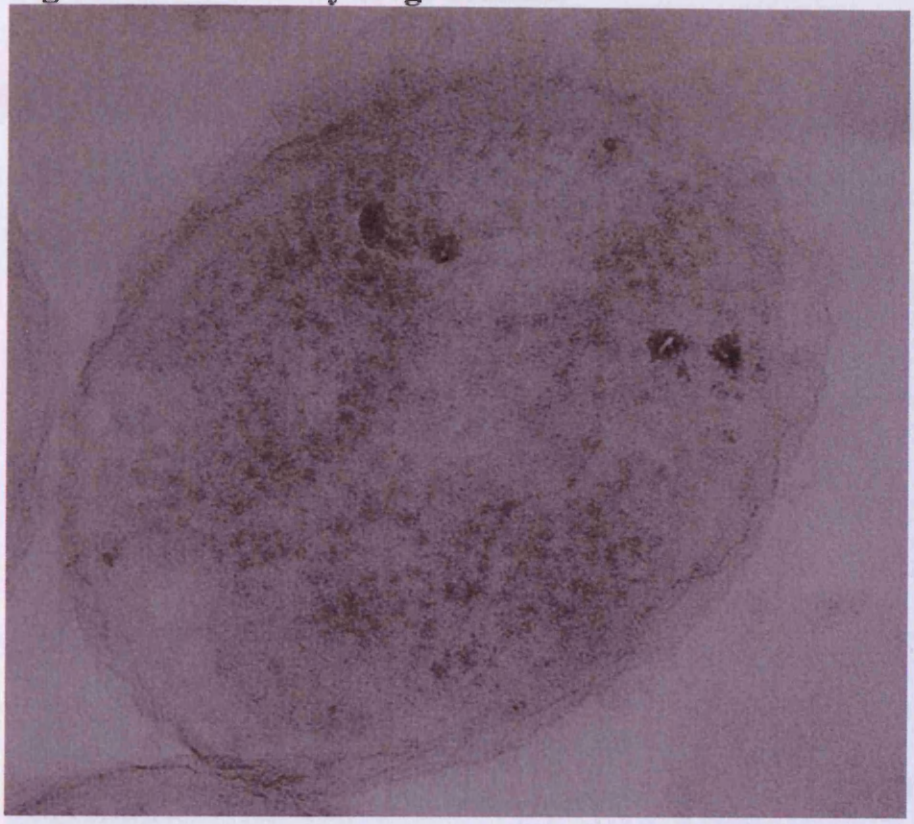

100nm

Fig. A3.5: Control hydrogenosomes

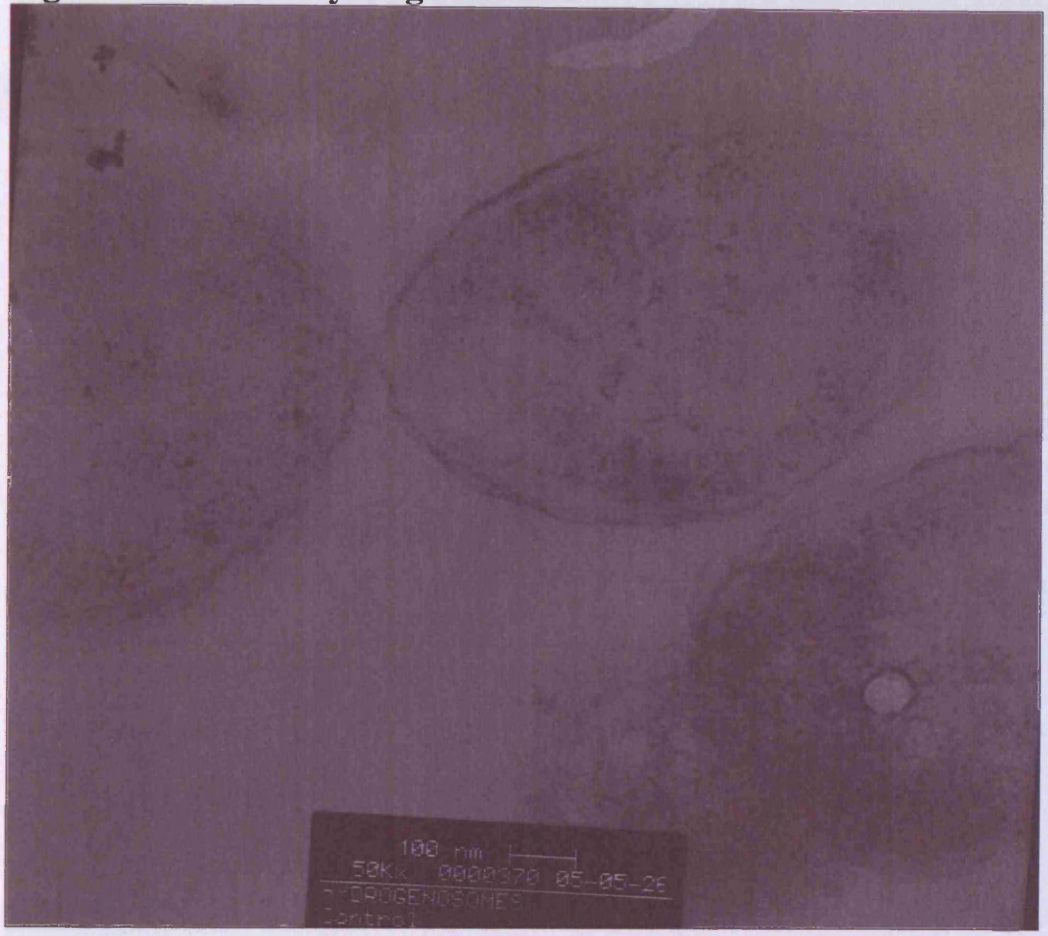

Scale bar on image is 100nm

Fig. A3.6: Control hydrogenosomes

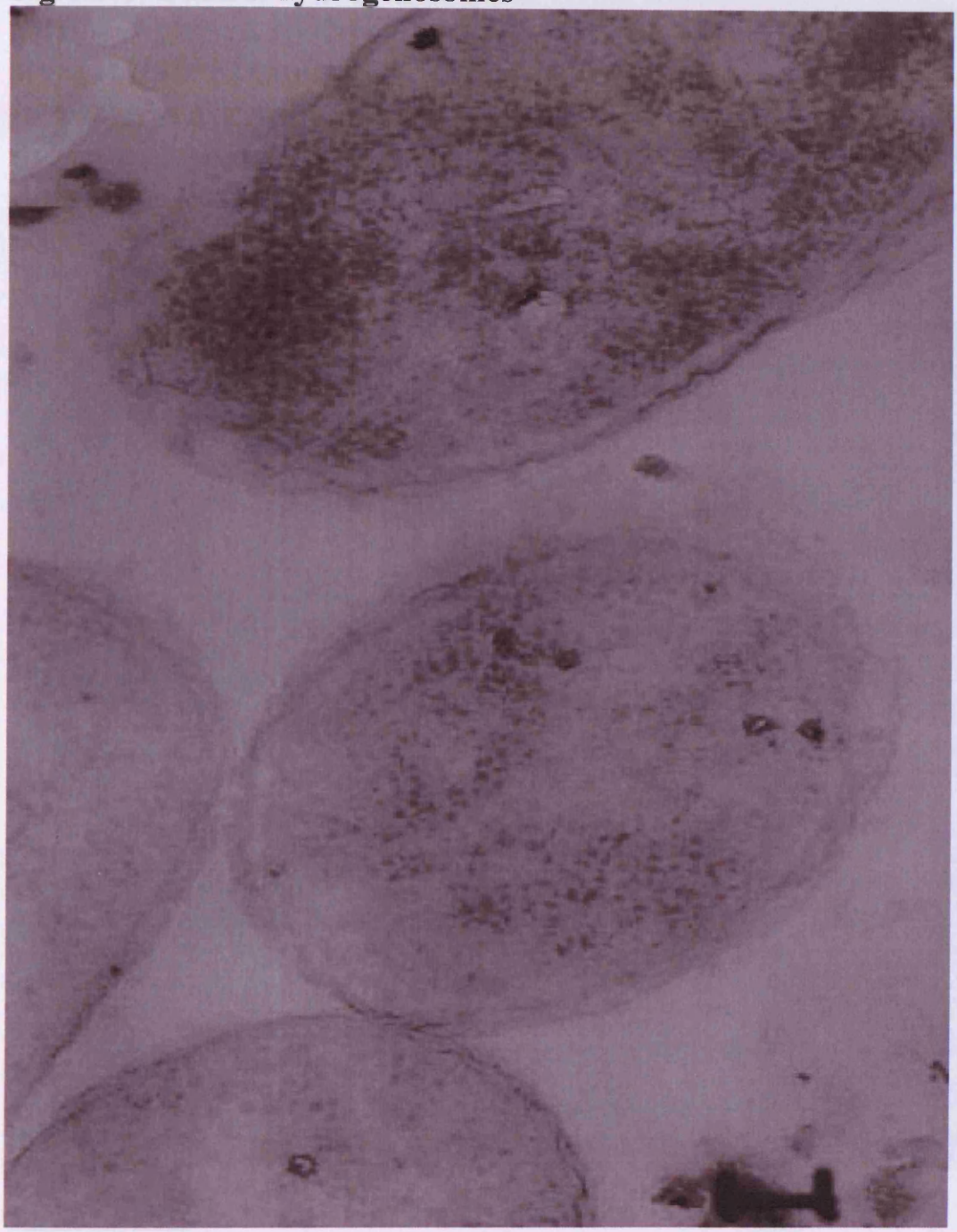

100nm

HYDROGENOSOMES ISOLATED FROM DFMO-GROWN *T. vaginalis*

"DFMO-grown hydrogenosomes" (Appendix Fig. A3.7-A3.15) were isolated from cultures grown overnight in tryptose/yeast/maltose (TYM) medium containing 5mM difluoromethylornithine, an irreversible inhibitor of ornithine decarboxylase, which therefore inhibits polyamine metabolism.

Fig. A3.7: DFMO-grown hydrogenosome

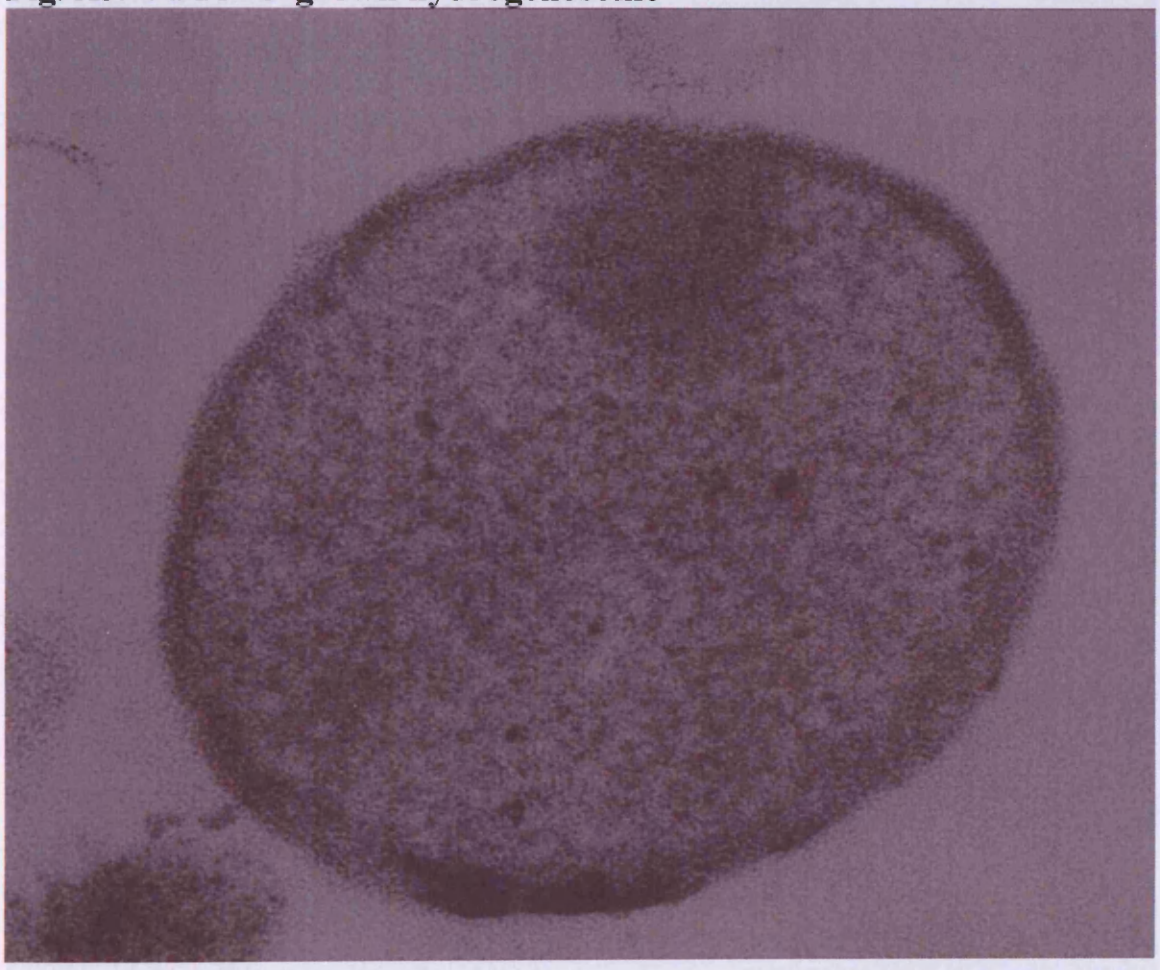

100nm

Fig. A3.8: DFMO-grown hydrogenosomes

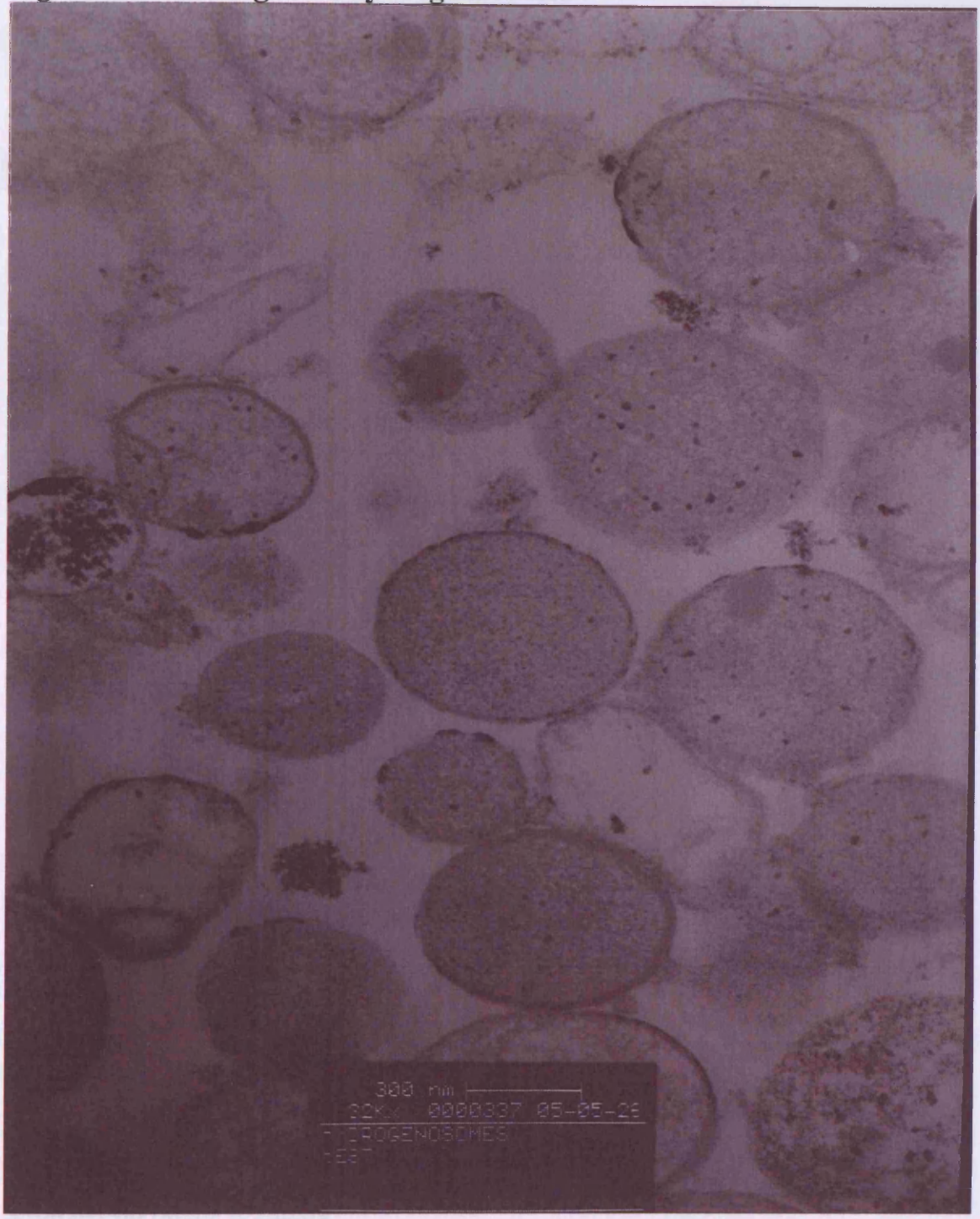

Scale bar on image is 300nm

Fig. A3.9: DFMO-grown hydrogenosomes

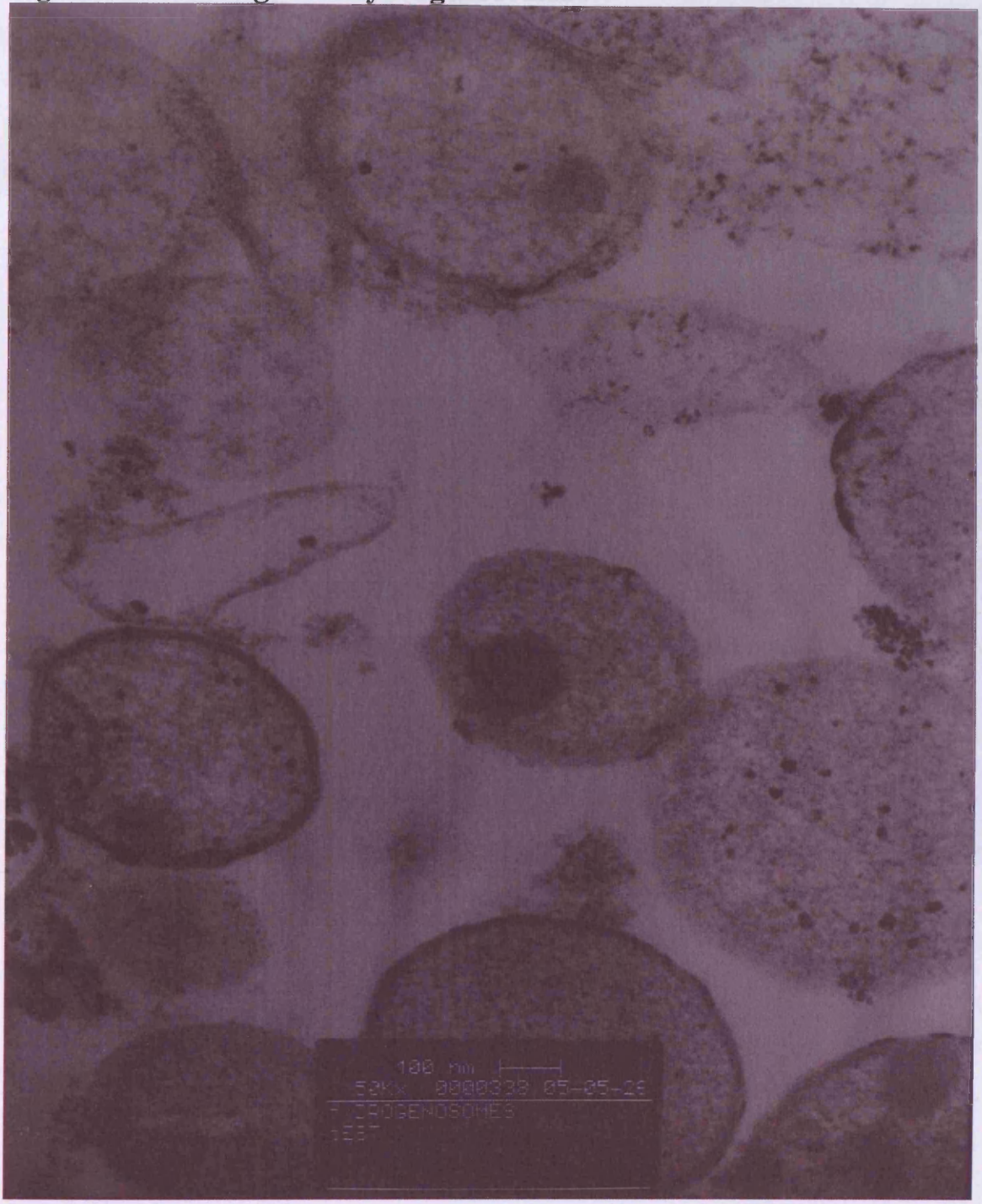

Scale bar on image is 100nm

Fig. A3.10: DFMO-grown hydrogenosomes

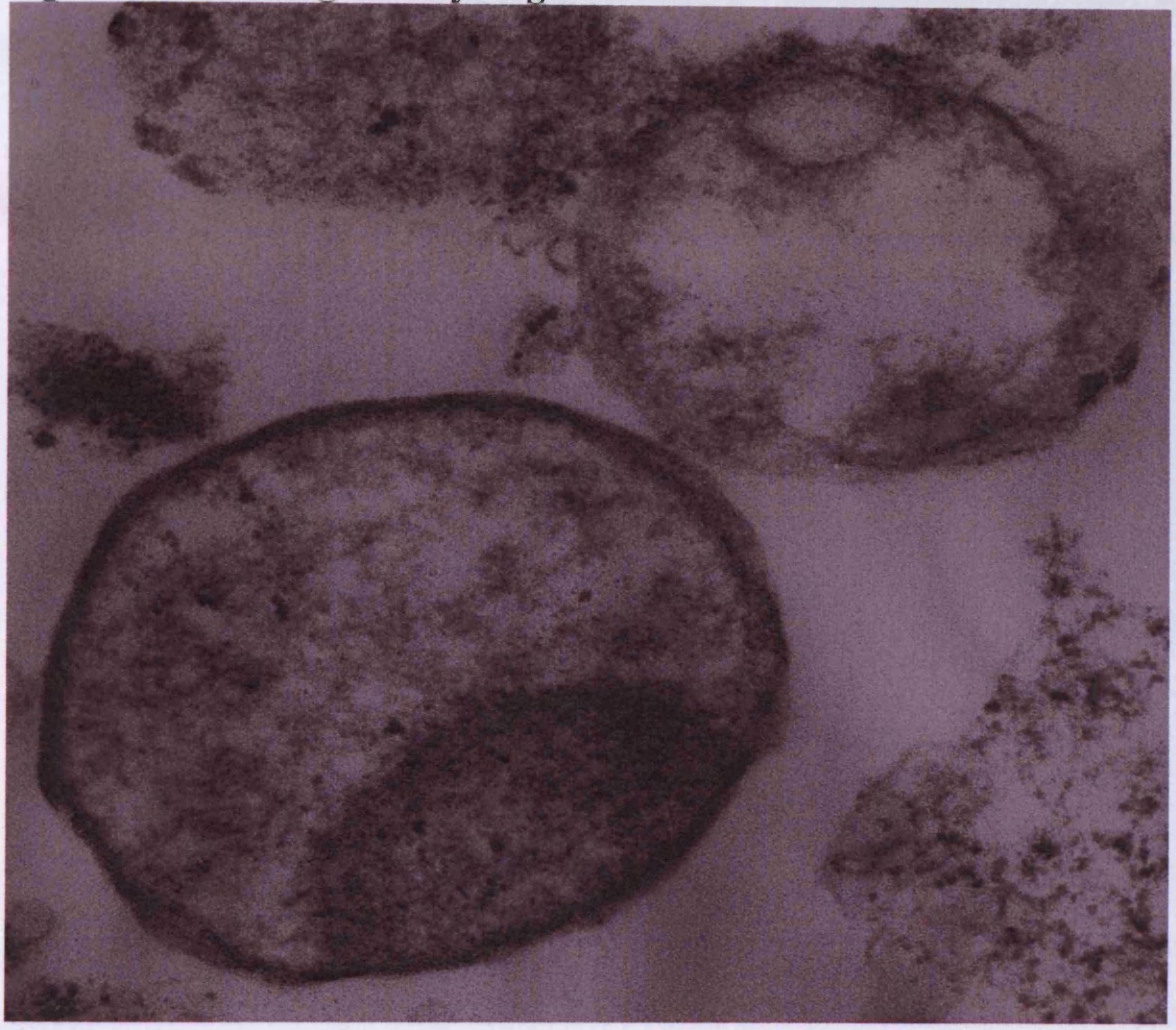

100nm

Fig. A3.11: DFMO-grown hydrogenosomes

Scale bar on image is 100nm

Fig. A3.12: DFMO-grown hydrogenosomes

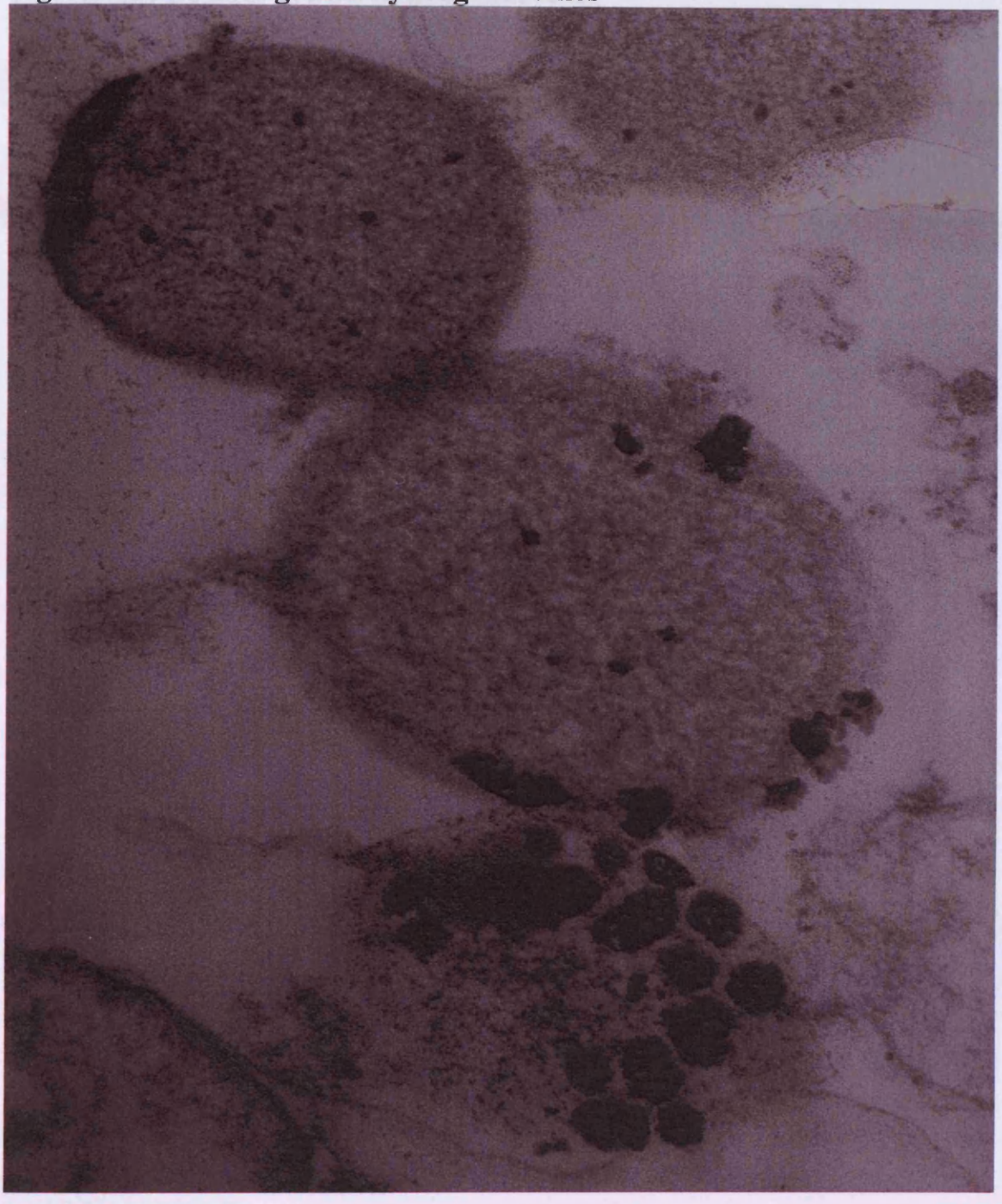

100nm

Fig. A3.13: DFMO-grown hydrogenosomes

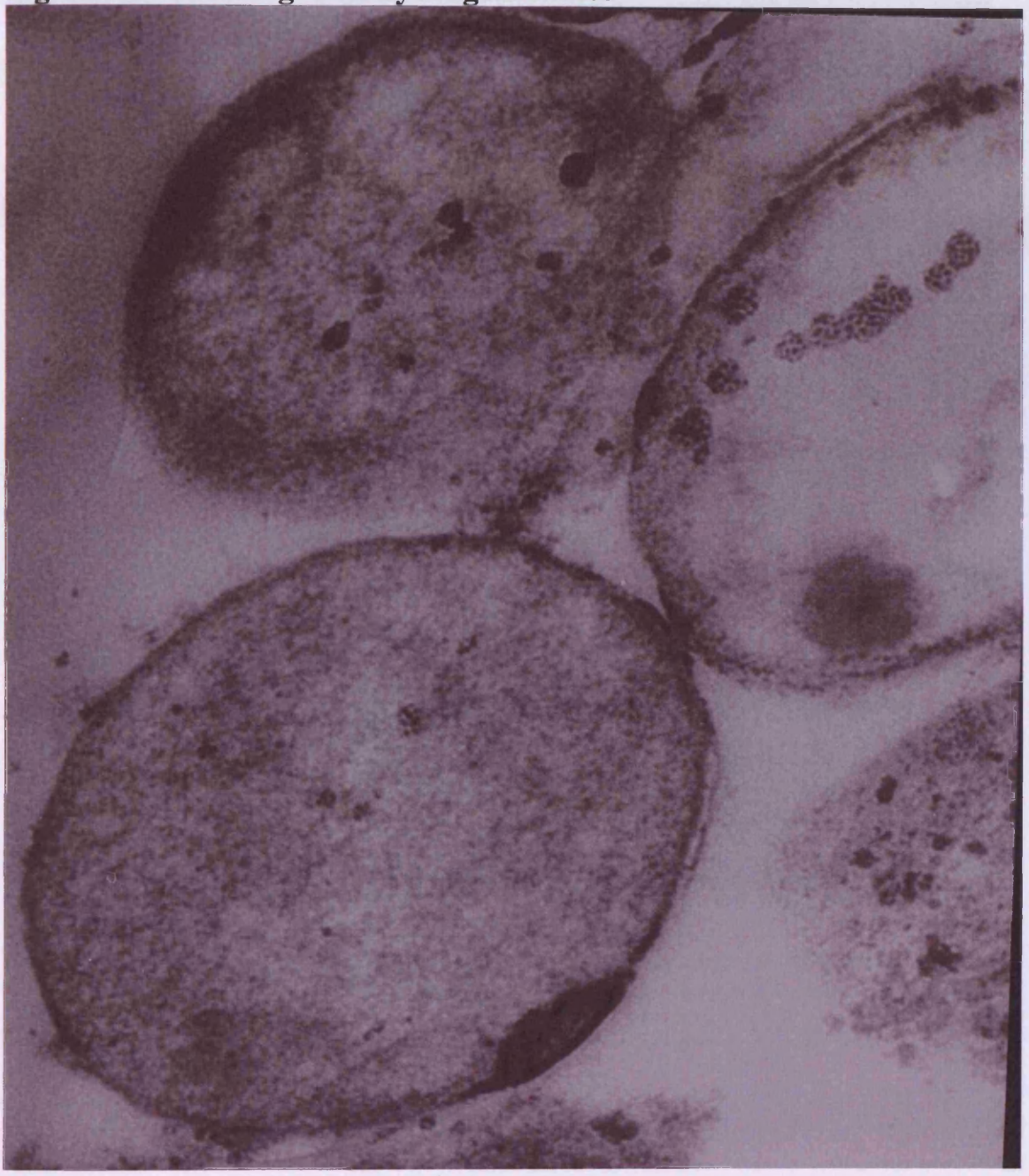

100nm

Fig. A3.14: DFMO-grown hydrogenosomes

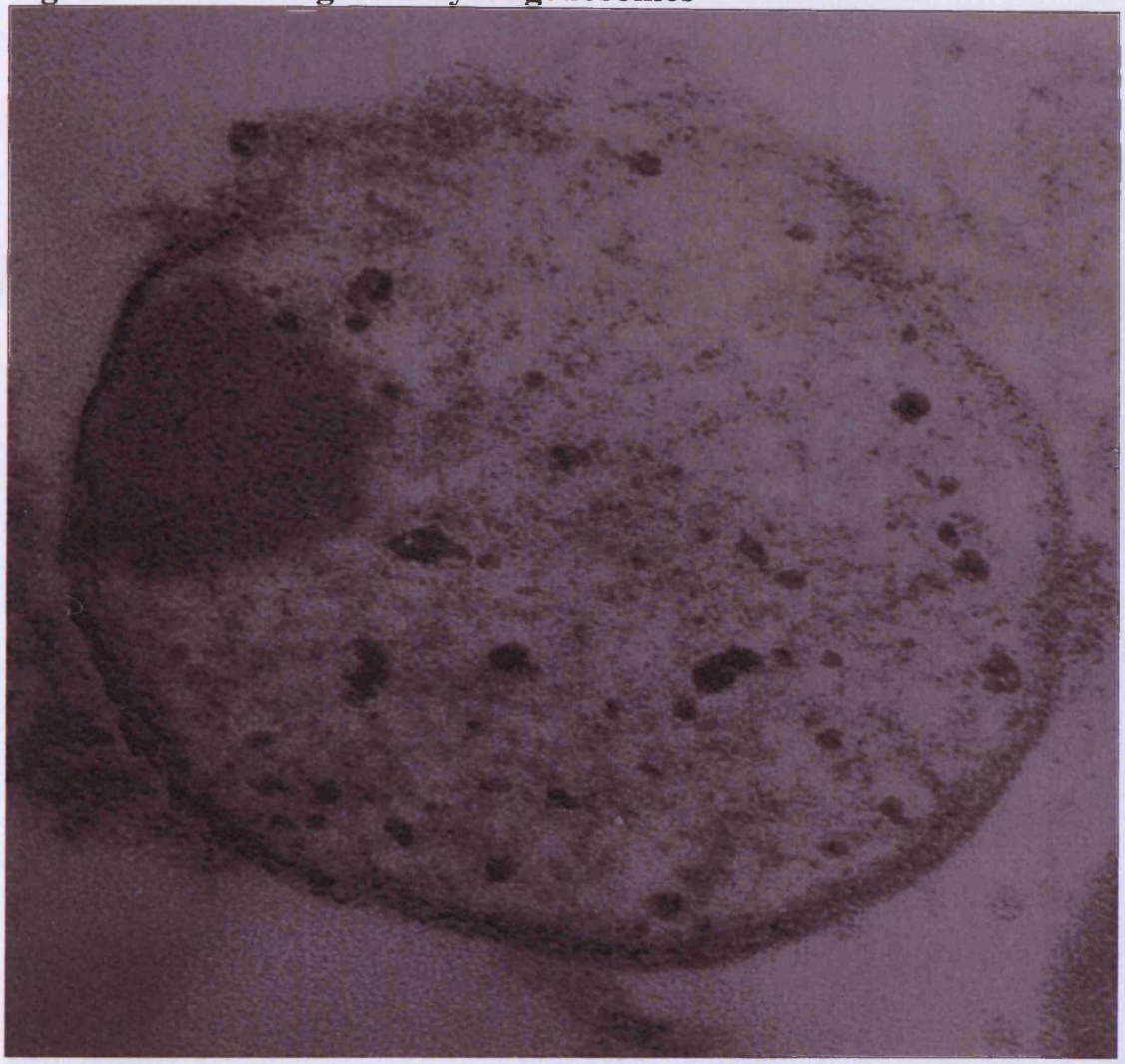

100nm

Fig. A3.15: DFMO-grown hydrogenosome

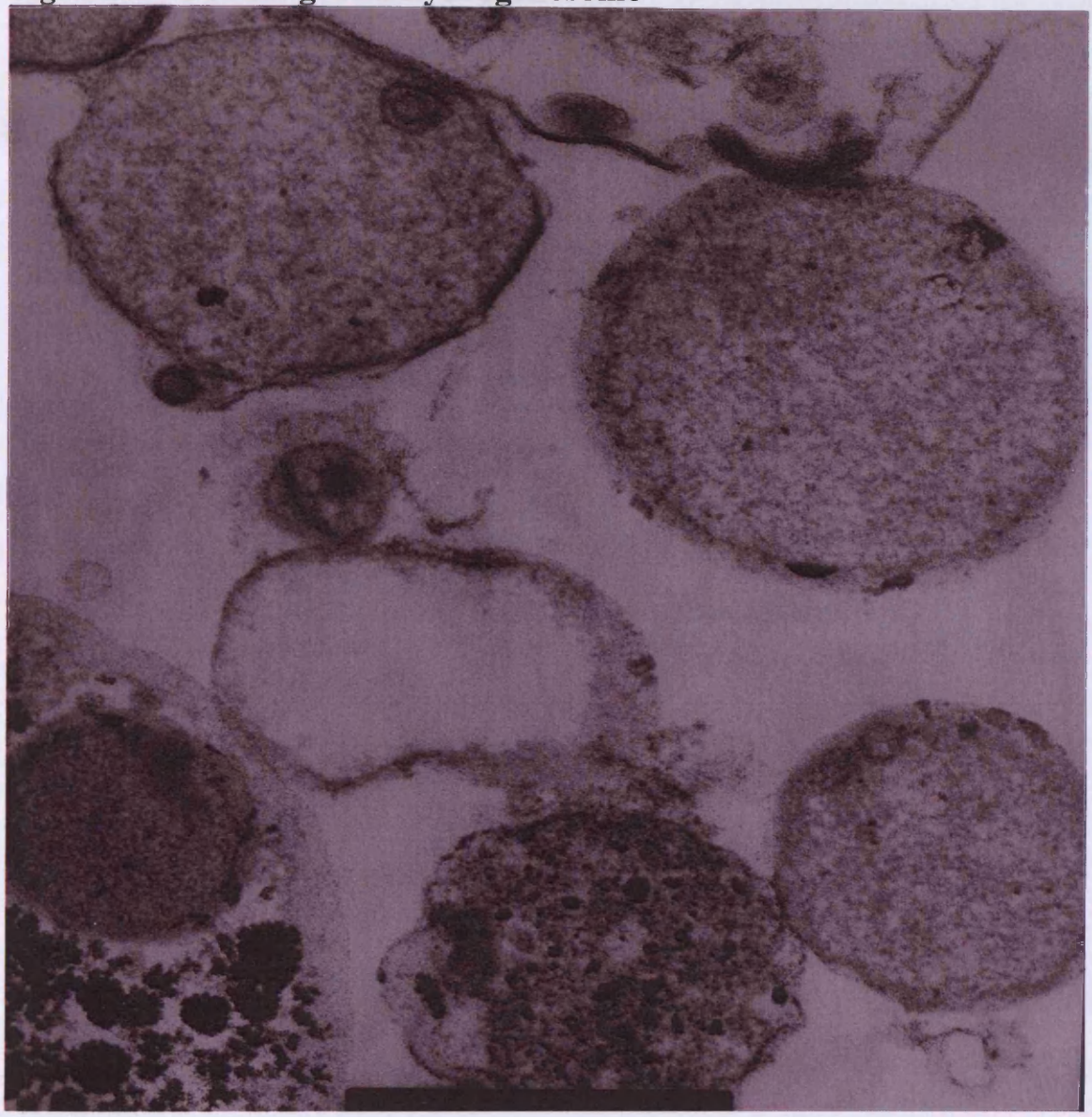

100nm

Publications:

Kristina M. Harris, Burt Goldberg, Giancarlo A. Biagini, David Lloyd. *Trichomonas vaginalis* and *Giardia intestinalis* Produce Nitric Oxide and Display NO-Synthase Activity. *Journal of Eukaryotic Microbiology.* **53**:182-183.

Manuscripts in preparation:

Kristina M. Harris, Burt Goldberg, Giancarlo Biagini, Rhian E. Lewis, David Lloyd. Mitochondria-like organelles in *Giardia intestinalis* produce nitric oxide and display NO synthase activity.

Kristina M. Harris, Burt Goldberg, Mark van der Giezen, Giancarlo A. Biagini, David Lloyd. Hydrogenosomes from *Trichomonas vaginalis* produce nitric oxide and display NO-synthase activity.

Irina A. Guschina, David Lloyd, John L. Harwood, Burt Goldberg, Kristina M. Harris. Phospholipids from *Trichomonas vaginalis* and Absence of Cardiolipin from *Trichomonas vaginalis* and *Giardia intestinalis.*

Kristina M. Harris, Rhian E. Lewis, Burt Goldberg, David Lloyd. Effects of Difluoromethylornithine on the Arginine Dihydrolase Pathway in *Trichomonas vaginalis.*

Kristina M. Harris, Burt Goldberg, Anthony Hayes, David Lloyd.
Effects of Polyamine Depletion by Difluoromethylornithine on Hydrogenosomes in *Trichomonas vaginalis.*

Published Abstracts and Oral Presentations:

Kristina M. Harris, Burt Goldberg, Giancarlo Biagini, David Lloyd.
T. vaginalis and *Giardia intestinalis* produce nitric oxide under aerobic conditions and show NO-synthase activity.
International Society of Protistologists Conference
June 20-24, 2006
Lisbon, Portugal
Winner of Jahn/Bovee Award for Best Student Speaker

Kristina M. Harris, Burt Goldberg, Anthony Hayes, Rhian E. Lewis, David Lloyd.
Effects of Polyamine Depletion by Difluoromethylornithine on Hydrogenosomes in *Trichomonas vaginalis.*
International Society of Protistologists Conference
June 20-24, 2006
Lisbon, Portugal

Kristina M. Harris, Burt Goldberg, Giancarlo Biagini, David Lloyd.
T. vaginalis and *Giardia intestinalis* produce nitric oxide under aerobic conditions and show NO-synthase activity.
Gregynog All-Wales Microbiology Symposium
March, 2006
Gregynog, Wales, UK

Kristina M. Harris, Burt Goldberg, Giancarlo Biagini, David Lloyd.
T. vaginalis and *Giardia intestinalis* produce nitric oxide under aerobic conditions and show NO-synthase activity.
Postgraduate Clinical and Biomedical Research Conference
November 25, 2005
Cardiff University, Cardiff, Wales, UK
Winner of Postgraduate Society Award

Kristina M. Harris, Tom Templeton, Victoria C. Hough, Burt Goldberg, Nigel Yarlett. Monoamine oxidase from *Cryptosporidium parvum.*
Polyamines in Parasites International Meeting
June, 2004
Pace University, New York, NY, USA

Published Abstracts and Poster Presentations:
Kristina M. Harris, Burt Goldberg, Anthony Hayes, Rhian E. Lewis, David Lloyd.
Effects of Polyamine Depletion by Difluoromethylornithine on Hydrogenosomes in *Trichomonas vaginalis*
International Conference on Anaerobic Protists
September, 2005
Alghero, Sardinia, Italy

Kristina M. Harris, Burt Goldberg, Anthony Hayes, Rhian E. Lewis, David Lloyd.
Effects of Polyamine Depletion by Difluoromethylornithine on Hydrogenosomes in *Trichomonas vaginalis*
Postgraduate Poster Evening
May 24, 2005
Cardiff University, Cardiff, Wales, UK

Kristina M. Harris, Victoria C. Hough, Martha P. Martinez, Nigel Yarlett.
Purification and Properties of spermine:spermidine N^1-acetyl transferase from *Trichomonas vaginalis*.
New England Science Symposium
March, 2002
Harvard University, Cambridge, Massachusetts USA